Novel insights on gamma-rhythmic gain modulation and repetition-related plasticity in awake primate area V1

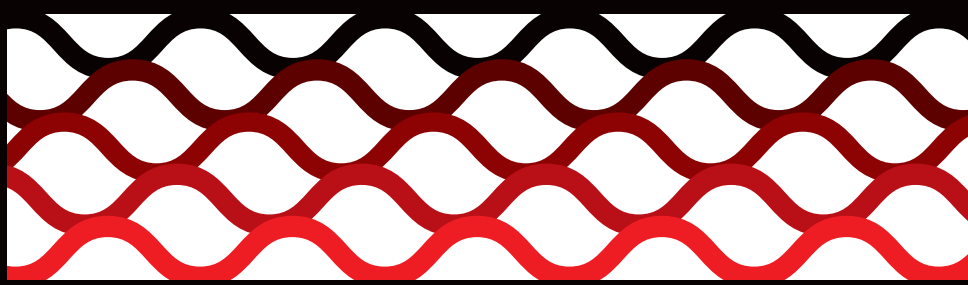

Martina Pandinelli

DONDERS SERIES

RADBOUD UNIVERSITY PRESS

Radboud Dissertation Series

Novel insights on gamma-rhythmic gain modulation and repetition-related plasticity in awake primate area V1

Martina Pandinelli

The research presented in this thesis was carried out at the Ernst Strüngmann Institute (ESI) for Neuroscience of Max Planck Society, in Frankfurt am Main, Germany.

Novel insights on gamma-rhythmic gain modulation and repetition-related plasticity in awake primate area V1
Martina Pandinelli

Radboud Dissertation Series
ISSN: 2950-2772 (Online); 2950-2780 (Print)

Published by RADBOUD UNIVERSITY PRESS
Postbus 9100, 6500 HA Nijmegen, The Netherlands
www.radbouduniversitypress.nl

Design: Proefschrift AIO | Guus Gijben
Cover: Claudia Kernberger
Printing: DPN Rikken/Pumbo

ISBN: 9789465152585
DOI: 10.54195/9789465152585
Free download at: https://doi.org/10.54195/9789465152585

RADBOUD
UNIVERSITY
PRESS

Novel insights on gamma-rhythmic gain modulation and repetition-related plasticity in awake primate area V1

Proefschrift ter verkrijging van de graad van doctor
aan de Radboud Universiteit Nijmegen
op gezag van de rector magnificus prof. dr. J.M. Sanders,
volgens besluit van het college voor promoties
in het openbaar te verdedigen op

dinsdag 12 mei 2026
om 14.30 uur precies

door

Martina Pandinelli
geboren op 5 maart 1996
te Bagno a Ripoli (Italië)

Promotor:
Prof. dr. P. Fries

Copromotor:
Dr. M.L. Schölvinck (Ernst Strüngmann Institute, Duitsland)

Manuscriptcommissie:
Prof. dr. F.P. de Lange
Dr. T.J. van Kerkoerle
Prof. dr. G. Gregoriou (University of Crete, Griekenland)

Novel insights on gamma-rhythmic gain modulation and repetition-related plasticity in awake primate area V1

Dissertation to obtain the degree of doctor
from Radboud University Nijmegen
on the authority of the Rector Magnificus prof. dr. J.M. Sanders,
according to the decision of the Doctorate Board
to be defended in public on

Tuesday, May 12, 2026
at 2.30 pm

by

Martina Pandinelli
born on March 5, 1996
in Bagno a Ripoli (Italy)

Supervisor:
Prof. dr. P. Fries

Co-supervisor:
Dr. M.L. Schölvinck (Ernst Strüngmann Institute, Germany)

Manuscript Committee:
Prof. dr. F.P. de Lange
Dr. T.J. van Kerkoerle
Prof. dr. G. Gregoriou (University of Crete, Greece)

Table of contents

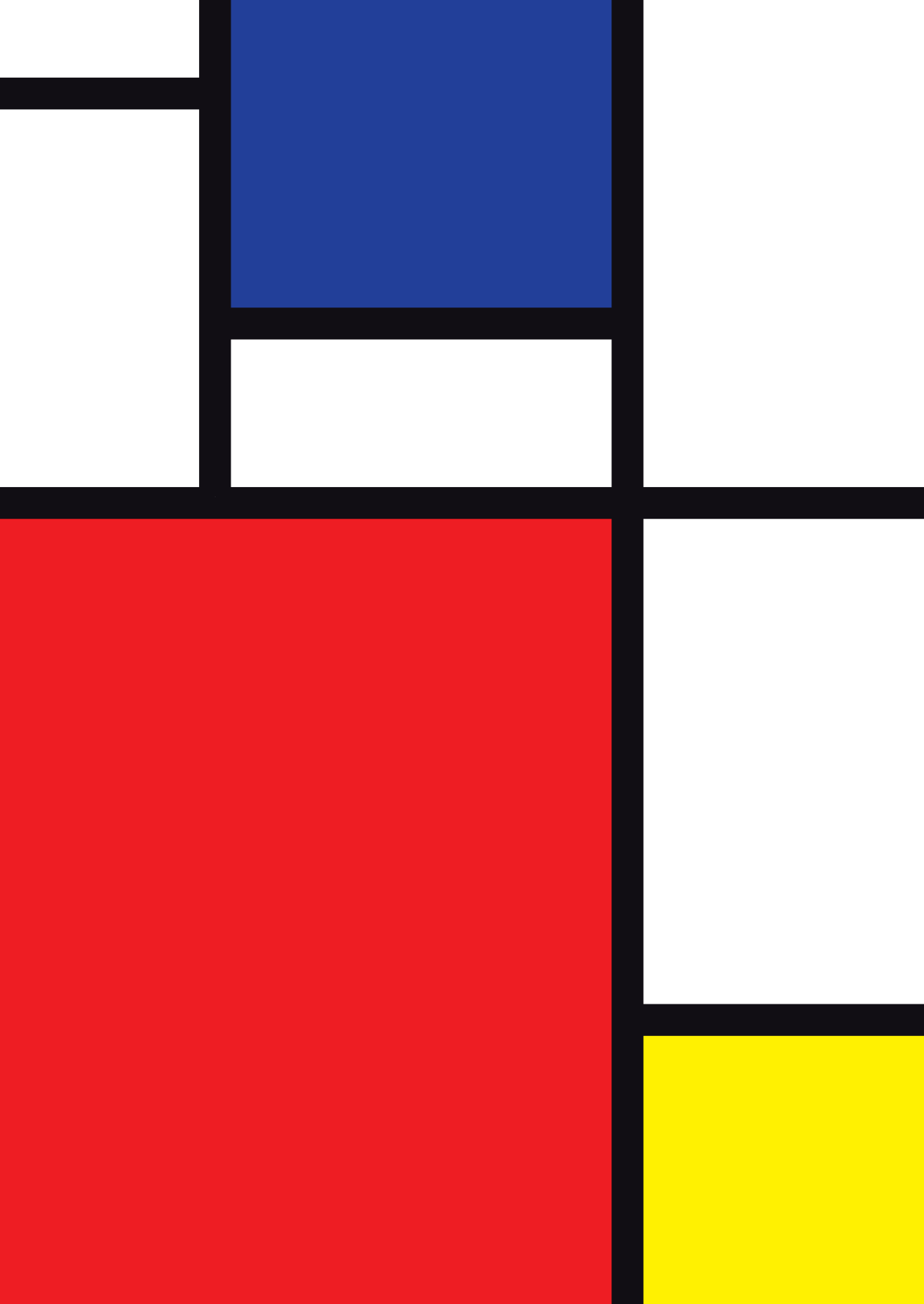

Chapter 1

General Introduction

Introductory remarks

This thesis is the result of experimental work conducted in the Fries lab, to the end of broadening the neuroscientific understanding of how the brain encodes and transmits information. All the experiments were carried out in a non-humane primate (NHP) experimental model, and involved intra-cranial recordings of neuronal activity in the form of local field potentials (LFPs) and multi-unit activity (MUA), in the primary visual cortical area, V1, while the animal was awake. The research work carried out focused on revisiting two well-studied topics in neuroscience: the brain oscillatory activity in the gamma range (≈40-90 Hz) (Fries 2009), and the neuronal spiking activity, and on further clarifying the relationship they entertain with each other and their behavior in particular stimulation conditions.

To this end, Chapter 1 will introduce the background knowledge for the understanding of the work conducted and described in the research chapters, Chapter 2 and Chapter 3. Chapter 2 will examine the interaction between gamma-band rhythmic activity and MUA, by investigating gamma rhythmic modulation of the neuronal MUA gain in response to the presentation of a visual stimulus. Chapter 3 will investigate the behavior of gamma-band activity and MUA in the particular stimulation condition of stimulus repetition. Chapter 4 of this thesis will eventually discuss findings and open questions leading to future research perspectives.

General Introduction

Gamma-band brain oscillations and the interaction with neuronal spiking activity and its gain modulation

The research questions addressed in the current thesis work stem from long standing and widely discussed topics of neuroscience, namely oscillatory activity in the brain, especially in the gamma range, and its relationship with neuronal spiking. Evidence has accumulated over time supporting the functionality of brain oscillations, especially in the gamma band, as syntactic organizers of the spiking activity (Buzsáki and Chrobak 1995, Buzsáki 2010). Brain rhythms in the gamma range constitute functionally relevant operational patterns that the brain uses for concerting the organization of local and more distant networks, in order to flexibly support the routing of information and the subsequent production of cognitive functions (Singer and Gray 1995, Bosman, Schoffelen et al. 2012, Fries 2015). Recently, computational and modeling experiments demonstrated the higher efficiency of networks of coupled oscillators resembling closely the biology of the brain, compared to non-oscillating networks (Effenberger, Carvalho et al. 2025, Singer and Effenberger 2025), shedding new light and interest on the topic. The presence of oscillations seems to constitute an advantage for the brain to be able to compute highly parallelized computations in a high-dimensional state space, therefore oscillations are not a simple epiphenomenon of brain activity, i.e. a consequence of it, but they hold a functional relevance (Singer 2018, Singer and Effenberger 2025). Spiking activity and the modulation of the neuronal gain are, on the other hand, equally important phenomena setting the basis for the encoding of information about the stimuli presented to the brain and adapting the neuronal response to the ever changing environment and state of the brain (Salinas and Sejnowski 2000, Salinas and Thier 2000). Despite the plethora of studies on these topics, some questions remain open to investigate, especially regarding the interaction of these two brain activity patterns, the oscillatory activity and the neuronal spiking response and its gain, in relation to stimulus response. Specifically, the interest of this work converges on how gamma band oscillations affect neuronal spiking activity by modulating its gain in the context of stimulus representation in the brain, and on the behavior of gamma oscillation and neuronal spiking activity in the context of repeated stimulation conditions.

Introduction outline

This introduction will set the background for the scientific questions leading this thesis work by presenting a summary of the topics involved in the investigation. Oscillatory brain patterns, specifically in the gamma range, have the ability of

organizing spiking activity, by synchronizing neurons' activity in meaningful temporally structured windows of activation: an account of brain oscillations will be given, focusing on gamma band activity and its mechanisms and functions. A presentation of the topic of gain modulation will follow, to set the basis for an understanding of how neuronal spiking output can be modified by ongoing brain activity and environmental influence. Gamma-band oscillations are particularly well observed in areas like the primary visual area V1, because they get activated by most visual stimuli, and due to V1 circuitry of recurrently connected excitatory and inhibitory neurons that supports the generation of such activity patterns. V1 is also well studied for the basic neuronal responses to the presentation of a visual stimulus, and how these responses change in various environmental or stimulus related conditions through the modulation of their neuronal gain. As V1 poses itself as the perfect brain location to study the interaction of gamma-band activity and the modulation of the neuronal gain, V1 will be described in the aspects that are mostly relevant to the current investigation. Finally, an introduction to the topic of stimulus repetition will be offered, and an outline of the thesis work will be presented.

Oscillatory activity in the brain

Brain oscillations are evolutionarily preserved rhythmic patterns of activity widely observed across brain areas. Evidence of synchronized oscillatory activity was found in the brains of various species and phyla of mammals, and oscillations were preserved during the increase of size of mammalian brains (Buzsaki, Logothetis et al. 2013). Evidence of oscillatory activity was even found in invertebrates (Bazhenov, Stopfer et al. 2005), and oscillations were described as originating in developing neuronal networks already during pre-natal brain formation, as organoid studies revealed (Trujillo, Gao et al. 2019). Typically, oscillatory patterns of activity in the brain of mammals can range from 0.5 Hz to 500 Hz (Buzsáki and Draguhn 2004, Buzsáki 2006, Buzsáki and Moser 2013, Singer 2018), and they are traditionally organized in defined bands or frequency ranges (Fig.1.1). Naturally, there are differences concerning the functionality and meaning that the various patterns of oscillatory activity have assumed in different species over the course of evolution. For example, gamma band synchronization in mice visual area V1 that functionally resembles the one described in the same cortical area in monkeys has a lower frequency range (25-40 Hz in mice compared to the 40-90 Hz in monkeys) (Fries 2009, Veit, Hakim et al. 2017, Hakim, Shamardani et al. 2018). A higher frequency gamma (~60 Hz) was also described in mice, but this is not functionally relatable to the primate visual gamma, because it is increased by movement and inhibited strongly by visual stimuli (Veit, Handy et al. 2023). Yet, oscillations as a

temporal patterning of neuronal activity remains a strikingly preserved feature of brain activity.

Brain oscillations of various frequencies interact with each other and work in concert across brain areas (Buzsáki and Draguhn 2004, Buzsáki and Moser 2013), and are generally described as to be organized in a hierarchy where faster oscillations nest in the slower ones facilitating the retention of information at a local level and the integration of it at a more global one (Buzsáki 2006). This feature of brain rhythms offers important advantages in terms of organization and optimization of the neuronal computation to the brain.

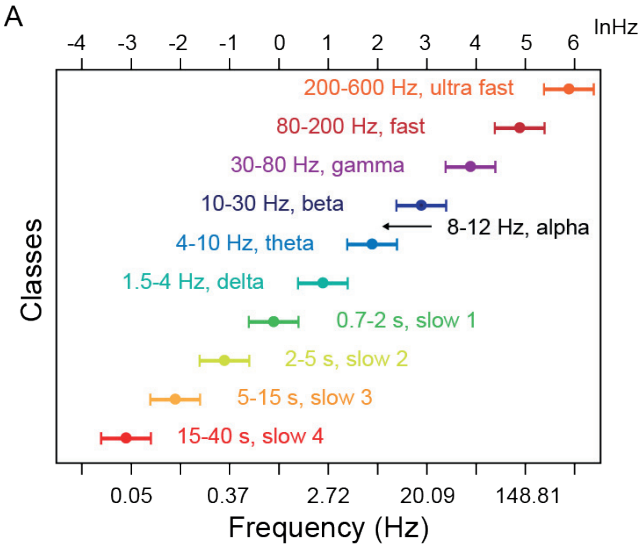

Fig. 1.1 Brain oscillations frequency ranges (*A*). This figure shows the traditional classification of oscillatory activity in the brain according to frequency bands. The alpha band, generally classified as ranging between 8 and 12 Hz (Buzsáki and Draguhn 2004) was missing in the original figure and was inserted with an edit. Figure adapted from (Buzsáki and Draguhn 2004).

Mechanisms of brain oscillations

Rhythmic activity in the brain is commonly originated from local or more extended networks of neurons presenting a specific cell composition and organizational motifs (Singer 2018). Usually, the establishment of an oscillatory firing pattern depends on the presence of recurrent inhibitory connections to an excitatory neuron that generate a negative feedback loop. Every time the excitatory neuron fires, the connected inhibitory neuron is excited, and will consequently fire with a small delay, inhibiting the activity of the same excitatory neuron to which it is recurrently connected (Kopell, Ermentrout et al. 2000, Börgers and Kopell 2003).

Functional relevance of brain oscillations

Very debated during the course of time has always been the question whether these rhythmic patterns of activity hold a functional meaning for the brain, or simply represent a byproduct of neuronal spiking activity, and are therefore to be considered epiphenomena (Ray and Maunsell 2015, Singer 2018). Convincingly, oscillatory activity is capable of temporally parsing neuronal spiking, which means to organize neuronal spiking in a temporal manner (Buzsaki, Logothetis et al. 2013, Singer 2018), which is also energy efficient (Buzsáki and Chrobak 1995, Buzsáki and Draguhn 2004). Due to the alternation of excitatory and inhibitory phases of an oscillatory cycle, excitatory post-synaptic potentials (EPSPs) will have a higher or lower chance to effectively integrate. Because individual cells integrate inputs in short time windows, information, may it be contained in a barrage of spikes with a specific rate (as supporters of the rate-code integration theory sustain) or in a coincidental arrival of spikes (as supporters of coincidence detection theory sustain), has to be anyways coordinated in time (Ahissar 1998, Ainsworth, Lee et al. 2012, Peter 2020). Oscillatory activity in the brain offers the opportunity to precisely time neuronal spiking and favor information transfer between neuronal assemblies that resonate at a similar frequency (Fries 2005, Fries 2015). To better explain the two integration theories mentioned above, according to the rate-code integration theory, information is contained in the spike rate, i.e. average firing rate in a restricted time window is essential for the transmission of information. On the other hand, coincidence detection theory supports a temporal code, i.e. that coincident arrival of spikes is the basis for information transmission (Ahissar 1998, Ainsworth, Lee et al. 2012).

Another interesting property of oscillatory activity is that of being capable to serve the dynamic organization of cellular assemblies in functional networks. For cognitive processes and behaviour to be put in action, the integration of signals has to be quick, and many brain areas even distant from each other, have to be coordinated. The anatomical connections between cells would require too long of a time to be structurally re-arranged for this process to be enacted in an useful time, while oscillatory activity is capable to support the formation of functionally relevant cell assemblies almost instantly, by coordinating cells' activity locally, and in distant networks. This way, the flexibility required to timely switch from one functional assembly to another can be guaranteed (Varela 1995, Varela, Lachaux et al. 2001, Singer 2018).

Gamma – band oscillatory activity

The gamma rhythm is a specific frequency band of the brain oscillatory activity commonly classified as ranging between 40 and 90 Hz (Fries 2009), and it well recapitulates all the characteristics of brain rhythms described in the previous section of this introduction. Gamma-band activity is one of the most widely observed, described, studied and debated ranges of oscillatory activity in the brain. Associated with many cognitive functions and observed in many animal species ranging from mammals to invertebrates (Wehr and Laurent 1996, Laurent 2002), gamma-band activity started to gain importance in the landscape of research addressing brain oscillation after a series of seminal studies in the visual cortex of anesthetized cats, were gamma activity was prominently activated during stimulation with gratings or moving bars (Eckhorn, Bauer et al. 1988, Gray, König et al. 1989, Gray and Singer 1989, Engel, König et al. 1991, Engel, Kreiter et al. 1991). Evidence of gamma activation following visual stimulation was later reported also for other kinds of stimuli, including free vision in awake animals (Gray and Viana Di Prisco 1997, Fries, Reynolds et al. 2001, Bichot, Rossi et al. 2005).

Many other cortical and extra-cortical brain areas show gamma activation (Wehr and Laurent 1996, Stopfer and Laurent 1999, Csicsvari, Jamieson et al. 2003) . For example, gamma was reported in awake and behaving cats and monkey's visual areas and auditory cortex, in human visual and somatosensory cortical areas (Bauer, Oostenveld et al. 2006, Fries, Scheeringa et al. 2008, Wyart and Tallon-Baudry 2008), and also in the spinal cord (Brown, Salenius et al. 1998, Schoffelen, Oostenveld et al. 2005). Gamma band synchronization was also studied and reported in hippocampus of mice and rats (Bragin, Jandó et al. 1995, Csicsvari, Jamieson et al. 2003, Sirota, Montgomery et al. 2008). All the reported gamma rhythms might hold a different functional significance according to the anatomical area they originate from and the cognitive function under investigation. Visually activated gamma in NHP area V1 is the type of gamma-band rhythm that this thesis work will be concerned with.

Gamma – band activity in the visual system

Gamma has been widely studied and characterized in relation to visual processing, and especially in visual area V1. In this cortical area, gamma power has been demonstrated to progressively increase with stimuli of increasing size and contrast, and with strength of the input (Roberts, Lowet et al. 2013, Peter, Uran et al. 2019, Lewis, Ni et al. 2021, Gieselmann and Thiele 2022). Interestingly, the pattern of gamma activation was also demonstrated to depend on the structure of an image. When an image is homogeneous, gamma activity is reported to be stronger, while when an image presents mismatches or discontinuities, gamma is reported to be

weaker. This is in opposition with the effects reported for firing rates described by the traditional receptive field (RF) center-surround modulation effect (Gieselmann and Thiele 2008, Peter, Uran et al. 2019). In addition, gamma oscillations were shown to be strongly activated in V1 following stimulation with chromatic stimuli or surfaces. Color is, therefore, another relevant stimulus feature for gamma activation (Zweig, Zurawel et al. 2015, Peter, Uran et al. 2019, Stauch, Peter et al. 2022) (see also Chapters 2, 3).

Long range connections responsible for horizontal connectivity across the columns of the visual cortex may also play a role in the modulation of gamma oscillatory activity (Vinck and Bosman 2016). Since horizontal connections were demonstrated to mainly link together columns with a similar orientation preference in V1 (Angelucci, Bijanzadeh et al. 2017) (see also below), these could be responsible for the modulation of gamma strength in different stimulation conditions: for example they could determine the increase or decrease in gamma strength witnessed, respectively, with homogeneous stimuli or with discontinuous ones (Peter, Uran et al. 2019). Long-range interneurons might also be represent the necessary anatomical connection to allow gamma synchronization to establish between remote areas of the brain, because they exhibit several times thicker myelinated axons than pyramidal cells, thanks to which electrical impulses travel faster (Jinno, Klausberger et al. 2007). The effect of long range and lateral connections on modulating gamma band activity (Chapter 3) and its interaction with neuronal spiking MUA (Chapter 2 and 3) will be discussed at many points during this thesis work.

Gamma – band activity as organizer of neuronal spiking

The interest in gamma-band activity and in clarifying how this rhythmic pattern interacts with neuronal gain stems from some of its characteristics. Firstly, gamma has cycle durations in the range of milliseconds, which makes it the preferential candidate to effectively support synaptic integration processes that happen in the same time scale. Secondly, gamma has been functionally acknowledged to be capable of organizing neuronal spiking activity at a local level and network synchronization at a more global one, favoring information transfer. These aspects will be clarified in the following paragraphs.

Due to its short cycle length, the gamma rhythm has more than any other rhythm the potential to support neuronal integration in the restricted milliseconds-long time windows that are necessary to guarantee integration at a synaptic level. 40 – 80 Hz frequencies, correspond in fact to cycles of 25 to 12ms (Fries 2009), and the spikes of neurons synchronized by this rhythm will generally tend to concentrate in

half of the cycle (the half that guarantees excitation) due to the modulatory activity of the oscillation, so that the window of opportunity for neuronal activation for sending and receiving input will be restricted to 12 to 6ms, exactly the same time range available for synaptic integration so that spikes would effectively summate in the postsynaptic neuron (Fries 2009).

One classical hypothesis about the functional role of gamma in the visual system, and more generally in the brain, is the Communication through Coherence (CTC) hypothesis (Fries 2005, Fries 2009, Fries 2015). CTC highlights the role of gamma oscillations in organizing neuronal spike output from and input to a local network, and more globally its role in supporting selective and functional routing of information via the dynamic re-organization of cellular assemblies according to the current cognitive demand. Locally, gamma oscillatory activity modulates neuronal membrane potentials of the neurons neuron to respond to an input stimulus, and to send spiking output grouped in time with increased efficacy. At a more global scale, CTC postulates that gamma coherence between neuronal populations can be adjusted *ad-hoc* so to guarantee optimal transmission of relevant information (Fries 2005, Fries 2009, Fries 2015). In attentional selection processes the gamma-band phase coherence between a sender group of neurons and a receiver one has been demonstrated to increase for attended vs non-attended stimuli, and this way support preferential downstream routing of the related information. This was shown in V1 – V4 studies (Bosman, Schoffelen et al. 2012, Grothe, Neitzel et al. 2012, Grothe, Rotermund et al. 2018). When attention is directed at a target, this will be preferentially sent to a receiver group of neurons by means of selective entrainment and phase coherence (Womelsdorf, Schoffelen et al. 2007, Lakatos, Karmos et al. 2008, Bosman, Schoffelen et al. 2012, Grothe, Neitzel et al. 2012, Grothe, Rotermund et al. 2018).

Origin and modulation of gamma oscillations

A crucial role in the generation of gamma band oscillatory activity has to be attributed to inhibitory interneurons (Buzsáki and Wang 2012). The brain areas where the gamma rhythm is commonly described have in common the presence of local inhibitory neurons acting on excitatory neurons via recurrent connections and GABAergic synapses. Peri-somatic inhibition enacted by local interneurons was demonstrated to be effective in determining the installment of rhythmic synchronization with inhibitory post-synaptic potentials (IPSPs), rather than excitatory EPSPs (Lytton and Sejnowski 1991). Two models are regarded as the most accountable for gamma generation. The first model is based on inhibitory – inhibitory reciprocal connections, and is generally referred to as I-I or interneuron-network gamma (ING) (Wang and Buzsáki 1996, Chow, White et al. 1998,

Traub, Bibbig et al. 2000), the second model is based on excitatory – inhibitory connections, and it is commonly called the E-I model or pyramidal-interneuron network gamma (PING) (Lytton and Sejnowski 1991, Börgers and Kopell 2003, Börgers, Epstein et al. 2005).

According to the I-I model, the only necessary elements to originate a gamma cycle are reciprocally connected inhibitory interneurons with a time constant given by their $GABA_A$ channels, and an appropriate amount of drive to induce spiking activity (Bartos, Vida et al. 2007, Buzsáki and Wang 2012). The sufficient drive to trigger the activation of the gamma cycle can be provided both via tonic and stochastic inputs to the recurrent neuronal network (Brunel and Wang 2003, Ardid, Wang et al. 2010, Economo and White 2012). In the case of an E-I model (Börgers and Kopell 2003, Börgers and Kopell 2005), excitatory neurons are mutually connected with inhibitory neurons, and the activation of the gamma rhythm can similarly be triggered by tonic or stochastic drive to the network. Between the spiking of the pyramidal neurons and the interneuron, a synaptic delay of around 5 ms elapses. This delay, together with decay time constant of the IPSPs determines the preferred frequency of the gamma cycle (Börgers and Kopell 2005, Buzsáki and Wang 2012).

Traditionally, studies in rodents have identified Parvalbumin positive (PV^+) basket interneurons as the locally coupled type of inhibitory cells connecting with the pyramidal cells in the generation of the gamma cycle (Buzsáki, Anastassiou et al. 2012). More recent studies, still in rodents, have identified also a role for Somatostatin positive interneurons (SST) and Vasoactive Intestinal Peptide (VIP) positive interneurons (Cardin, Carlén et al. 2009, Veit, Hakim et al. 2017, Veit, Handy et al. 2021). In NHP, the generation of gamma rhythms was mostly studied via non-cell-type specific causal manipulations, so it is not clear which specific interneurons contribute mostly to the oscillation (Psarou 2024).

Gain Modulation

Gain modulation is recognized to be one of the few canonical computations of the brain, i.e. one of those general mechanisms used across the whole brain to serve many modalities, brain states, and cognitive functions (Salinas and Thier 2000, Reynolds and Heeger 2009, Ohshiro, Angelaki et al. 2011). Neuronal gain refers to the "sensitivity of a neuron to changes in input" (Ferguson and Cardin 2020), and can be measured in terms of the slope of the ratio between the incoming signals the neuron receives, and its firing rate in response to them, or more simply the slope of the neuron's input-output (I/O) response curve (Silver 2010, Ferguson and

Cardin 2020). Modulation of the neuronal gain achieves the scope of regulating the amplitude of the neuron's response to an input without affecting the neuron's selectivity for the features of the stimulus, or the characteristics of its RF (Andersen and Mountcastle 1983, Salinas and Thier 2000, Ferguson and Cardin 2020).

One example of gain modulation is contrast-invariant tuning, a mechanism described in the visual system where neurons respond to stimuli of different contrast intensity without changing their orientation preference or spatial frequency tuning (Ferster and Miller 2000, Alitto and Usrey 2004, Finn, Priebe et al. 2007). Normalization is another special form of gain modulation where the summed activity of a local pool of neurons divides and this way scales the neuronal responses (Carandini and Heeger 2011).

Functions of gain modulation

In an ever-changing environment that constantly challenges the brain with variable stimuli, gain modulation represents the perfect computational strategy to guarantee the necessary flexibility to encode the input information in an efficient way, and elaborate adequate responses to salient stimuli. For example, neurons should be able to detect weak stimuli, and at the same time not saturate their response to strong stimuli (Ferguson and Cardin 2020). Therefore, gain modulation acts via adaptation so that differences in sensory inputs over a wide range of intensities can be more easily detected and represented (Demb 2007, Farley, Quirk et al. 2010). This was reported in many brain areas linked to different sensory modalities, like the primary auditory cortex of awake rats and monkeys (Fishman and Steinschneider 2012, Natan, Carruthers et al. 2017), in cat primary visual cortex (Cardin, Palmer et al. 2008), and in macaque MT (Kohn and Movshon 2003), to mention a few.

On the other hand, gain modulation is essential not only in relation to external stimuli conditions, but also for adapting responses to changing brain states. The brain can change between states of quiet wakefulness, arousal, sleep, and many others that engage different levels of activation thanks to the mechanism of gain modulation, which operates to make sure the input signals are encoded and processed appropriately. For example, the states of arousal and locomotion are found to increase the gain of neurons in visual cortical areas (Niell and Stryker 2010, Vinck, Batista-Brito et al. 2015). Functional relevance of gain modulatory processes can also be found in the enhancement of relevant information when the gain is modulated by attention (Reynolds, Pasternak et al. 2000, McAdams and Reid 2005).

Different kinds of gain modulation

There are different kinds of gain modulation. If on the one hand, a neuron increases its net output response to the incoming input stimulation or has a leftward shift in its I/O curve that does not change the net output, but increases the output response for lower input intensity, this is referred to as multiplicative modulation (Fig.1.2A, light-blue arrows). If on the other hand, the net output response of a neuron is reduced, or the I/O curve of the neuron is shifted rightwards, the gain modulation mechanism in place is called divisive (Fig.1.2A, green arrows). Both these mechanisms of multiplicative and divisive gain modulation can be exerted either on the incoming signal to a neuron or on the response of a neuron to an incoming signal, according, respectively, to an input-gain modulation model (Fig.1.2A, left panel) or an output-gain modulation one (Fig 1.2A right panel). More precisely, in case of an input-gain modulation, the sensitivity of the neuron to the stimulus is affected, via a multiplicative or divisive scaling of the input signal, and a resulting shift of the I/O response curve towards the left (multiplicative modulation) or the right-hand side (divisive modulation). An output-gain modulation multiplicatively or divisively scales the net response neuronal firing, altering the maximum output (Silver 2010, Ferguson and Cardin 2020). Importantly, both input- and output-gain modulation do not affect the stimulus selectivity, i.e. the tuning curve, of the modulated neuron (Reynolds and Desimone 1999).

There are other cases of transformation of the I/O response curve that are not multiplicative, but are represented by simple upward or downward shift (Fig.1.2B). These mechanisms are referred to as additive or subtractive operations and differ from multiplicative gain modulation processes because they maintain the sensitivity of the neurons, while changing their stimulus selectivity (Silver 2010, Ferguson and Cardin 2020).

Mechanisms implementing gain modulation

The mechanisms allowing multiplicative or divisive gain modulation at a cellular level are mainly the regulation of synaptic input, and the strong role of inhibition mediated by GABAergic interneurons, and the neuromodulatory influence of the brain state (Ferguson and Cardin 2020).

The regulation of the overall level of synaptic inputs to a neuron in conjunction with environmental factors such as the stimulus drive and the neuromodulatory influence of the current brain state can affect the spontaneous fluctuations in the membrane potential (V_m), which can in turn regulate the gain of single neurons (Chance, Abbott et al. 2002, Cardin, Palmer et al. 2008). Sub-threshold input drive

to a neuron can also contribute to the modulation of its gain thanks to stochastic resonance, since noisy background synaptic input can drive some sub-threshold signals to surpass detection threshold (Bulsara, Boss et al. 1989).

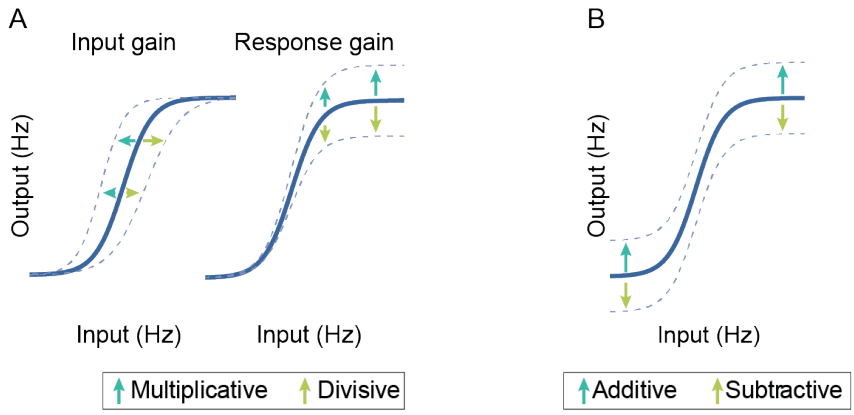

Fig. 1.2. Different types of gain modulation. (*A*) Gain modulation can be multiplicative, and increase the neuronal gain, or divisive, and reduce the neuronal gain. Multiplicative modulation is represented by the light-blue arrows in the figures, divisive modulation by the green arrows. Multiplicative and divisive modulations change the shape of the neuronal input/output curve and can impact the input (left-hand side) or the output (equivalent to the response, right-hand side) gain of the neuron. (*B*) Transformation of the I/O response curve can also be represented by a shift of the curve. In this case, the stimulus selectivity of the neuron in question changes, and the modulation is referred to as additive (light-blue arrows) or subtractive (green arrows). Figure adapted from (Ferguson and Cardin 2020).

Inhibition imposed by GABAergic neurons can also determine gain modulation. GABAergic inhibitory neurons comprehend classes of interneurons like PV^+, SST^+ or VIP^+ expressing interneurons (Katzner, Busse et al. 2011, Lee, Kwan et al. 2012). All of these cell types may be involved in specialized gain modulation processes (Natan, Rao et al. 2017), and their activity is often influenced by other parameters, like brain or behavioral state and the kind of stimulation. Shunting inhibition also represents a crucial mechanism for gain modulation, allowing the dampening of incoming excitatory input to a neuron, without affecting its V_m (Mitchell and Silver 2003). All of these mechanisms can contribute to generating multiple different kinds of gain modulation, depending on how they are combined.

Mechanisms such as depolarization and change in membrane conductance that do not dependent on direct modulation of the synaptic input drive, only determine additive or subtractive shifts in the I/O response function, since they affect the neuron's rheobase and consequently the level of depolarizing current necessary for

spiking (Salinas and Thier 2000, Silver 2010), changing neuron selectivity towards a stronger or weaker stimulus, rather than its sensitivity. These mechanisms, though, can also modulate the gain of a neuron in a multiplicative or divisive way if combined with the other synaptic input regulating processes, like for example shunting inhibition (Shu, Hasenstaub et al. 2003, Vogels and Abbott 2009).

Note that all the mechanisms described above to implement gain modulation apply to the postsynaptic neuron as a whole, or to the summed synaptic input drive to it. This consideration will be followed up in the discussion presented in Chapter 4, in the *Considerations and future perspectives for gamma rhythmic gain modulation studies* paragraph.

The role of inhibitory activity is crucial for the brain's computations, just like it was specified for the generation of gamma oscillatory activity, it is again here for neuronal gain modulation. More considerations about the role of inhibition in regulating neuronal gain and its interaction with gamma band activity will follow in Chapters 2, 3, and 4.

Gain modulation and gamma-band oscillatory activity

The question of whether – and how – the gamma-band rhythm modulates the neuronal gain stems from one of CTC's fundamental arguments, namely that oscillatory modulation of the neuronal gain gives an advantage to information transmission processes because "inputs that consistently arrive at moments of high input gain benefit from enhanced effective connectivity" (Fries 2015). What does this entail? There are three main predictions about gamma-band modulation on the gain of neurons that can be derived from the CTC hypothesis:

1. Multiplicative gain modulation

Gain modulation imposed by gamma band rhythmic activity is supposed to be multiplicative. The effect of gamma-band oscillatory modulation on the neuronal gain is not merely additive, i.e. it does not correspond to a upwards or downwards shift of the I/O response curve, which is in practice represented by a constant neuronal response to the presentation of a stimulus superimposing additively onto phases of higher or lower excitability during the gamma cycle. On the contrary, the gain modulation imposed by gamma should be multiplicative, such that input aligned to beneficial gamma phases will benefit from genuinely enhanced gain.

2. Input-gain modulation model

The nature of the modulation imposed by gamma is predicted to resemble an input-gain mechanism. This means that gamma-rhythmic gain modulation should act on the neuronal sensitivity, shifting the I/O curve sideways. This is consistent with the CTC observation that the inhibitory activity involved in the generation of the gamma cycle will periodically inhibit inputs to the downstream neuron.

3. Preserved selectivity

One of the roles postulated by CTC for gamma-band activity is that of supporting the preferential transmission of an attended stimulus in selective attention processes. In order to guarantee this, the gain-modulation mechanism implemented by gamma has to act specifically on the subset of synaptic inputs that are attentionally selected, and not on the overall pooled synaptic input to a neuron. On this ground, gamma should be able to selectively amplify synaptic inputs corresponding to a specific stimulus, on top of not altering the neuronal tuning properties, which is already implied in the definition of multiplicative input gain modulation.

Stemming from these considerations, the main topic of gamma-rhythmic gain modulation will be addressed in Chapter 2, trying to define if this modulation exists and surpasses the mere effects of an additive kind of modulation, towards a multiplicative one. On the other hand, Chapter 2 will try to assess if the model imposed by gamma modulation corresponds to an input or an output gain. It will not be possible to elucidate all aspects and predictions highlighted in the above paragraph in the course of the current dissertation, for example, input selectivity of the gain modulation will not be tested (but more considerations on this topic will follow in Chapter 4).

Visual area V1

The area we chose to investigate gamma band activity and the neuronal spiking activity in the form of continuous MUA is the primary visual area V1 of NHP. V1 is particularly suitable to address these topics, because it shows prominent gamma-band activation for the majority of the visual stimuli, as it was described in the previous paragraph about gamma-band oscillatory activity, and it is also one of the areas where basic characteristics of neuronal response and gain modulation to stimuli were studied. V1 is at the basis of the cortical visual hierarchy in the mammalian brain, and it is the first processing station after retina and the lateral geniculate nucleus (LGN) of the thalamus, where complex computations about

the visual stimuli are performed (Priebe and Ferster 2012). This means that information that is relayed non-specifically by the retina and LGN, is organized according to selective features like edges and orientations (Priebe and Ferster 2012). The basic computation attributed to V1 is, in fact, to recognize oriented edges, and this represents the first basic step towards object segregation and recognition (Tschechne and Neumann 2014, Peter 2020). V1 is also sensitive to color information: based on these specific characteristics the stimulation paradigms that will be presented in Chapters 2 and 3, namely an oriented bar on a colored background, was defined.

Structure and function of V1

V1 is organized as a retinotopic map of the visual field (Tootell, Hadjikhani et al. 1998, Blasdel and Campbell 2001) so that RFs of neurons responding to spatially neighboring parts of the visual field are positioned close by in V1. RFs of neurons in V1 are small compared to higher visual processing areas, and represent the visual scene with a level of detail that decreases with eccentricity, i.e. when deviating away from the fovea, the center of fixation (Harvey and Dumoulin 2011).

On a histological level, the organization of V1 in NHP is based on the existence of functional columns (Sincich and Horton 2005). V1 is organized in columns of neurons with specialized function that span the thickness of the cortex until the white matter (Hubel and Wiesel 1968, Hubel and Wiesel 1979). Two prominent selectivities of columns of neurons in V1 are ocular dominance and orientation. Ocular-dominance columns receive information from specific layers of the LGN conveying inputs that are segregated for the right eye and the left eye. This way, segregation is maintained to the input into area V1. On the other hand, orientation selective columns are organized so to respond to specific oriented contours. (Kandel, Koester et al. 2021). Besides the columnar organization, another structural feature of V1 is that of being organized into blobs and inter-blobs (Kandel, Koester et al. 2021). Initially, it was thought that blobs responded specifically to color information, while the orientation selective neurons were to be found in the inter-blobs (Livingstone and Hubel 1988). More recent studies proved instead that both blobs and inter-blobs respond to color information (Wachtler, Sejnowski et al. 2003). A scheme of this organization is presented in Fig1.3A.

V1 has typically been referred to as striate cortex, due to the clear organization of its structure in six layers (Hubel and Wiesel 1968), with a layer 4 that is visible to the naked eye as “stria Gennari”. The layers, or laminae have been described for their specialized functions from the outermost, layer one (L1), to the innermost, layer

six (L6). L4 represents the preferential input layer to V1 with connections arriving from LGN (Solomon 2021). Layer L4 projects forward connections to L2 and L3, which represent the main output layers to higher visual areas. L2 and L3 also represent the preferential layer for gamma-band activity generation, together with a subset of L4, L4B (Vinck and Bosman 2016), since they not only receive input from L4, but also present an extensive network of lateral and recurrent connections, perfect network substrate for the generation of such a rhythm, and also project further to upper cortical areas, supporting the role of feedforward transmission of information to which gamma is traditionally associated (Bosman, Schoffelen et al. 2012, van Kerkoerle, Self et al. 2014, Bastos, Vezoli et al. 2015, Michalareas, Vezoli et al. 2016). Some of the input information from the LGN reaches L5 and L6 as well, layers that are reached by top-down feedback connections from L2 and L3, project than back to the LGN, and are responsible for communication with the motor system (Kandel, Koester et al. 2021). The L1 mostly contains dendritic processes serving as horizontal connections and interneurons. This information is summarized in Fig1.3B.

On a cellular level, V1 is mainly composed of two functional cellular types, the simple and the complex cells, whose characteristics explain the emergence of the basic computation in V1, the encoding of oriented edges. The simple cells present the typical ON/OFF RF, responding to light in the center of the RF, and dropping quickly the response when stimulated in the surrounding area (Priebe and Ferster 2012). Simple cells recognize end encode spatial changes in local illumination which might indicate the presence of a boundary, and this makes it possible to encode for the edge of an object. The integration of the information encoded by several simple cells is performed by a complex cell, which responds to oriented light information, and puts together several pieces of the receptive field presenting the indication of an edge and characterized by the same orientation selectivity. Complex cells are capable of summating information from simple cells with feature invariance, defining oriented edges (Hubel and Wiesel 1962, Hubel and Wiesel 1968, Priebe and Ferster 2012).

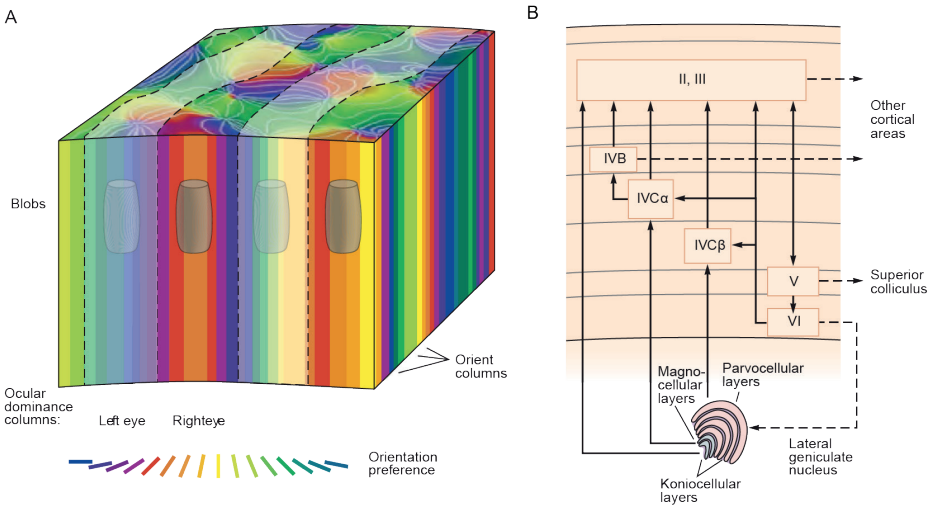

Fig. 1.3. Structural architecture of V1 layers. (*A*) Histological organization of a patch of V1 cortical area. The tissue has a columnar organization of ocular-dominance and orientation specific columns. Oriented columns spanning the 360 degrees of possible orientations are organized in a hyper-column. Blobs and inter-blobs respond to orientation and color information. (*B*) The circuitry between V1 layers and other visual areas is summarized. V1 mainly receives input from LGN, and input is distributed in L4 and L5/L6. L2 and L3 receive input from L4 and represent the main output layers to higher visual processing areas, while L5 and L6 receive top-down feedback connections form L2 and 3 and are the main output layers feeding back into LGN and communicating with the motor system. L1 mainly contains dendritic processes acting as horizontal connections. Figure adapted from (Kandel, Koester et al. 2021) chapter 21

Stimulus repetition and plasticity

Both gamma-band rhythmic activity and neuronal spiking activity were assessed in a quite consistent body of literature in relation to repeated presentations of a stimulus. The interest in studying the response of the brain to a repeated identical input stems from two levels of observation about the natural process of vision. First of all, on a stimulus level, any visual scene constituting the input to the visual processing system, contains repeated information. In each landscape or scene presented to the eye, some features like contours, oriented edges or colors, are represented a plethora of times (Torralba and Oliva 2003). These statistical regularities are the building blocks for the composition of an image. On a behavioral level, on the other hand, it is also commonly observed that in the scanning of a visual scene, the eyes tend to revisit the same image locations or objects multiple times (Wilming, Harst et al. 2013), so that, again, the repeated input to the visual system represents a phenomenon of importance for the processing of visual information. The information reaching the brain will be, as a consequence,

redundant, and it is of interest to understand how the brain makes use of these regularities and optimizes its computation in relation to it.

Many studies have addressed the topic of stimulus repetition reporting interesting findings. Early fMRI studies indicated that blood oxygen level dependent (BOLD) signals decreased without affecting behavioral performance, or even with an improvement of it (Grill-Spector and Malach 2001). The effect of stimulus repetition was also initially reported to increase synchronization over the lower frequency bands, like alpha and beta (Gilbert, Gotts et al. 2010, Gilbert and Li 2013). Enhancement of oscillatory activity in the alpha-beta band in response to repeated stimuli can be linked to a top-down information flow (von Stein and Sarnthein 2000), as confirmed by studies associating lower frequency bands with feedback receiving layers in V1 (Bastos, Vezoli et al. 2015), and possibly cover the functional meaning of signalling the increased predictability of the repeated stimuli. Another study showed that stimulus repetition not only increased the strength of gamma activity, a rhythm generally associated with feedforward signaling (Bastos, Vezoli et al. 2015), but also increased gamma synchronization between areas V1 and V4 of the monkey cortex (Brunet, Bosman et al. 2014). Later studies confirmed and reinforced the findings of a decrease in firing rate and increase in gamma band synchronization in response to visual stimuli, adding that there's a specificity to this effect, since each repeated stimulus independently shows signs of repetition-dependent change in the neuronal response to it (Stauch, Peter et al. 2020, Peter, Stauch et al. 2021, Psarou, Parto-Dezfouli et al. 2025). This evidence taken together supported the hypothesis that repetition suppression of the neuronal spiking in combination with higher power in oscillatory activity represents a mechanism to increase the efficiency of brain computation by increasing the temporal precision of the lower spike number, so that behavioral performance is not affected (Grill-Spector, Henson et al. 2006, Gotts, Chow et al. 2012).

(Stauch, Peter et al. 2020) described a cellular mechanism to explain how gamma power increase comes about in conjunction with decrease in spike rates. Gamma band activity is very likely to intervene in processes of plasticity like the Hebbian spike-time-dependent plasticity (STDP) (Caporale and Dan 2008), because STDP is critically dependent on the temporal relationship between two neurons' spiking, and the gamma cycles not only provides a frame for spikes' alignment that makes them more efficient, but it also works at a time scale that perfectly matches the times necessary for synaptic integration (Fries 2009, Singer 2021). STDP is well known for being able to change the strength of a synapse by reinforcing it, when the pre-synaptic neuron fires before the post-synaptic one, or weakening it, in the opposite

case. It is possible therefore, that gamma-activated processes of STDP influenced the reciprocal connection weight and consequently pattern of activity of neurons linked together in the generation of a gamma cycle in the context of stimulus repetition. If we assume that the gamma cycle is generated by a characteristic sequence of excitation followed by inhibition after a small delay, (E - I), other less driven excitatory neurons (*e*) connected locally will fire only after the E-I primary cycle, if they can fire at all. It is possible that the E-I connection will be reinforced due to the appropriate temporal spiking sequence of the two neurons, while the connection with the other *e* neurons of the circuit will be weakened, because they fire in delay, according to the rules of the STDP. This could lead to a substantial increase of the strength of oscillatory activity in the gamma range, together with a concomitant decrease of the independent neuronal spiking in the local network. This model explains a potential mechanism for the effects described above.

This abundance of studies addressing the topic of stimulus repetition effects investigated the most various group of stimuli type, and reported consistently the same results when describing the behavior of gamma-band activity and MUA. From here, the interest arose in verifying if a similar pattern of behavior for gamma-band and MUA could be found in the context of the repetition of the specific stimuli that were used for the task designed to address the abovementioned topic of gamma rhythmic gain modulation that will be presented in Chapter 2. The results for this study will be presented in Chapter 3.

Finally, a clarifying distinction has to be made between stimulus repetition and the more general phenomenon of adaptation. Repetition refers to a type of stimulation paradigm where the same visual (in the case of the current work) stimulus is repeated multiple times, and the interest is in observing and describing the brain response to it. Adaptation on the other hand, refers to the observed phenomenon of reduction of neuronal responses over time as a consequence of prolonged presentation of a stimulus (Weber and Fairhall 2019). Repetition is a characteristic of the stimulation paradigm, while adaptation is a phenomenon of the neural activity. This is the meaning with which these two terms will be used throughout the course of this dissertation. It is not to be excluded that adaptation processes intervene in determining the reduction in firing rate usually described in stimulus repetition paradigm based studies.

Thesis outline

In light of the considerations presented above, this thesis will investigate two main scientific questions:

1. How does gamma rhythmic activity modulate the gain of the MUA response to a visual stimulus?
2. How do gamma band oscillatory activity and MUA behave in the context of non-classical stimuli repetition?

Questions 1 will be addressed in Chapter 2 by revisiting a previous study (Ni, Wunderle et al. 2016), with a new stimulation paradigm and new analysis methods. The study will assess the effect of gamma-band oscillation phase on the MUA gain modulation in response to a visual stimulus. The working hypothesis of the study is that gamma imposes a multiplicative gain modulatory effect, i.e. that gamma is capable of changing the neurons' sensitivity to a stimulus. The multiplicative nature of this gain modulation effect entails that the MUA response to the presentation of a stimulus cannot be described as a mere sum of a constant stimulus response added on top of gamma phases of higher or lower excitability determined by the ongoing gamma oscillatory activity. The study will also characterise the modulation imposed by the gamma rhythm on MUA by identifying the model, input or output gain, according to which gamma is modulating the MUA gain, and assess the absolute phase of gamma modulation.

Question 2 will be addressed in Chapter 3 and will also revisit previous findings, namely that stimulus repetition typically leads to V1 firing rates to decrease and gamma activity to increase. The idea to re-investigate the behavior of gamma-band oscillatory activity and MUA in relation to stimulus repetition stemmed from the abundance of trials collected during the recordings, and from the realization that the visual stimuli presented in the paradigm used in Chapter 2 were different from the stimuli generally used in other repetition studies, and had not yet been studied in relation to the repetition effect. Classical studies about stimulus repetition consistently reported the same results for gamma-oscillatory activity and MUA (Brunet, Bosman et al. 2014, Peter, Stauch et al. 2021, Stauch, Peter et al. 2021, Psarou, Parto-Dezfouli et al. 2025), so the study aims to assess if the classical effects could be found for the novel set of visual stimuli used in Chapter 2.

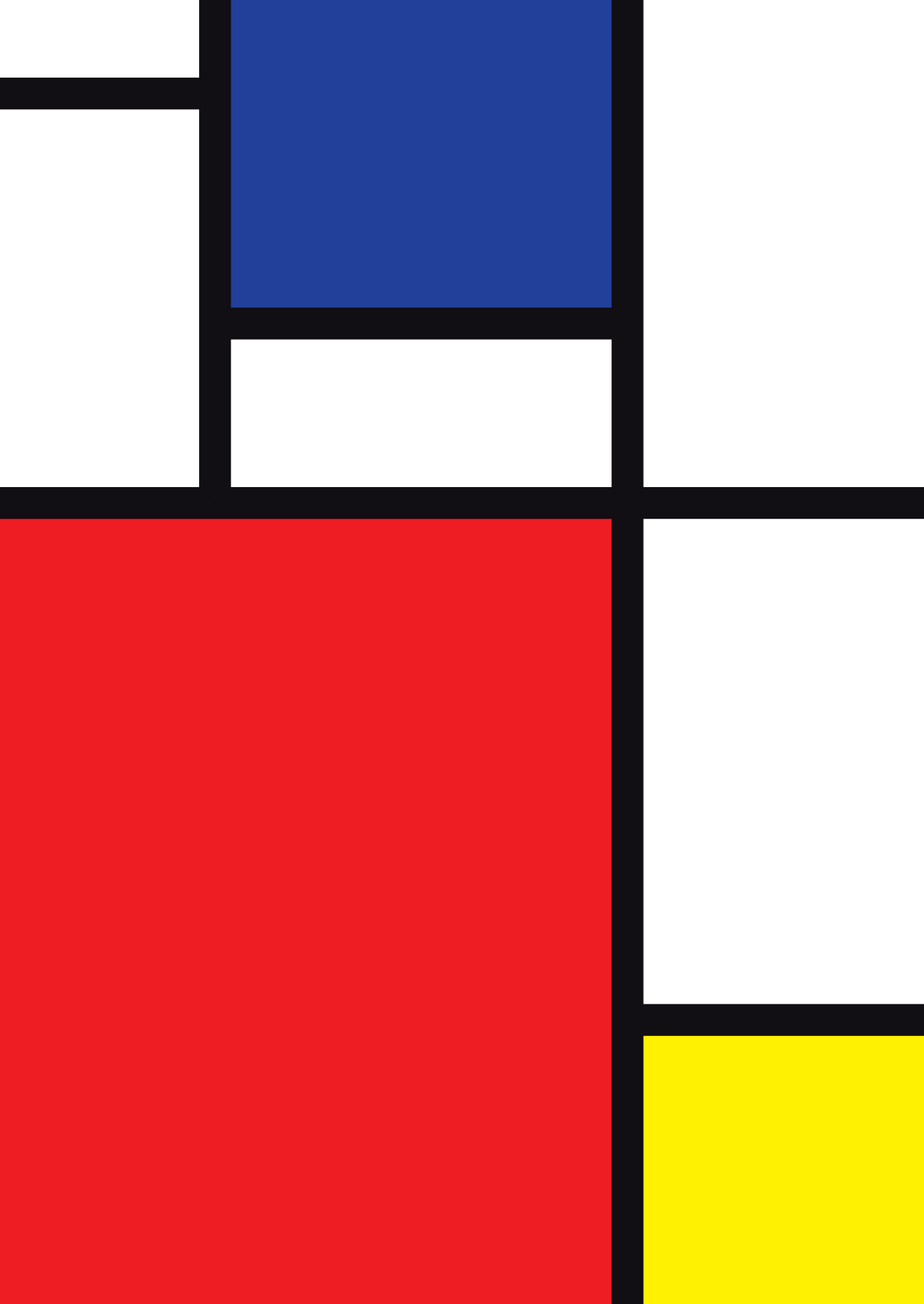

Chapter 2

Gamma rhythmic gain modulation: new perspectives

In preparation as: Martina Pandinelli, Tim Naeher, Eleni Psarou, Iris Grothe, Pascal Fries. Gamma rhythmic gain modulation: new perspectives.

Abstract

Oscillatory activity in the gamma band (30–80 Hz) is a widespread and functionally significant phenomenon known to synchronize neuronal spike timing, promoting coincident synaptic input to downstream targets and enhancing the efficacy of communication. The gamma rhythm was demonstrated to rhythmically modulate the neuronal gain in response to a stimulus change, and behavioral reaction times. This supports the Communication-through-Coherence (CTC) hypothesis, which proposes that gamma phase gates input strength, enhancing the effective connectivity of inputs aligned with high-gain phases. However, the absolute phase of this gamma modulation still remains unclear, and it has also not yet been clarified whether this phase-dependent gain modulation reflects input gain (increased sensitivity) or output gain (scaled responses) modulation. To address these questions, we investigated gamma-phasic modulations of visual responses in awake macaque V1, using a fixation task. We induced sustained gamma activity with a uniform red background, and then presented a black bar probe stimulus at varying contrasts to evoke a multi-unit activity (MUA) response and assess the applicable gain modulation model. Our results show that the LFP gamma phase rhythmically modulates MUA responses, with a consistent preferred phase between –30° and 30°. Significant modulations were observed across many frequency bands, including the alpha, beta and gamma band and even at higher frequencies. Mid-contrast stimuli showed stronger modulation, consistent with an input gain model.

Introduction

Oscillatory activity in the gamma-band range (30 – 80 Hz) is a rhythmic event widespread across many brain areas (Fries 2009, Buzsáki and Wang 2012), and has recently been described as a network activity pattern capable of serving as functional operational unit of local circuits. This allows the expression of many different cognitive functions, according to the brain state and the specific neuronal circuitry from which gamma rhythm originates (Fernandez-Ruiz, Sirota et al. 2023). At a local circuit level, it has already been long known that gamma activity synchronizes spike output and can thereby lead to coincident inputs at postsynaptic neurons, which can increase the impact of the synaptic output of the presynaptic neurones (Salinas and Sejnowski 2000, Salinas and Sejnowski 2001, Azouz and Gray 2003, Azouz and Gray 2008). Moreover, in local circuits, gamma also entails rhythmic synchronization of local inhibitory inputs, which is expected to rhythmically modulate the response to excitatory input, that is, to rhythmically modulate input gain (Fries 2009).

Experimental evidence demonstrated gamma-rhythmic gain modulation in awake behaving non-human primate (NHP) area V4, with an experiment that elicited gamma activation and then probed the modulatory impact of its phase on MUA response to the change of a visual stimulus (Ni, Wunderle et al. 2016). Specifically, a grating was presented to induce sustained spiking and gamma activity. When the grating underwent a change in colour at an unpredictable time, this produced synaptic inputs to V4 at random phases of the ongoing gamma. Those gamma phases modulated the subsequent spike response to the stimulus change. That is: gamma rhythmically modulated the gain. Intriguingly, gamma also rhythmically modulated reaction times (RTs); and the gamma phases leading to the shortest RTs were close to the gamma phases leading to the strongest spike responses. This suggests that the modulation exerted by gamma phase on MUA is a phenomenon whose consequences are not restricted to the level of local neuronal communication, but that has a direct impact on the behavioural outcome of the cognitive process in question. Gamma phase not only modulates neuronal gain, but also has a functional importance.

Gamma-phasic gain modulation is a central tenet of the Communication-through-Coherence (CTC) hypothesis (Fries 2005, Fries 2015). CTC posits that local rhythmic neuronal activity rhythmically modulates gain, and inputs that consistently arrive at high-gain phases will have a high input gain, whereas inputs that arrive at random phases will have a lower input gain. Therefore, depending on the phase

at their arrival, stimuli might benefit from an enhanced representation at a neuronal level, and consequently an enhanced effective connectivity, and this might confer them an advantage in progressing in the cortical processing hierarchy (Womelsdorf, Schoffelen et al. 2007, Ni, Wunderle et al. 2016). This was hypothesized to be a mechanism behind the selective routing of attended information in attentional processes. Attention enhances the effective connectivity between areas V2 and V4 for the bottom-up inputs conveying the attended stimulus (Reynolds, Chelazzi et al. 1999). In addition, when two visual stimuli induce two local gamma rhythms in awake macaque V1, and one of them is attended, then the gamma driven by this attended stimulus, the "attended gamma", manages to entrain and synchronize V4, whereas the "non-attended gamma" does not. Thereby, the spikes from the attended V1 group will arrive in V4 at consistent gamma phases (Bosman, Schoffelen et al. 2012, Grothe, Neitzel et al. 2012). Another study showed that the phase relation at which V1 and V4 synchronize is actually optimal for leading to short reaction times as well (Rohenkohl, Bosman et al. 2018). Finally, a most recent study proved the concept that gamma phase synchronization is causal for effective and selective information processing (Drebitz, Rausch et al. 2025).

One prediction stemming from these experimental evidences is that the rhythmic gain modulation in the postsynaptic neuronal group is a rhythmic modulation of the gain of synaptic inputs, rather than the spike outputs. These are two alternative forms of gain modulation: Input gain, also referred to as contrast gain modulation, because it resembles the increase of contrast in the input to the postsynaptic neuronal group; and output gain, also referred to as response gain modulation, because it scales the response of the postsynaptic neuronal group (Ferguson and Cardin 2020). When neuronal responses are plotted as a function of stimulus contrast or stimulus strength, an input-gain modulation corresponds to a leftward shift of the neuronal response curve, such that the sensitivity of the neurons to the same stimulus is enhanced; by contrast a response gain modulation corresponds to a scaling of the responses that is similarly strong for all stimulus strengths, such that the strongest absolute response increases occur for the strongest stimuli (Ferguson and Cardin 2020).

A previous study had directly tested whether selective visual attention modulates neuronal output gain or input gain in NHP V4 (Reynolds, Pasternak et al. 2000). In this study, bar shaped patches of black and white gratings of varying contrast were presented, and cued so that the monkey could perform an attentional selection task. The neuronal responses in the attend-in conditions were found to be more strongly modulated for lower and mid-level contrast stimuli, rather than high contrast ones. This finding is coherent with an input gain modulation model (Reynolds, Pasternak et

al. 2000). Here, we aimed to test whether the rhythmic gain modulation generated by local rhythmic activity was a modulation of input or output gain.

Furthermore, we aimed to test whether the phases of maximal and minimal gain were aligned across neurons. The latter hypothesis could not be tested in (Ni, Wunderle et al. 2016), because the gamma rhythmic gain modulation was examined in V4, and the stimulus response latencies were long and scattered, and moreover, they were triggered by small changes in a strong pre-existing grating stimulus.

For these reasons, here we tested the model of gamma-rhythmic gain modulation in awake macaque V1, where response latencies are shorter, to verify the modulation imposed by gamma-band activity onto MUA in response to the presentation of a stimulus. We designed a visual fixation task where we used a uniform red background to induce an ongoing strong gamma activation. We then tested the effect of the ongoing gamma oscillatory activity with a stronger probe stimulus to evoke the MUA response. The probe stimulus assumed the shape of a simple black bar, to match the feature preference of the area under investigation, V1, and was also presented in a range of contrasts in order to be able to test the type of gain modulation (input or output).

Results

Conceptualization of the study and task design

As gamma-band activity in V1 is characteristically oscillatory, we decided to test the influence of gamma-rhythmic phase on MUA in response to a visual stimulus (Fig. 2.1A). To this end, we designed a passive visual fixation task as shown in Fig.2.1B. After an initial Inter Trial Interval (ITI) of 0.7 s, the monkey was required to fixate a central fixation dot and to keep fixation for the entire duration of the trial to obtain a reward. After fixation was attained, a red coloured full-screen background (FSB) was presented in 90% of the trials, to induce strong gamma activity (Shirhatti and Ray 2018, Peter, Uran et al. 2019, Stauch, Peter et al. 2022), while the FSB was kept grey in the remaining 10% of the trials, as a control condition. In both the red and grey FSB condition, after 1.40 to 1.65 s had elapsed, a visual stimulus in the shape of a small black bar was flashed on the screen for 0.2 s at a random time, inside the RF. If fixation was maintained throughout, a reward was subsequently delivered.

The black bar presented on top of the FSB was oriented to evoke maximal MUA responses (see Methods), and its presentation served to test the effect of gamma

phase on the MUA response to the bar itself. For this reason, the bar was presented at a variable time after the onset of the FSB, so that the phase of the gamma cycle at which the stimulus would hit V1 could be random and unpredictable at each trial. We decided to test gamma phase with a black bar stimulus, first of all to adapt the stimulation to the preference of the area under investigation, V1, that is tuned to simple visual features like contours and edges. In addition, we decided to use a simple bar stimulus to remove any potential phase confound effect that could arise from the use of a grating, a stimulus that entails a spatial frequency of its own, and could therefore entrain the gamma rhythm, so that the phase analysis that we intend to carry out could be biased. Fig.2.1C shows a grand average over trials and recording sites of the LFP power in the grey and red FSB time period, over a time window of 0.5 s before the presentation of the black bar stimulus. A clear gamma peak is present in the red FSB condition, and a smaller peak, in a lower gamma-frequency range is observable for the grey FSB condition. The exact peak of gamma-band activity for the later analyses was extracted for both red and grey FSB conditions separately per each recording site by using the fitting-oscillations-and-one-over-f (FOOOF) method (Donoghue, Haller et al. 2020).

The black bar stimulus was presented always at full contrast in the grey FSB condition, while it could assume 6 different contrast levels in the red FSB condition, ranging from 5% to 100% (see Methods, and Fig.2.1B, right hand side panel for a visual representation of how the bar stimulus appeared on the screen during the experiment). This served us to verify if gamma phase modulated the MUA response according to an input- or an output-gain model ((Reynolds, Pasternak et al. 2000), see below). Fig.2.1D presents the grand-average MUA responses, averaged over recording sites and trials, to the black bar presentation, separately for each of the contrast conditions in the red FSB condition, and for the grey FSB condition. As expected, among the red-FSB conditions, the MUA response grows according to stimulus contrast. The strongest overall MUA response occurred for the grey FSB condition.

The gamma rhythm imposes an ongoing modulation on MUA

We first demonstrated that the gamma peak observed in the LFP power spectrum (Fig.2.1C) represented in fact an oscillatory pattern of MUA. To this end, we tested whether gamma activity modulated MUA before black bar stimulus presentation, i.e. we checked if we could demonstrate the existence of an Ongoing Modulation (OM) imposed by gamma on the MUA. To this end, we selected a 0.15 s time period from the red FSB condition, right before black bar stimulus presentation (Fig. 2.2A), and we extracted the phase at the peak gamma frequency for this time period. Then, for each point of the phase time series, and each trial, we binned the

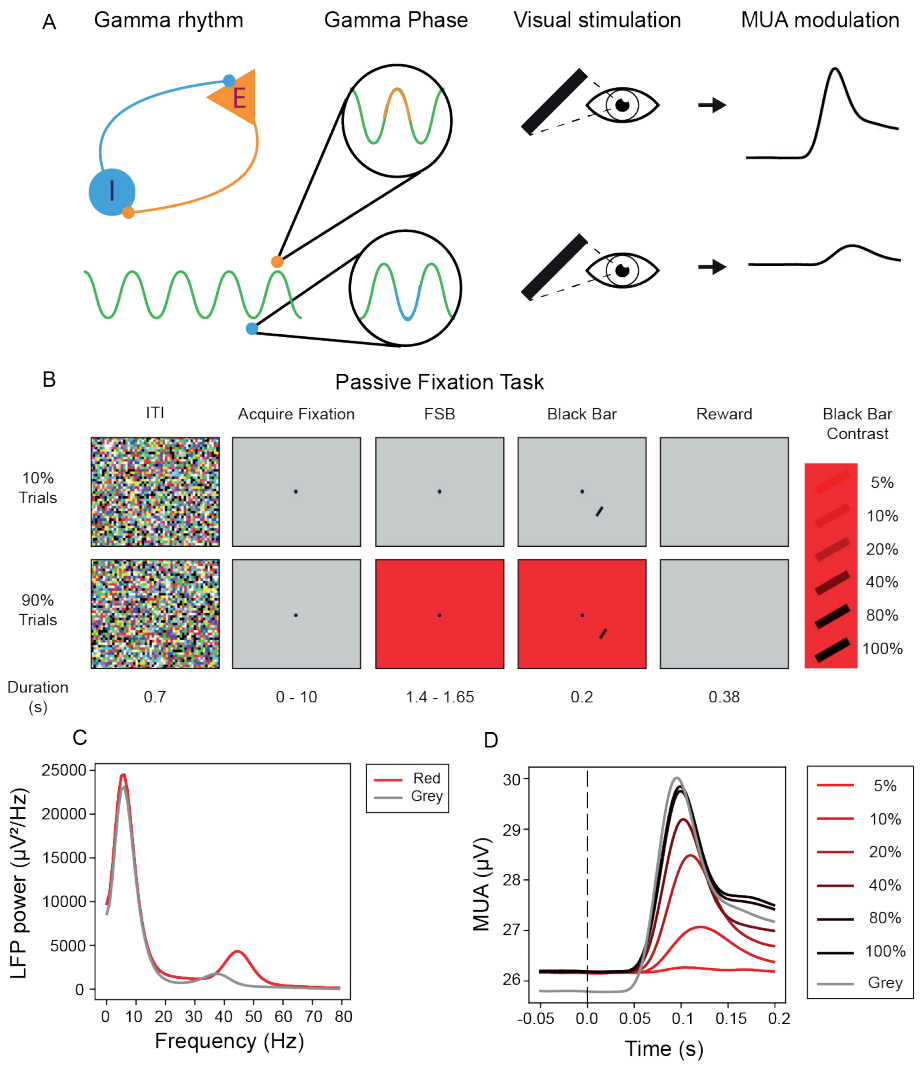

Fig. 2.1. Conceptualization of the study, task paradigm and stimuli, and stimulus induced LFP power and MUA responses. (*A*) Schematic illustration of the hypothesized mechanism underlying gamma-rhythmic gain modulation. Gamma oscillatory activity originates via a characteristic sequence of excitation and inhibition. Its phase is thought to rhythmically modulate MUA response to the presentation of a stimulus. (*B*) Schematic representation of the task used to test gamma-phasic MUA gain modulation. The upper row represents the grey condition, the lower row represents the red condition. The side panel shows the different visual stimuli that can be presented in each trial. (*C*) Raw power spectrum for the last 0.5 s of the FSB time period, before bar stimulus presentation, averaged over trials and recording sites. (*D*) MUA response to stimulus presentation averaged over trials and recording sites in the Black Bar time window, for each stimulation condition. Raw MUA is expressed, after convolution with a Gaussian kernel (SD=12.5ms).

corresponding MUA values into six phase bins, according to the extracted phase values. The phase bins were defined according to the Ni, Wunderle et al. (2016) paper, as bins containing the same number of trials, and centered respectively at -150˚, - 30˚, -90˚, 30˚, 90˚, 150˚ degrees. We fitted a cosine function to the average MUA spike rate value of the six phase bins, in order to assess periodicity, and tested the resulting amplitude against shuffled controls. Gamma significantly modulated MUA in the FSB period (Fig.2.2B, see methods).

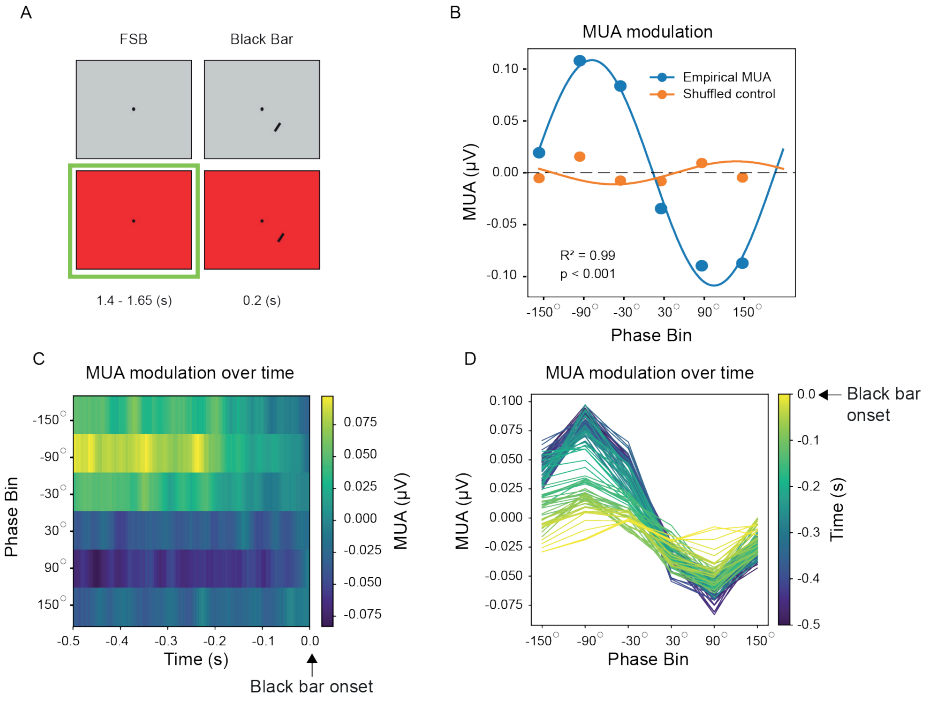

Fig. 2.2. Gamma-rhythmic ongoing oscillatory modulation of MUA spike rates. (*A*) The green square shows that the red condition FSB before the presentation of the black bar was the time window selected to calculate ongoing oscillatory modulation imposed by the gamma rhythm. The gamma modulation is calculated for the last 0.15 s of the red condition only. (*B*) Empirical gamma-modulated MUA (blue dots and line), against shuffled control (orange dots and line). Goodness of cosine fit is expressed by R^2 metric for the blue curve. P-value for the statistical test is reported in the figure, from a non-parametric randomization test based on random pairing of MUA spike rate with gamma phase bin during the red FSB period. The figure presents one exemplary recording session. Each of the dots represents the average MUA firing rate over trials, for each phase bin. (*C*) Evolution of the gamma-phasic modulatory effect on MUA over time, averaged over all trials and recording sites, for each phase bin. (*D*) Evolution of the gamma-phasic modulatory effect on MUA over time, averaged over all trials, and recording sites.

The FSB time window is long, ranging from 1.4 to 1.65 s, and despite the fact that LFP gamma activity evoked by the red FSB stayed strong and consistent throughout the whole time window before the presentation of the black bar (Suppl. Fig. 2.2B), we reasoned that there could be a decay in the strength of the OM imposed by gamma on the MUA during the course of time. Therefore, we assessed the behavior of the OM across the time windows preceding the black bar appearance. Fig.2.2C, and Fig. 2.2D show the decay of OM modulation strength on MUA, as a function of time relative to black-bar onset. These results informed some of the considerations for the following analyses (see below, estimation of sTP).

Gamma rhythm: Additive or Multiplicative Modulation? A schematic overview

We draw here a schematic overview of the reasoning behind our following analysis. The rationale follows closely the one described in Ni, Wunderle et al. (2016).

We have demonstrated the existence of an OM imposed by gamma on the MUA before stimulus presentation. When the system is presented with the black bar stimulus at a random phase of the FSB-induced gamma, the response could be such that it can be described in terms of an Additive Modulation (AM, Fig. 2.3A), or a Multiplicative Modulation (MM, Fig. 2.3B). In case of an AM, the MUA response elicited by the black bar corresponds to a constant response (Fig.2.3A, lower panel), simply riding on top of the OM that is imposed by gamma. The constant response adds up – from which the name of this modulation – onto phases of higher or lower excitability of the ongoing modulated MUA (Fig.2.3A upper panel). On the other hand, what we aim to find evidence for, if possible, is that the modulation imposed by gamma on the MUA is not as trivial as an AM, but instead corresponds to an actual modulation of the MUA response, an MM, that goes beyond an AM as an emergent property of the system (Fig.2.3B). This means that the MUA response to the black bar is not merely a constant response riding on phases of lower or higher excitability, but rather that the response itself is actually modulated, becoming higher or lower according to the incremental or detrimental phase of the gamma cycle.

If the MM is to be found in our data, this can be demonstrated beyond any doubt by subtracting from the empirically recorded data an estimate of the AM, calculated by adding a constant MUA response to a visual stimulus (an average of the MUA response to the black bar across trials) on top of the OM activity. If there is a remaining component after this operation, this demonstrates that the MUA response is actually modulated multiplicatively (Fig.2.3C).

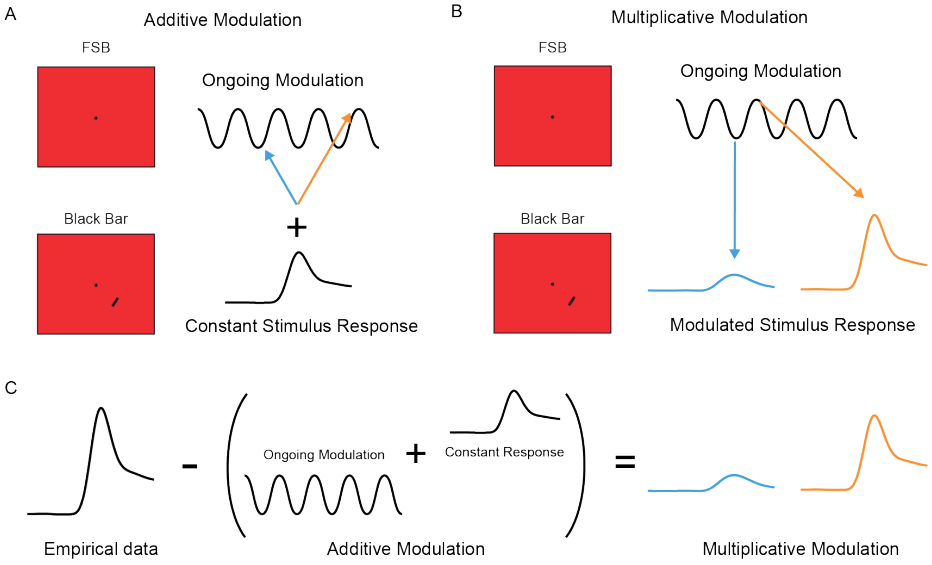

Fig. 2.3. Schematic illustration of Additive and Multiplicative modulation components of the signal, and schematic overview of the analysis rationale to extract Multiplicative modulation component from empirical data. (*A*) Additive Modulation: a constant MUA response to a visual stimulus rides on top of, i.e., is *added* onto the ongoing modulation imposed by the gamma rhythm. The constant response to the black bar stimulus (bottom panel of the image) will summate on top of phases of lower (blue arrow) or higher (orange arrow) excitability of the gamma rhythm (top panel of the image). The top and bottom panels on the left of the image present a schematic of the time period of reference, FSB or Black Bar time windows. (*B*) Multiplicative modulation: phases of higher or lower excitability of the gamma rhythm modulate the MUA response to a visual stimulus, increasing or dampening the neuronal response. Stimuli reaching the brain at phases of lower excitability of the gamma cycle (top panel, blue arrow) correspond to lower MUA responses to the black bar stimulus (bottom panel, blue trace). Stimuli that are, instead, reaching the brain at phases of higher excitability of the gamma cycle (top panel, orange arrow), correspond to higher MUA responses to the black bar stimulus (bottom panel, orange trace). Left-side top and bottom panels of the figure as explained before in *A*. (*C*) From the empirical data (left side panel) we subtract an estimate of the additive modulation (central panel) to find the multiplicative modulation (right panel). The estimate of the additive modulation is calculated by mathematically adding a constant MUA response, as the average over all trials belonging to the same condition, onto the ongoing modulated MUA response per each phase bin.

The gamma rhythm imposes a multiplicative modulation on the MUA response

To assess what kind of influence the phase of gamma oscillation had on the MUA (AM or MM), we first extracted the exact time point (TP) of input arrival in V1, i.e., the time sample at which the ERP response began in the LFP trace (Fig.2.4A). We estimated phases at gamma peak frequency for each trial and recording site at TP with a custom phase extraction algorithm based on Patel, Psarou et al. (2024)

(see methods), and we grouped the trials into 6 non-overlapping phase bins (Fig.2.4C), according to phase value, as explained above. We then grouped corresponding MUA responses into the respective bins, and averaged over trials to obtain one empirical MUA response value per each phase bin (Fig.2.4D, blue trace, and see methods for MUA trace averaging procedure details). To obtain an estimate of the AM, we repeated the phase extraction at gamma peak frequency, but this time not at TP, but defining a surrogate time point (sTP), 0.15 s before presentation of the black bar stimulus (Fig. 2.4B). sTP was located at – 0.15 s, because this allowed to calculate the AM for the duration of a typical MUA response to the bar, but also close enough in time to the MUA response to have a good estimate of the OM, which was shown to decrease in time (Fig.2.2C, D), so that we would not overestimate this modulatory component. Once again, we binned phases in 6 bins, grouped corresponding MUA responses into the respective bins, and averaged over trials to obtain the estimate of the OM (see Fig.2.3C and methods as a reference). To this estimate, we added the estimate of the Constant Response (CR) to black bar stimulus presentation to obtain our estimate of AM (Fig.2.4D, red trace), for each phase bin. We proceeded to subtract the estimate of AM from the Empirical MUA response, in order to define the MM component in our data (Fig.2.4E). We quantified the periodicity of the MM by fitting a cosine function, and repeated the procedure for each recording site and contrast condition (Fig. 2.5B).

In order to statistically test the MM, we extracted the amplitude of the cosine modulation for each recording site, the Modulation Depth (MD, Fig. 2.4E), and tested it across the whole frequency spectrum from 4 to 80 Hz, against the Bias Estimate, a metric that estimated the positive bias inherent to the cosine fitting procedure without pre-determined phase (Fig. 2.5A, see Methods). Fig. 2.5A shows the MD and Bias Estimate spectra across frequencies per each contrast level, and presents the significant frequencies. We find that the MM is significant in the lower frequency range, corresponding to alpha-beta band, for all contrast conditions, while significance in the gamma range and high gamma range can be found for 20%, 40% and 80% contrast levels. The grey condition MM appears to be significant throughout the whole frequency spectrum. The statistics was ran per each recording session, given that the recording channels on the electrode were spaced by only 50 um, so we could assume that the signal picked up by each recording site during one session was highly correlated, and therefore we averaged over recording sites within each session. The statistics for each recording site as a unit of testing is presented in the supplementary material (Suppl. Fig. 2.3). After averaging across recording sites, we found that the absolute gamma phase leading to the strongest MM was between -30° and 30°, for all contrast conditions (Fig. 2.5B).

Since the strength of the lower frequency component in the power spectrum could have biased our phase estimation algorithm, and our results for the MD and bias estimate spectra, and also for the absolute phase estimation, we decided to repeat the analysis with pre-whitened data (Suppl. Fig. 2.4 A, B). The results were generally confirmed, even after pre-whitening of the data (Suppl. Fig. 2.4, C, D).

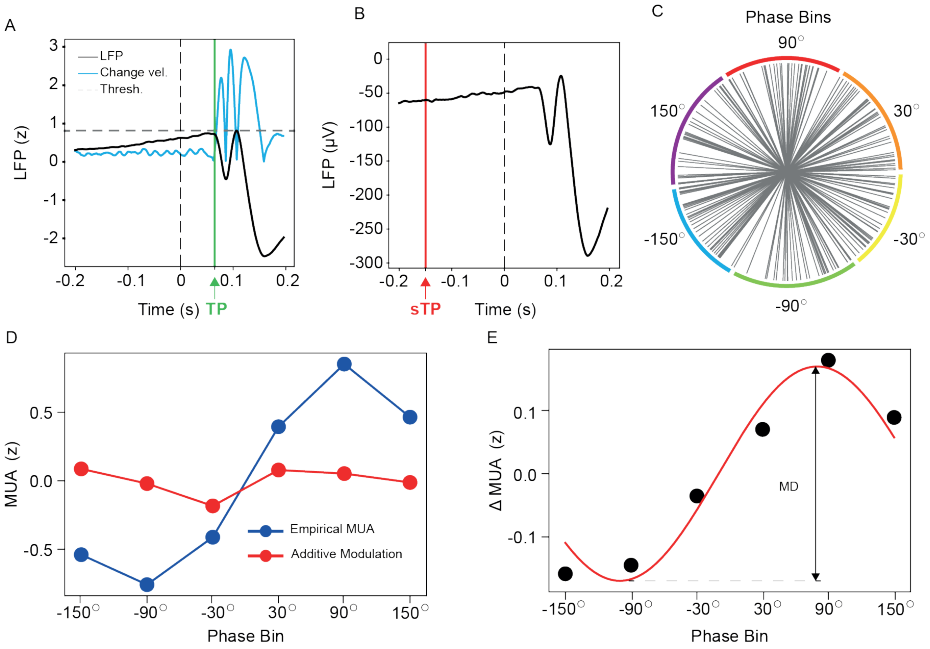

Fig. 2.4. Finding the multiplicative modulation in the empirical data. (*A*) The time point of input arrival in V1 (TP) is estimated by calculating the velocity of change of the event-related potential (ERP) and taking the first time sample for which the velocity of change surpasses 1.5 times the SD of the signal, after stimulus presentation. TP is used as the time marker where to perform phase extraction to organize the trials in phase bins. The figure presents one exemplary recording site. (*B*) The time point for phase extraction to estimate the additive component is defined as surrogate TP (sTP) and fixed at -0.15 s from the time of black-bar presentation on the screen. (*C*) Phase binning. Trials were binned into 6 non-overlapping phase bins, respectively centered at -150˚, -90˚, -30˚, 30˚, 90˚, 150˚ degrees. (*D*) Empirical and additive MUA activity. Each dot in the figure represents the average over trials of MUA responses per each phase bin; the figure presents results for one exemplary recording session. (*E*) Multiplicative modulation extracted after subtraction of the additive modulation from the empirical signal. A cosine function is fitted to the data points to quantify the size of the modulation. The figure presents one exemplary recording session.

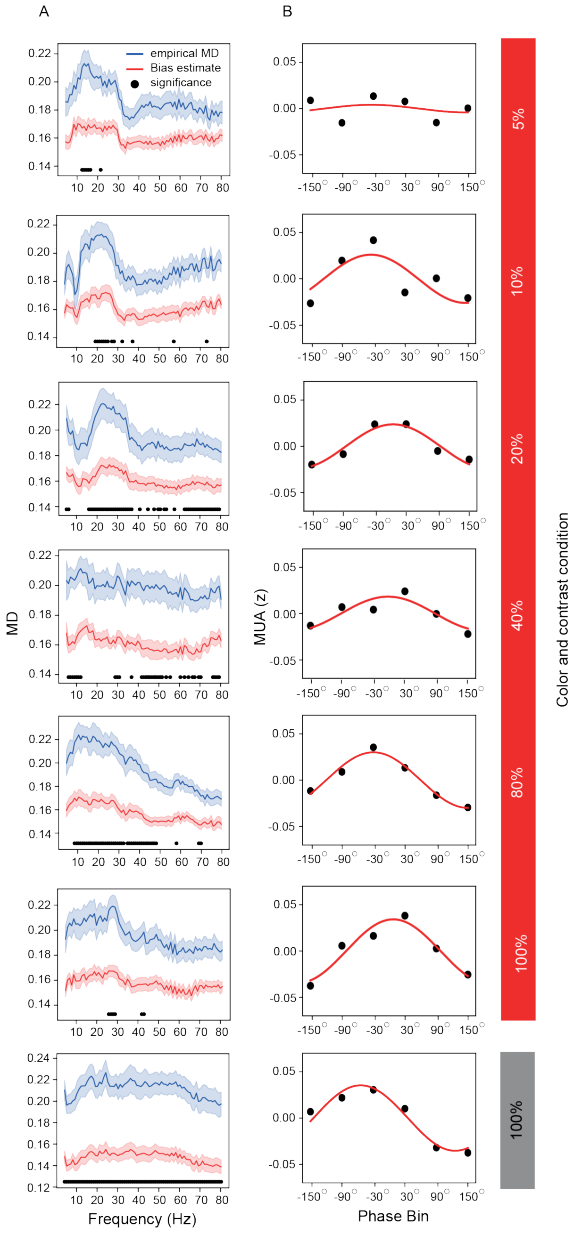

Fig. 2.5. Multiplicative modulation and statistical testing Method 1. (*A*) Statistical testing. Blue lines present the spectrum of the amplitude of the cosine modulation, Modulation Depth (MD), red lines present the spectrum of the Bias Estimate. Black dots represent frequencies for which the difference between the 2 is significant. The statistics is run considering one recording session as a unit of observation. (*B*) Multiplicative MUA modulation and fitted cosine function for each contrast level of the black bar visual stimulus. The results present the grand average over all recording sites. The lateral bar on the right-hand side indicates color condition of the FSB and contrast condition of the black-bar stimulus.

Finding the Multiplicative Modulation: an alternative method

We decided to assess the MM effect of gamma oscillation phase also with another method, alternative to the one described in (Ni, Wunderle et al. 2016) and presented above, to estimate the AM. For this second method, we took again the sTP, but estimated phases at the peak of gamma band, not only for the precise sTP time sample, but for the 0.15 s window of samples preceding the sTP (Fig. 2.6A). The AM was calculated for each of these time samples by taking a 0.15 s window after the time sample considered for each iteration. In this procedure, we made sure to not cross the threshold of the time 0, when the black bar was presented. Once the phase was extracted for each time sample, trial and recording site, we binned the phase values into 6 bins (Fig. 2.6B, C), and grouped corresponding MUA responses into the respective bins. With this procedure we expanded the data points at our disposal to calculate the OM before the presentation of the black bar. This resulted in an overall stronger OM component, because the amount of data points at our disposal for the average was higher, and therefore stronger overall AM once we added the estimate of the constant MUA response to the black bar. This method achieved a slightly overestimated AM, so that we could prove with more certainty the existence of an MM in our data. Once we obtained the new estimate of AM for each phase bin, we proceeded to subtract it from the Empirical data to find the new MM. We repeated the same statistical testing procedure described above to test the frequency specificity of MM effect, based on MD metric. We found that alpha-beta frequencies were again statistically significant for all contrasts tested. Contrasts from 20% to 100% and the grey condition showed a significant modulation for the gamma band and higher gamma band (Fig. 2.7A). Again, we tested the periodicity of the MM by fitting a cosine function to the data points we extracted per each phase bin, and repeated the procedure for each recording site and contrast condition (Fig. 2.7B).

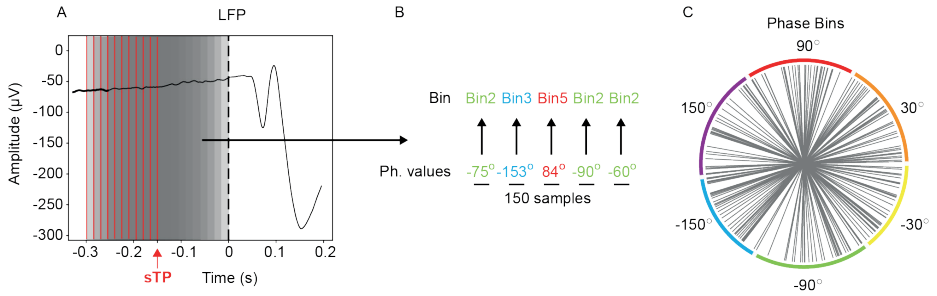

Fig. 2.6. Graphic representation of Method 2 to find the additive component of the signal. (*A*) Each time sample of a 0.15 s time window is associated with their respective phase value. Additive modulation is calculated considering a surrogate MUA response of 0.15 s after the time sample under consideration. (*B*) Phase values for each time sample are binned into 6 phase bins. The same procedure is repeated for each trial and each recording site separately. MUA surrogate ERP values associated with the same phase bin value will be later averaged to find the additive component. (*C*) Same as panel C in Fig. 2.4.

This demonstrated again that the absolute gamma phase leading to the strongest MM was between -30° and 30°, for all contrast conditions (Fig. 2.7B), after averaging over all recording sites.

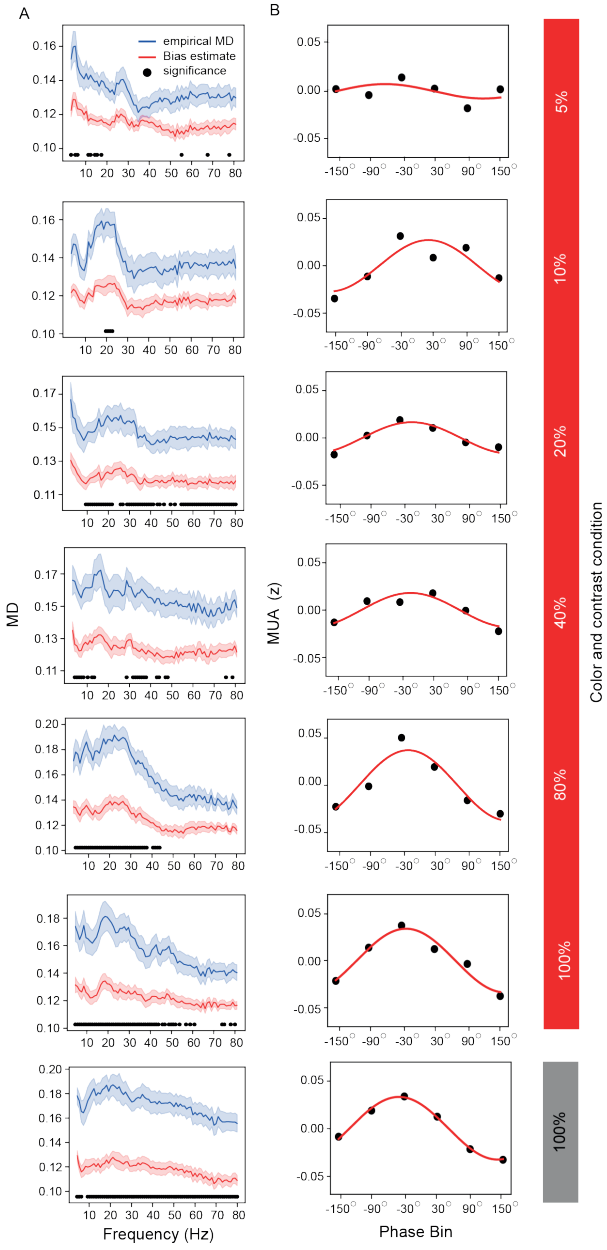

Fig. 2.7. Multiplicative modulation and statistical testing for Method 2. (*A*) Same as in Fig. 2.5, panel A. (*B*) Same as in Fig. 2.5, panel B. The lateral bar on the right-hand side indicates color condition of the FSB and contrast condition of the black-bar stimulus.

The gamma rhythm modulates MUA responses according to a quasi-input gain model

We investigated if the modulation imposed by gamma phases on the MUA response corresponded to an input-gain or an output-gain model (Reynolds, Pasternak et al. 2000) by plotting the grand average MD as a function of black-bar contrast. The highest modulation was found for the 40% contrast level (Fig. 2.8A). This evidence is most consistent with an input-gain model for the gamma-rhythmic modulation of MUA responses, because the biggest MM was found for a mid-level contrast. However, the pattern of contrast-dependent MM showed additional features, like increases for the lowest and highest contrast, that were not fully in line with a pure input-gain model (Reynolds, Pasternak et al. 2000), and further research is required to arrive at a firm conclusion in this regard.

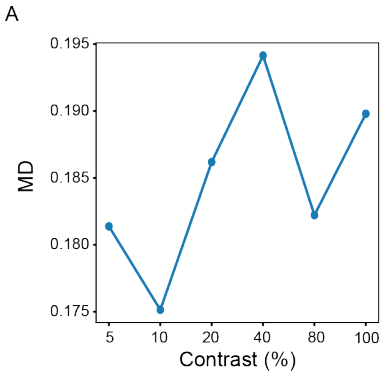

Fig. 2.8. Dependence of gamma-phasic modulation of MUA neuronal responses to visual stimulus presentation as a function of black-bar contrast. (*A*) Grand average MD value over all recording sites. The highest MD value is at 40% contrast, consistent with an input gain model type of modulatory effect.

Discussion

Summary

We find that gamma rhythmically modulates the MUA response to a simple visual stimulus, and that the absolute gamma phase leading to the strongest response lies between -30˚ and 30˚. This oscillatory modulation could not be demonstrated to be specific for gamma-band activity, but rather we found a broader significance for the effect across the alpha-beta, gamma, and high gamma range, depending on the contrast condition. The model according to which the modulation is exerted by the gamma band could not be defined with certainty, as to be pertaining to

an input or an output gain one, but we found a higher modulation for mid-level contrast stimuli, pointing in the direction of an input gain model.

Limitations of the study

The current study tried to address questions about gamma-phasic gain modulation. Some of the features of the paradigm used to this end, can be interpreted as limitations, and might need to be revisited in the future to gain a clearer understanding of the phenomena under examination. The stimuli used in the task, for example, were specifically tailored to elicit a very strong gamma rhythmic activation, particularly the red colored FSB, and its combination with a probing black bar stimulus. This kind of stimulus is different from the stimuli used in the body of literature of vision related studies, that generally implies gratings, or other simple stimuli on neutral colored backgrounds (Womelsdorf, Schoffelen et al. 2007, Grothe, Neitzel et al. 2012, Ni, Wunderle et al. 2016, Grothe, Rotermund et al. 2018), so it might be difficult to put our results in relation to previous ones. Moreover, the stimuli used here are not natural, and therefore do not allow us to generalize our findings to a naturalistic vision processes. In order to make claims about the functioning of V1 and the role of gamma oscillatory activity it will be necessary to address the same questions in the context of more physiological experimental paradigms. Additionally, still concerning the nature of the stimuli used here, the fact that we are addressing our research questions using colored stimuli poses some challenges to the interpretation of our results, since color is a stimulus feature still poorly investigated and understood in the context of visual processing. Lastly, our task design involved the use of a colored noise mask in the ITI. This was set up in order to reduce as much as possible the adaptation effects potentially stemming from the repeated and prolonged usage of a FSB of red color. The colored ITI might have had effects on the data that we could not account for with precision, also due to the fact that the monkey was not required to maintain fixation during this time interval.

Comparison to the Ni study

The findings of the current study summarised above overlap in part with the ones of Ni, Wunderle et al. (2016). The 2016 study also found significant modulatory effects on the MUA gain for both the gamma and the lower alpha-beta frequencies, as highlighted in the current study by both methods implied to investigate the existence of an MM. In the case of the 2016 study though, the specificity of gamma band activity was more consistently proven by the clearer peaks around the gamma band in the MD spectra, and also by the fact that the effect was specific for the gamma band for what concerned behavioural performance. Our findings might

differ from what was previously reported for several different reasons. Not only the area under investigation is different, we are addressing V1, rather than V4, but also the paradigm differs significantly for the stimuli used.

Specifically, Ni, Wunderle et al. (2016) triggered gamma oscillation and tested the impact of its phase with the same stimulus. A grating appeared on the screen and induced the gamma rhythm, and then its colour changed to test the MUA response in relation to it. In the case of the current study instead, two stimuli are used: a red FSB to induce gamma, and a small black bar appearing on top of the FSB to test the MUA response according to gamma phase. This might create differences in the visual processing stream followed by the stimuli and in the neuronal activity outcomes, because the two visual objects pertaining to the stimulation might entertain complex interactions. For example, the black bar stimulus overlapping onto the coloured background poses the challenge of foreground figure–background segregation (Lamme 1995, Roelfsema 2006), and this process may co-occur with the gain modulation effect.

One piece of information added by the current study to the results already reported in 2016, refers to the interpretation of the absolute gamma phase of MUA gain modulation. We could demonstrate that the preferred gamma phase for MUA gain modulation lies between -30˚ and 30˚, when we estimated the periodicity of the modulation on the grand average MM of MUA across all recording sites and sessions. This result was confirmed by both methods used to estimate the AM, and consequently calculate the MM.

The phase modulation model

CTC (Fries 2005, Fries 2015) postulates that gamma rhythmic activity is capable of organizing spikes so that they will be restricted and synchronized to specific time windows, increasing the precision and impact of the spiking output. In addition, gamma-band activity is also capable of rhythmically modulate input to the local circuit engaged in gamma activity in accordance to its phase (Fries 2009, Fries 2015). Accordingly, input gain modulation can be theoretically predicted as the preferential mechanism for gain modulation in the context of a gamma modulated local network. According to our results, input gain modulation could not be unequivocally demonstrated.

One reason for these mixed effects that we reported might be found in the results described in (Wunderle 2015). This study tried to determine the role of lateral input to a local network in determining which specific kind of gain modulation, input or

output gain, this network will engage in. The study showed that the final outcome of the modulation model via lateral connections to a local network, actually depends on a broader set of direct and indirect connections with higher levels of the cortical hierarchy, up until the callosal tracts between hemispheres. Ultimately, the status of the extended network the local network is connected with determines the modulation model, and this can correspond to a mixed modulation model as well. It is possible that in the case of our experiment, the presence of a red FSB, being so large and prominent, might have triggered feedback inputs from higher cortical areas, like V4, and this might have influenced the final outcome of the modulation.

Low frequency components significant peaks in MD

One aspect of our findings concerns the results obtained when testing the specificity of the modulation effect. Gamma could not be demonstrated to be the only frequency responsible for this modulation. Rather, it was interesting to notice how the MD spectra presented clear peaks in the lower alpha-beta band for almost all contrast levels tested, and also for the grey condition. This result was investigated further by performing a pre-whitening of our data, since we hypothesized that the strong low-frequency component could have biased our phase estimation algorithm, and the final result. The results for the pre-whitened data, where the low frequency component is removed, are shown in Suppl. Fig. 2.4. We noticed that the results stayed consistent with the ones obtained with the raw data. We had therefore to pose the question of why this could possibly be.

One hypothesis to explain this phenomenon is that figure-background segregation processes might be activated as soon as the black bar appears on the screen, given that the black bar test stimulus can be interpreted as a foreground stimulus on top of the red FSB background. Evidence of segmentation and figure-ground organization in early visual areas were found in many studies on NHP (Lamme 1995, Self, van Kerkoerle et al. 2013, Poort, Self et al. 2016). These processes are implemented via an early figure enhancement and a later background suppression enacted by the many feedforward, feedback and lateral connections to V1 (Self, van Kerkoerle et al. 2013, Poort, Self et al. 2016). The feedback and lateral connections through which figure-background segregation processes are exerted, might interfere with or inhibit those inhibitory mechanisms that trigger gamma oscillatory activity, reducing the impact of the modulation imposed by gamma in time (see Fig. 2.2C,D), and also in the general impact that the frequency band has on the modulation compared to other frequency bands.

Interestingly, additional evidence coming from experiments in rodents, might reinforce this speculation that inhibition of the inhibitory mechanisms influences gamma band activity impact on the neuronal gain. In mice, it was demonstrated that those interneurons involved in the generation of the gamma rhythm in the visual areas, the SST interneurons, are modulated by other inhibitory neurons, of the VIP kind. These VIP interneurons are driven together with the SST generating the gamma rhythm by the presentation of a visual stimulus, and they are particularly strongly responsive to low contrast and small stimuli. These neurons were proven to locally linearly scale gamma power by suppressing it, and also to reduce global gamma coherence (Veit, Handy et al. 2023). In the case of our experiment, the connection of the local gamma-generating network with speculative modulatory interneurons of the kind described in the abovementioned study, might have contributed to reduce the impact of gamma band modulatory activity. This might be especially true for the lower contrast conditions of the black bar stimulus that we presented, for which the MD spectrum showed the clearest peaks in the lower alpha-beta band, and not in the gamma one. In support of this claim, some studies describing the connectivity pattern and interneuron types in the cortex of NHP allow to speculate that the function of VIP interneurons found in primates could be consistent with a disinhibitory mechanism such as the one described in rodents in the abovementioned study. (Defelipe, González-Albo et al. 1999, Callaway 2004, Glatigny, Geffroy et al. 2024).

Alpha and beta frequency bands have anyways been previously described as taking part to visual information processing between V1 and V4. Specifically, while gamma has been traditionally labelled as the carrier of feedforward information in the visual processing stream, frequencies in the alpha-beta range have been demonstrated to be the preferential frequency channels for feedback information, in monkeys and humans (van Kerkoerle, Self et al. 2014, Bastos, Vezoli et al. 2015, Michalareas, Vezoli et al. 2016). In the current study, the nature of the visual stimuli presented to the monkey (i.e. the salient FSB red stimulation and the superposition of the black bar on it, activating foreground-background segregation processes) may inherently trigger a strong activation of the feedback connections to area V1, thus a consistent flow of information travelling backwards from higher visual areas. Given that oscillatory activity in the alpha-beta range preferentially covers the feedback-carrier role, this might be particularly well represented in the MD spectrum.

Additionally, besides the feedback propagation just mentioned, alpha band has also been described as to originate by generators present in vision-specialised areas of the thalamus, and inhibit information flow to visual areas in a feedforward manner

according to its phase. The relay stations of the thalamus sending connections to visual area V1 were indeed shown to modulate the incoming of sensory information in humans (Dou, Morrow et al. 2022). For these reasons, it is not unlikely that alpha frequency range covered a role of importance in the modulation of neuronal gain in our task, partially masking or reducing the modulatory effect imposed by gamma. Beta activity, on the other hand, was also recently proposed to be involved directly in the visual processes by serving the role of preferential frequency channel for the magnocellular-dorsal pathway, processing information about the 'where' of a visual scene. (Di Dona and Ronconi 2023). According to this study, the role of beta would be especially relevant in all of those circumstances where spatial segregation of elements of a visual scene is necessary, because they provide the spatial framework for the object-segregation and recognition process. Because the task we presented to the monkeys involves such segregation process, these pieces of evidence taken together could add another explanation to why the beta frequency range is so well represented in our MD spectra.

Future perspective

In summary, while the current study adds information on the absolute phase of gamma-rhythmic gain modulation, it still leaves open questions as for what concerns the interpretation of the gamma gain modulation model, and also specific questions about the role of lower frequency bands like alpha and beta in the modulation of the neuronal gain. Gamma gain modulation was, anyways, demonstrated again, even though the specificity of the effect could not be stated. Future experiments using more naturalistic stimuli should further clarify the open questions in order to make it possible to expand the knowledge of gamma mechanisms in context of the physiological functioning of the brain.

Supplementary Material

Supplementary Figures

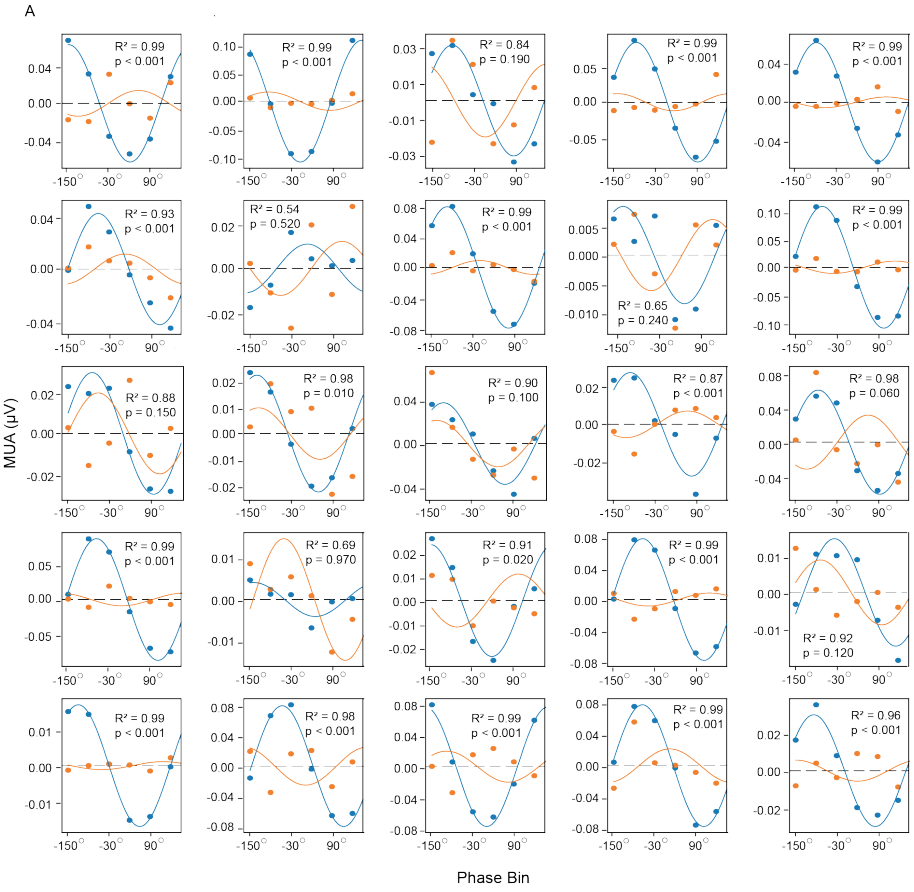

Suppl. Fig. 2.1. Ongoing modulation imposed by gamma oscillatory activity in the FSB time period for all recording sessions. (*A*) Each panel of the figure presents the same plot as in Fig. 2.2B. Each panel of this figure shows pre-stimulus gamma modulation on the MUA spike rates for one recording session, averaging over all the recording sites belonging to the recording session.

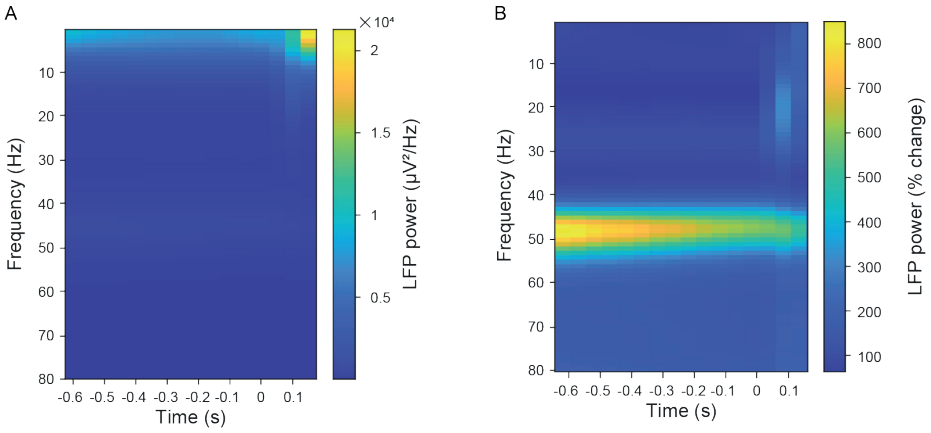

Suppl. Fig. 2.2. Time resolved power spectra. (*A*) Raw power spectrum for the red condition, across the FSB time window and the Probe time window. (*B*) Power spectrum for the red condition across FSB and Probe time windows, expressed as percent change relative to the baseline. The last 0.2 s of the corresponding FSB time window of the gray condition were used as baseline, and power is expressed as percentage change to it.

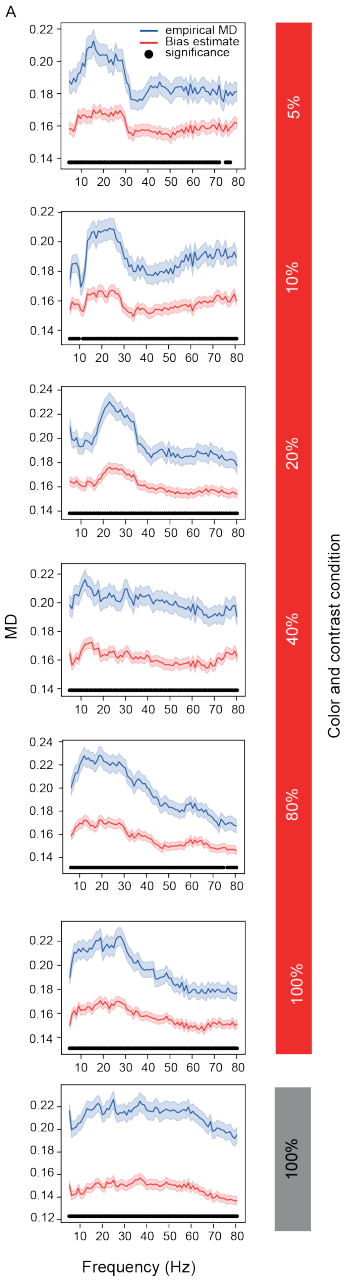

Suppl. Fig. 2.3. Channel by channel multiplicative modulation and statistical testing. (*A*) Same as in Fig.2.5 panel A, and Fig. 2.7 panel A. The statistics is run considering one recording channel, instead of one session, as a unit of observation. The lateral bar on the right-hand side indicates color condition of the FSB and contrast condition of the black-bar stimulus.

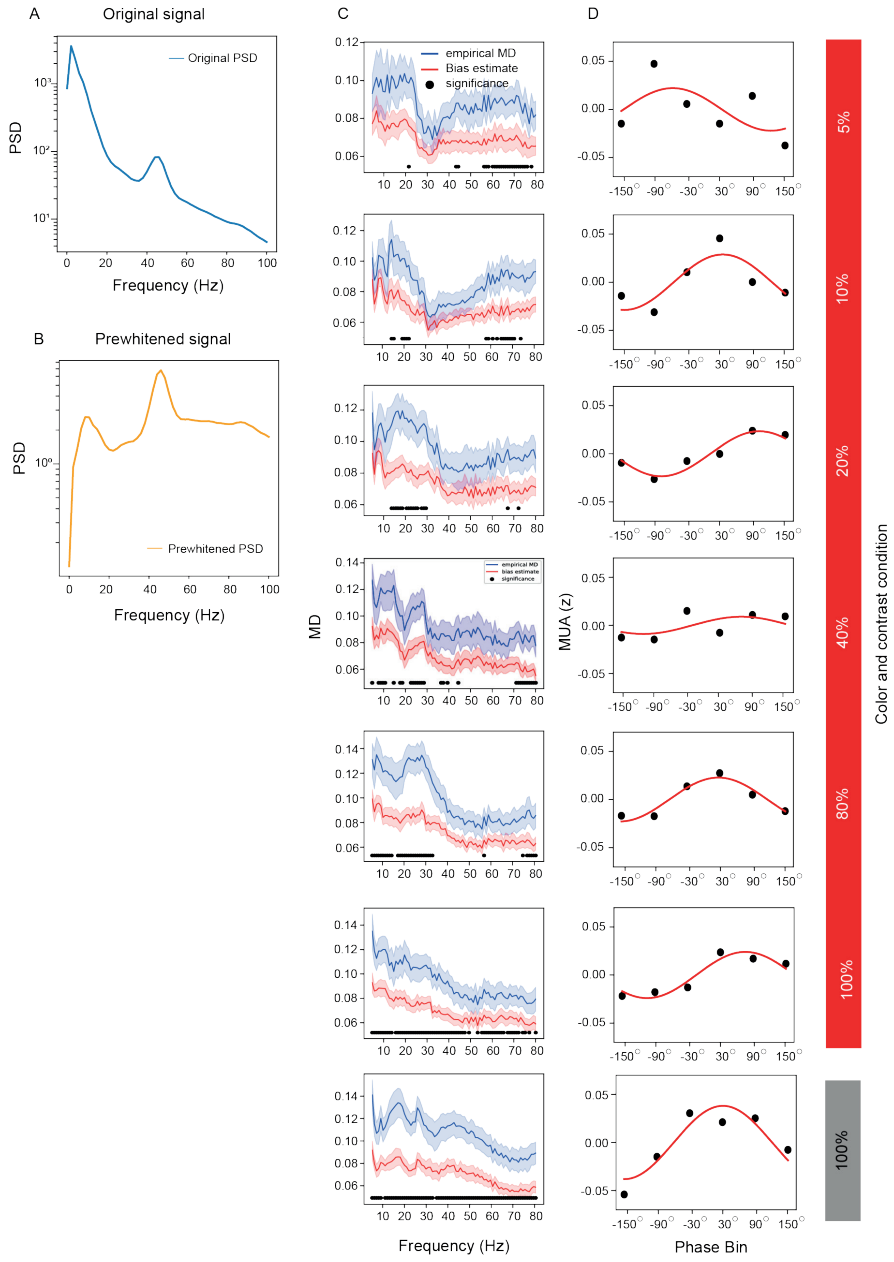

Suppl. Fig. 2.4. Multiplicative modulation and statistical testing for pre-whitened data. (*A*) Power spectral density spectrum of the original LFP signal for one exemplary recording session. (*B*) Power spectral density spectrum of the pre-whitened LFP signal for one exemplary recording session (*C*) Same as in Fig. 2.5, panel A. (*D*) Same as in Fig. 2.5, panel B. (*E*) Same as in Fig. 2.5, panel C. The lateral bar on the right-hand side indicates color condition of the FSB and contrast condition of the black-bar stimulus.

Materials and Methods

Surgical procedures

All experimental procedures involving non-human primates (NHPs) were conducted in accordance with German and European ethical regulations governing the protection of animals. The research project was reviewed and approved by the German regional authority, the Regierungspräsidium Darmstadt.

One adult male rhesus macaque (Macaca mulatta), 20 years old and weighing 13 kg, was used in this study. The use of a single monkey instead of the more common two to three monkeys has been motivated in a previous publication and a recent preprint (Fries and Maris 2022, Psarou, Katsanevaki et al. 2024). All surgical procedures on the experimental animal were performed under general anesthesia, and appropriate postoperative care—including administration of analgesics and antibiotics—was provided to ensure animal welfare.

Head-post implantation was performed using a two-step procedure as detailed in Psarou, Vezoli et al. (2023). Following this, a custom-designed modular titanium recording chamber for acute recordings was implanted. The chamber was positioned on the skull over the occipital region of the left brain hemisphere, targeting the cortical area corresponding to primary visual cortex (V1).

Visual Stimulation

An LG 32GK850G-B monitor (LG Electronics Inc., Seoul, South Korea) was used to display the visual stimuli, and gamma correction was applied for all tasks (gamma: 1.57). The eyes of the monkey were 83.5 cm from the screen. The exact timing of black-bar stimulus presentation was captured by a custom-built photodiode signal elicited by the presentation of a small square stimulus, simultaneous to the black bar, and hidden from the monkey's view in the upper-left corner of the monitor.

Receptive field (RF) estimation

The position and orientation preference of the RF were determined by first identifying all electrode contacts on the laminar probe sitting in the cortical tissue, as detailed in the following section, and then averaging across the neuronal responses of those selected channels. The spacing between electrode contacts was only 50 µm. Therefore RF positions and orientation preferences were expected to be consistent across simultaneously recorded contacts.

RF position was assessed at the start of each recording session, using the Fiorani, Azzi et al. (2014) back-projection method. In each trial of a fixation task where the monkey was required to maintain fixation on a central fixation point, a moving bar scanned the entire monitor in one of eight possible directions. The moving bar travelled at a speed of 8 deg/s and measured 0.1 dva in width. A total of 80 correct trials were collected, with ten successful trials per movement direction.

To determine the RF position, MUA-based spike density functions were accumulated over time, generating a spatial response map that identified the RF location. This process included correcting for response latency to maximise the back-projection response. MUA responses were then smoothed using a Gaussian function for each movement direction, the 10th and 90th percentiles were then selected, and an ellipse was fitted to thosedata points, in order to identify the MUA-response based RF position.

Orientation tuning task

RF's orientation preference was determined using a dedicated orientation tuning task. In each trial, a bar measuring 0.1 dva in width and 0.3 dva in length was displayed at the RF location in one of six possible orientations, while the monkey maintained fixation on the central fixation spot. A trial was deemed successful if fixation was sustained throughout. A total of 60 correct trials were collected, with ten successful trials for each orientation. The preferred orientation was identified by comparing the MUA response amplitude across the six orientations (or the LFP response if the MUA signal was weak) and selecting the orientation that elicited the highest MUA response. During the task the colour of the background was maintained grey [128,128,128], and the bar colour was black.

Behavioral task

All training and recording sessions were performed, in a fully shielded recording booth with dim lighting, while the monkey performed the task sitting in a primate chair. For electrophysiological recordings the head of the monkey was fixated. The behavioural task was designed using a custom-built software developed in-house using MATLAB, ARCADE (Dowdall, Schmiedt et al. 2018),.

The monkey was trained to perform a fixation task, in which every trial started after the monkey acquired fixation on a central black dot (0.3 dva in diameter) displayed at the centre of a grey screen. Fixation had to be maintained within a 0.5 dva tolerance radius around the fixation dot. If the monkey maintained fixation

for the entire trial duration (ranging from 1600 to 1850 ms), the trial was considered successfully completed, and the monkey was rewarded with grape juice.

Each trial involved the presentation of a sequence of visual stimuli on the monitor. Trials began by displaying a grey full-screen background (RGB coordinates [128, 128, 128]) and the central fixation dot. The monkey had a maximum of 10 seconds to acquire fixation, though fixation was usually attained much sooner.

Once fixation was established, a full-screen coloured background (FSCB) appeared. In 90% of the trials (red-condition), the FSCB was red (RGB coordinates [255, 0, 0]), while in the remaining 10% (grey-condition), the background remained the same grey as the initial screen. The grey-condition served as a control condition for comparison with the red-condition. The FSCB segment lasted 1.4s, plus a randomly jittered time ranging from 0 to 0.25s before proceeding to the next segment of the trial.

Following the FSCB period, the coloured background (red or grey) remained on-screen, and a black-bar stimulus was presented in correspondence to the previously identified RF for 0.2s. The black bar measured 0.3 dva in length and 0.1 dva in thickness, and it was oriented according to the recorded neurons' preferred orientation. In the red condition, the black bar appeared at six different contrast levels (detailed below), whereas in the grey condition, it was always displayed at full contrast. After the bar disappeared, a waiting period of 0.1s elapsed before the monkey could receive a reward. If the monkey broke fixation at any point, the trial was immediately terminated, and no reward was given.

During the inter-trial interval (ITI) of 0.7s, a colourful noise mask was displayed on the screen. This mask consisted of rectangles with side lengths varying from 0.1 to 0.5 dva in 0.01 dva increments, each assigned a randomly selected colour from the full range of RGB coordinates. The purpose of this noise mask was to counteract potential colour adaptation effects.

Color contrast and normalized color space

The black bar stimulus was displayed at six contrast levels during the red FSB condition: 5%, 10%, 20%, 40%, 80%, 100%. Contrast was determined using the Weber contrast formula:

$$\frac{I - Ib}{Ib}$$

where *I* represents the luminance of the stimulus, and I_b represents the luminance of the background. To ensure appropriate contrast levels, the colour coordinates for both the red background and the black-bar stimulus were selected from the standardized CIELAB colour space (Gravesen 2015) and then converted into RGB coordinates.

Eye position

Eye position was recorded using the Eyelink 1000 system (Eyelink Inc., SR Research, Ottawa, Canada), at a sampling rate of 1000 Hz. Calibration was performed on the left eye at the start of each recording session, and the signal from the left eye was subsequently recorded.

Recordings

During each recording session, a single laminar probe was inserted into the cortical tissue through the intact dura. These laminar probes consisted of 16 recording contacts arranged in a single column, with a spacing of 50 microns (linear V-probes from Plexon Inc., Dallas, Texas, USA). The probe was introduced using a guide tube that rested on the dura, which served as the ground during recordings, while the probe's shank acted as the reference. Recordings were conducted inside a fully shielded booth functioning as a Faraday cage, effectively preventing line noise interference with the electrophysiological signals. As a result, no additional line-noise removal was required or performed.

Electrophysiological data were collected using systems from Tucker Davis Technologies (TDT, Alachua, Florida, USA). The raw signals were recorded and digitized at a sampling rate of 24.4140625 kHz using a TDT PZ2 pre-amplifier.

Data Analysis

The analysis presented here was in large part aiming to reproduce as closely as possible the methods used in Ni, Wunderle et al. (2016), therefore the following descriptions will contain pieces of text that are copies or close to literal copies of Ni, Wunderle et al. (2016), while avoiding the placement of those sentence parts in quotes, which would have impoverished readability.

Analyses were performed in MATLAB, using the FieldTrip toolbox (Oostenveld, Fries et al. 2011), and in Python with custom algorithms. All the analyses were conducted per each recording session or per each recording site separately (one recording site corresponds to one recorded valid channel, see below), as detailed in the main text, and per each contrast separately.

Preprocessing

The raw data were downsampled to 1000 Hz. For the LFP, preprocessing involved upsampling to 3,125,000 Hz, followed by downsampling to 25,000 Hz. The signal was then filtered using an IIR filter with a stop-band at 500 Hz before being further downsampled to 1000 Hz. For the MUA, preprocessing included upsampling to 3,125,000 Hz, applying a band-pass filter between 300 and 12,000 Hz, rectifying the signal, filtering with a stop-band at 500 Hz (IIR filter), and finally downsampling to 1000 Hz.

Recording site selection

In each recording session, one laminar probe was used for one penetration into the brain tissue. The probe was positioned based on real-time visual inspection of neuronal signals and their overall responsiveness to visual stimuli, ensuring that most recording sites exhibited strong MUA and LFP responses. However, some sites did not display clear RFs. These sites were identified through visual inspection and excluded from further analysis.

MUA responses

In order to obtain spike densities, MUA was smoothed with a Gaussian kernel, with a standard deviation (SD) of 12.5ms, truncated at +/-2 SD. In order to obtain MUA values for the empirical data and AM, MUA spike rates were first averaged over trials belonging to the same contrast condition, and then over time, by selecting a 10 ms window centered around the maximum peak of the MUA response to the black bar. For those contrast conditions where the MUA response to the black bar was very low, like 5% contrast, and a clear maximum peak could not be identified, we calculated an estimate of the peak time point for each recording site by first averaging over trials belonging to all contrast condition taken together, and then again finding the MUA peak response as the maximum value of the MUA response to the black bar. With this procedure we could estimate a confidence interval to evaluate the goodness of the estimate of the MUA peak for all channels and contrast conditions, by using the Full Width Half Maximum (FWHM) duration of the MUA response to the black bar per each channel, when averaged over all contrast conditions. The FWHM initial and final time samples defined a range of time points were it was most plausible to find the actual peak of MUA response to the black bar. If the peak time point calculated per recording site and contrast condition fell in the range it was automatically accepted, otherwise we would take the peak time point of the average across contrast conditions for that specific recording site.

Gamma peak frequency estimation

In order to extract the gamma peak frequency, a time window of 0.5s end-aligned to the black-bar stimulus presentation was selected, Hann-tapered, zero-padded to 1s, and Fourier transformed using Pyhton SciPy fast-Fourier transform function package. The spectra obtained with this procedure were then analyzed with FOOOF (Gerster, Waterstraat et al. 2022), in order to extract gamma peak frequency for each recording site. The frequency peak was ranging between 42 Hz and 46 Hz for the red condition, and 37 to 39 Hz for the grey condition, according to the recording site.

Precise timing of stimulus arrival in V1

In order to verify the effect of gamma phase modulation on MUA responses, it was necessary to extract phase at the estimated time of input arrival in V1 (TP). The estimation of this critical time point was performed per each recording site separately. For each channel, the ERP was calculated and z-scored over time points. Then, the absolute value of its first derivative was taken as the velocity of slope change. A threshold was set at 1.5 times the ERP signal's SD, and the critical time point was defined as the first time sample after black-bar stimulus presentation for which a threshold crossing could be detected.

Input-time phase extraction method

Once the precise time point of stimulus arrival in V1 was identified, we faced the challenge to estimate the spectral phases of the LFP at that critical time point, immediately preceding the ERP response to the stimulus. In our specific case, we needed to make sure that the spectral phase would be extracted from the LFP trace as close as possible to the ERP, but excluding any potential influence from the ERP itself. To address this problem, we used the phase estimation method presented in Patel, Psarou et al. (2024). This method is an expansion and improvement of the phase extraction procedure described in Ni, Wunderle et al. (2016), and in brief, aims at solving the edge issue by generating data after the edge limit by making use of an autoregressive model.

Data whitening

The auto-regressive phase estimation method could be inherently biased by power in the lower frequencies of the spectrum. In order to account for a potential distortion in our results caused by this phenomenon, we decided to repeat the phase estimation procedure with the same method (Patel, Psarou et al. 2024) with LFP data previously whitened. For each trial and each channel, an autoregressive model of order 1 (AR-1) was fitted using ordinary least squares (OLS) regression. The AR-1 coefficient (phi) quantified how much of the current signal value can be

predicted by its immediately preceding value. Once this coefficient was estimated, the signal was transformed by subtracting the lag-1 prediction (i.e.) from each time point, effectively removing the linear dependency on the previous sample.

The results using phase values extracted from pre-whitened data did not differ substantially from the results obtained using the original data (Suppl. Fig. 2.5), therefore we decided to present the latter in the main text.

Ongoing modulation of MUA by gamma rhythm

In order to calculate the ongoing modulation imposed by the gamma rhythm on the MUA during the full-screen red stimulus presentation, before the appearance of the black bar, we selected for each trial a time window of 0.150s immediately preceding the stimulus presentation (not the onset of the neuronal response), and we performed time resolved spectral analysis on it, by using the filter-Hilbert method. The filtering procedure was optimized for the analysis for the gamma frequency, by using the gamma frequency peaks previously extracted. We extracted the phase values for each of the 150 original time samples, we binned those values in 6 phase bins centered respectively at -150, -90, -30, 30, 90, 150 degrees, and then we averaged accordingly the correspondent MUA values for each of the time points. We later averaged MUA value for corresponding bins over trials, to obtain one MUA value per each of the phase bins. The obtained data points were then fitted with a cosine function to show the periodic modulatory effect. The R^2 value of the fit was obtained to evaluate the goodness of the fitting. The goodness of fit was tested against shuffled controls.

Additive component of the modulation

In order to demonstrate that the gamma phase imposes a multiplicative modulatory (MM) effect on the MUA, an additive modulation (AM) was calculated and subtracted from the empirically recorded data. Two methods were used to calculate the additive component of the modulation, and this was repeated for each frequency of the spectrum ranging from 4 to 80 Hz, to later test the specificity of the effect for gamma band activity.

The first method followed closely the approach of Ni, Wunderle et al. (2016), where the additive component of the modulation is described as a constant MUA response to the presentation of a stimulus riding on top of the ongoing oscillatory modulation, or adding on top of this ongoing modulation, from which the name. We calculated the AM component by first getting an estimate of the ongoing modulatory (OM) activity. First, we arbitrarily defined a time point during the red-

background epoch, far back in time enough from black-bar stimulus presentation to only capture activity of the ongoing gamma modulation, but close enough to the actual time point of input arrival in V1 so that we would have a fair estimate of the gamma modulation as close as possible to that time point. We defined this "surrogate" time point (sTP) of input arrival in V1 at minus 0.15s from black bar presentation. Then, per each trial, we extracted the phase at sTP using the phase extrapolation method described above for input-time. We then binned trials according to phase value into 6 bins, centered respectively at -150, -90, -30, 30, 90, 150 degrees, and we made sure each bin contained 35 trials. For each bin we collected the corresponding MUA, and averaged over trials. We then computed the constant MUA response as the global average MUA response over trials, regardless of phase bin. Finally, we mathematically added the two components, the constant MUA response and the ongoing modulation to obtain the additive component.

The second method that we used for estimating the additive component of the modulation followed the same rationale of the one described above, but it differed in the way ongoing gamma modulatory activity was calculated. Instead of choosing one single sTP before the presentation of the black bar, we chose a time window of 150 time samples, going further back in time, so that the estimation of a 150 samples additive component would be safely distant from the ERP even for the last time sample considered. We then extracted the phase at each time sample of the selected window, and proceeded in the same way described above to prove the existence of ongoing gamma modulatory effect. This method possibly overestimated the additive component of the modulation, because the amount of data points available for averaging was expanded, therefore the resulting MUA average was cleaner. This method allowed us to have stronger proof of the existence of a multiplicative component of the modulation, once this stronger additive component was subtracted from the empirical data.

Multiplicative modulation by input-time phase

In order to extract the MM component of the MUA modulation, per each contrast, frequency, recording site and phase bin, we subtracted the AM component described above from the empirical data. We then z-scored the MM components per each recording site, by calculating mean and SD across trials, and then subtracting this mean and dividing by this standard deviation, in order to later combine recording sites.

The phase-dependent modulation of the z-transformed multiplicative MUA response components was assessed by fitting a single cycle of a cosine function, with the peak-

to-peak amplitude defined as the modulation depth (MD). Both the amplitude and phase of the cosine function were fitted to avoid imposing strong assumptions about the phase that produces the strongest response. Cosine fits without a predetermined phase always yield a positive modulation depth, therefore we estimated this inherent bias. To do so, we randomly paired phases with z-transformed multiplicative MUA components and repeated the cosine fitting process 100 times. The average MD across these 100 randomizations served as the bias estimate, which is depicted as a red line in Fig.2.5B, Fig.2.7B, and Suppl. Fig. 2.2 D.

Gamma phase modulation model

Based on Reynolds, Pasternak et al. (2000) it is possible to describe the effect of a variable, in the case of the abovementioned paper selective attention, on MUA response to a stimulus with two models. The input gain model sees an increase in MUA through a shift in the sensitivity of the neurons. Namely, this means that the neurometric curve describing the MUA response to stimuli of increasing contrasts is shifted to the left, and it is possible to find the biggest difference in neuronal response for stimuli of mid-level contrast, when comparing for different conditions. On the other hand, the response gain model postulates that the effect of the variable is that of causing a net increase of the MUA by multiplying it by a constant gain factor. Therefore, the highest difference in MUA response between experimental conditions will be evident for the highest contrast stimuli in this model. Following this notion, we described which model gamma-phase modulation imposes on the neuronal gain. To this end, we plotted the average MD over all recording sites, for each contrast condition and check for which contrast level we could identify the highest value of MD. Because the peak MD was found for 40% contrast stimuli, we concluded that gamma phase imposes a Contrast Gain type of modulation on the MUA response.

Statistical analysis

For each recording session and frequency, we computed both the observed modulation depth (MD) and its corresponding Bias Estimate. The analysis yielded an MD spectrum and a bias spectrum per each recording session. We subsequently assessed whether consistent differences between these spectra were evident across recording sessions. To this end, paired t-tests were conducted for each frequency to compare MD and bias spectra across recording sessions. Importantly, statistical inference did not depend directly on the outcomes of these t-tests; thus, our conclusions were not subject to their underlying assumptions. Instead, the resulting t-values served solely as a quantitative measure of difference for the following analysis based on a non-parametric permutation test. In each of 10,000 permutations, the following

procedure was applied: for every session, the MD and Bias spectra were randomly either swapped or left unchanged; a paired t-test was then recomputed across recording sessions; and the maximum t-value observed across all frequencies was added to the permutation distribution. This final step controlled for the multiple comparisons across frequencies, as described by Nichols and Holmes (2002). Finally, we determined p-values by comparing the observed t-values to the permutation-based distribution in a two-sided test, with correction for multiple frequency comparisons. The same statistical testing procedure was used in Suppl. Fig.2.3, but the unit of observation used was the single recording site, rather than the recording session.

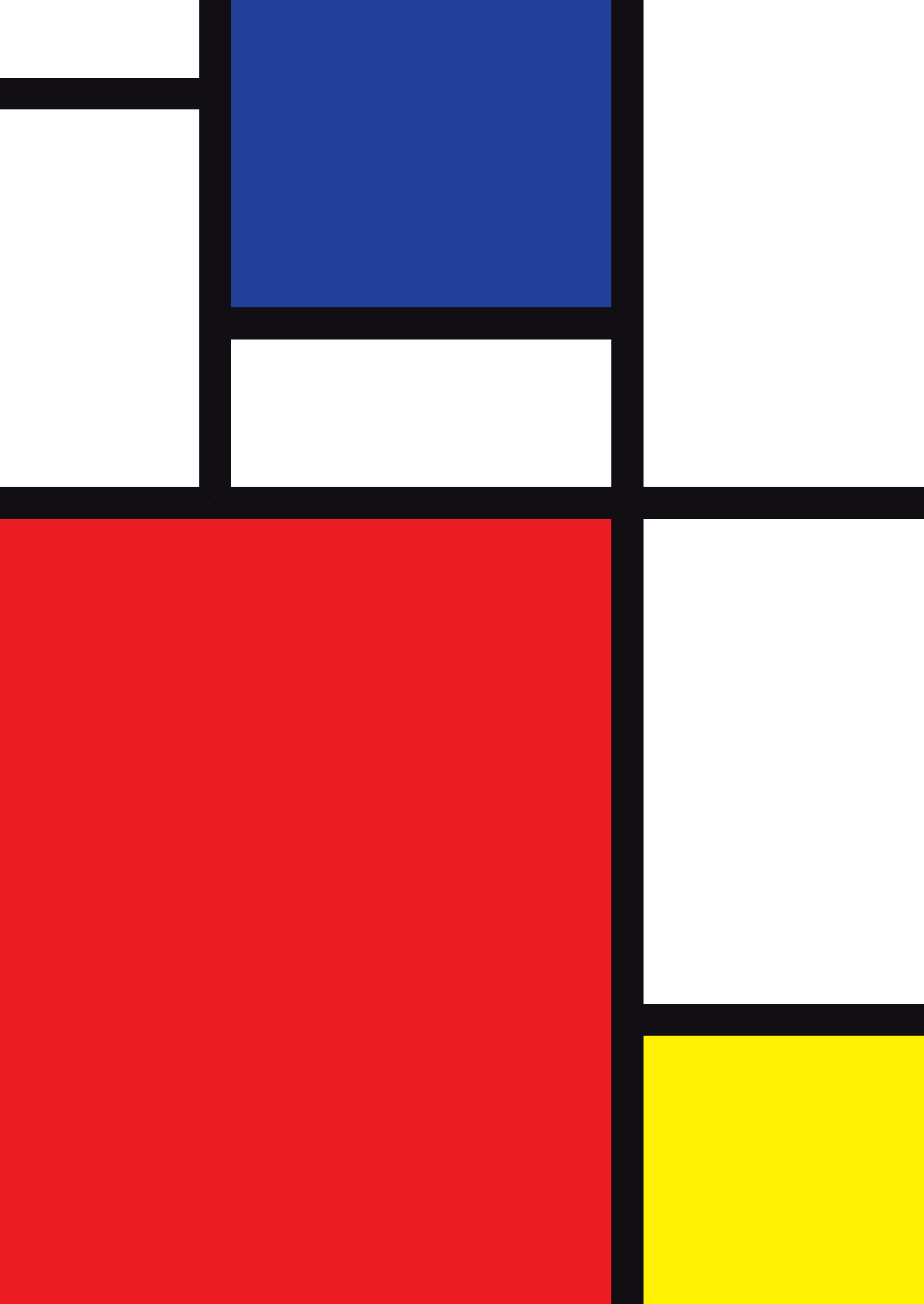

Chapter 3

Surprising effects of stimulus repetition on neuronal firing rates and gamma-band synchronization

In preparation as: Martina Pandinelli, Mohsen Parto-Dezfouli, Eleni Psarou, Iris Grothe, Pascal Fries. Surprising effects of stimulus repetition on neuronal firing rates and gamma-band synchronization in awake macaque V1.

Abstract

Stimulus repetition is abundant, because the environment is redundant and/or because it is redundantly sampled. This offers an opportunity to optimize the processing of repeated stimuli. Indeed, stimulus repetition leads to classically described neuronal response decreases, and to more recently described neuronal gamma synchronization increases (sometimes preceded by decreases for a few trials). Here, we used a full-screen colored background (FSCB) and a flashed black bar, while recording multi-unit activity (MUA) and local field potentials (LFP) from area V1 of an awake macaque monkey. We found that the FSCB repetition induced neuronal response increases (sometimes preceded by decreases for a few trials) and gamma synchronization decreases (preceded by increases for a few trials). These effects are largely opposite to the dominant previous findings. Intriguingly, these surprising effects reversed when we isolated the responses to the flashed black bar. We discuss these findings, considering differences to previous studies with regards to the subject of the study, the stimuli and the task. We notice that in studies reporting classical results for gamma, sometimes in combination with firing rates, the stimuli were typically (partly) predictive of the reward. Here, we found non-classical results for the FSCB that was not reward predictive, and classical results for the black bar that was reward predictive. Whether this has revealed a general effect of reward predictive versus non-predictive stimuli will require further investigation with stimuli and task designs tailored specifically for this question.

Introduction

Repetition is a key feature of visual experience on several levels. On a behavioral level, the eyes of a subject tend to perform return saccades, as a strategy to optimize foraging (Wilming, Harst et al. 2013, Psarou, Parto-Dezfouli et al. 2025), and thereby revisit the same objects. This brings the same stimuli repeatedly into the receptive fields (RFs) of a given neuron or neuronal group in retinotopically organized visual cortical areas, like primary visual cortex, V1. On a stimulus level, a natural visual scene can contain dynamic stimulus repetitions, when e.g. image elements move back and forth and thereby in and out of the mentioned RFs. On a combined stimulus and behavioral level, stimuli can contain spatial repetitions (Torralba and Oliva 2003), like e.g. trees in a forest, or faces in a crowd, and the behavioral sampling of these repeated items can stimulate those RFs repeatedly with similar stimuli. All these types of stimulus repetition offer the brain the opportunity to optimize its computation (Olshausen and Field 1996, Schwartz, Hsu et al. 2007).

Repetition of visual stimuli in experimental contexts has generally led to decreases in neuronal firing rates (Li, Miller et al. 1993, Desimone 1996) and in the fMRI BOLD (functional magnetic imaging blood oxygenation level dependent) response (Grill-Spector, Henson et al. 2006). This effect, classically described as repetition suppression, has no detrimental impact on behavioral performance (Grill-Spector, Henson et al. 2006). Maintained performance might be achieved by neuronal synchronization (Gotts 2003, Gotts, Chow et al. 2012) which might increase the impact of the synchronized neurons by means of feedforward coincidence detection (Salinas and Sejnowski 2001) or entrainment (Fries 2015). Indeed, increased neuronal gamma-band synchronization within and between awake macaque areas V1 and V4 has been reported as a result of stimulus repetition (Brunet, Bosman et al. 2014). This repetition-related gamma increase has been confirmed by studies that additionally demonstrated stimulus specificity of the repetition effect, both in monkeys (Peter, Stauch et al. 2021, Psarou, Parto-Dezfouli et al. 2025) and humans (Stauch, Peter et al. 2021).

In the present study, we report surprising findings obtained serendipitously while analyzing the effect of stimulus repetition in a dataset that had originally been collected to further investigate a different previously reported phenomenon: Visually induced gamma-band activity rhythmically modulates the gain of the spike response to a stimulus change (Ni, Wunderle et al. 2016). In the present experiment, we recorded multi-unit activity (MUA) and local field potentials (LFPs) from awake

macaque area V1, while inducing sustained gamma-band activity with a full-screen-colored background (FSCB) (Shirhatti and Ray 2018, Peter, Uran et al. 2019). On top of the FSCB and at an unpredictable time, we then presented in the RFs of the recorded V1 neurons, a black bar that evoked neuronal spike responses.

This paradigm differed in several aspects from previous studies that had described repetition-related changes in gamma-band activity. These previous studies had used sustained stimulation with gratings or natural stimuli (Brunet, Bosman et al. 2014, Peter, Stauch et al. 2021, Stauch, Peter et al. 2021, Psarou, Parto-Dezfouli et al. 2025), whereas here we used the FSCB and a flashed bar. Furthermore, in those previous studies, the stimuli that induced the investigated neuronal activity underwent changes or offsets that temporally predicted the reward. In the present experiment, reward was tightly predicted by the black bar, whereas the FSCB did not add to reward prediction.

This paradigm produced repetition-related changes in neuronal activity that were surprising, as they differed drastically from the results of those previous studies. The previous studies had confirmed numerous reports that stimulus repetition leads to MUA decreases (Brunet, Vinck et al. 2014, Peter, Stauch et al. 2021, Psarou, Parto-Dezfouli et al. 2025). Furthermore, they revealed that stimulus repetition can lead to initial gamma decreases for a few (typically 4-10) repetitions (Peter, Stauch et al. 2021, Stauch, Peter et al. 2021), always followed by gamma increases for the remaining repetitions (Brunet, Bosman et al. 2014, Peter, Stauch et al. 2021, Stauch, Peter et al. 2021, Psarou, Parto-Dezfouli et al. 2025). By contrast, the present study revealed that the repetition of the FSCB induced MUA increases, preceded by MUA decreases for some conditions and/or task period. The repetition of the FSCB consistently induced gamma increases for some initial trials followed by gamma decreases for the remaining trials. Even more surprisingly, the repetitions of the black bar induced MUA decreases and initial gamma decreases followed by gamma increases, largely following results from previous studies.

Results

Stimuli and task are illustrated in Fig. 3.1A. After an inter-trial interval with a randomly colored noise mask, each trial started with the presentation of a gray FSCB and a central fixation point (we refer to gray as a color, simply for ease of use). As soon as the monkey attained fixation, the FSCB color remained gray in 10% of the trials (gray-condition), or turned red in 90% of the trials (red-condition). The

sequence of gray- and red-condition trials was pseudorandom. After 1.41.65 s, while the FSCB remained unchanged, a black bar (width: 0.1 dva (degrees of visual angle), length: 0.3 dva) was flashed for 0.2 s into the previously mapped RF, while the monkey was required to keep fixation. In different trials, the bar was presented at different contrast levels, pseudorandomly chosen from 5%, 10%, 20%, 40%, 80%, or 100% in each trial of the red condition, and always at full contrast (100%) in the gray-condition (see Methods for definition of contrast). Thus, the trials of the red-condition contained approximately equal numbers of trials of the 6 distinct contrast conditions. If the monkey kept fixation, the bar was followed by a gray FSCB and reward.

This paradigm offered an interesting opportunity to investigate repetition-related changes in neuronal activity, because it differed from previous studies as outlined in the introduction. We studied neuronal activity in response to the repetition of the FSCB and the repetition of the FSCB with the black bar superimposed. Moreover, we studied the neuronal response to the repetition of the black bar in isolation, by subtracting the response to the FSCB.

To analyze neuronal activity, we defined three periods indicated by the blue-shaded rectangles in Fig. 3.1B, C. The "FSCB-transient" period started with the fixation onset, which also triggered the red FSCB onset in the red condition; the FSCB-transient period was 200 ms long. The "FSCB-sustained" period corresponded to the last 200 ms end-aligned to the onset of the black bar. Finally, the "bar-transient" period started with the onset of the black bar and was 200 ms long. As expected, the LFP (Fig. 3.1B) and MUA (Fig. 3.1C) averaged over all trials and recording sites showed phasic responses during the FSCB-transient period in the red condition, much smaller phasic responses during this period in the gray condition (as there was no color change, just fixation onset), and contrast-dependent phasic responses in the bar-transient period.

For each of the conditions and periods, we first computed the raw LFP power spectra averaged over recording sites and all trials (Suppl. Fig. 3.1). The raw LFP power spectrum is not very sensitive for showing rhythmical neuronal synchronization (Vinck, Womelsdorf et al. 2013). Nevertheless, these raw power spectra revealed gamma peaks or at least gamma bumps for all combinations of conditions and task periods. Note that clear gamma peaks were visible also for the FSCB-transient and FSCB-sustained periods of the gray condition. This was unexpected, and potentially due to a color-aftereffect, as few gray-condition trials were interspersed between many red-condition trials. We nevertheless opted to use the gray condition as a baseline condition for the

normalization of the red condition. This is mainly useful for the investigation of power spectra, which are otherwise dominated by a 1/f component. Importantly, when we analyzed the raw LFP power spectra, all results remained qualitatively identical.

For the normalization, we expressed the power during the red condition as percent change relative to the gray condition (from the corresponding task period). For the bar-transient period, this was done separately per contrast condition. This was first done per recording site, and the resulting LFP power change spectra were then averaged over recording sites. They showed prominent beta and gamma peaks for the FSCB-transient period (Fig. 3.1D), and they were dominated by a large gamma peak for both the FSCB-sustained period (Fig. 3.1E) and the bar-transient period (Fig. 3.1F). For the bar-transient period, they differed across contrast conditions, mainly in the alpha-beta range (Fig. 3.1F). For further analysis of the gamma-band power, we defined the gamma band, separately per task period, as the peak frequency in the average power change spectrum plus/minus 10% of that frequency, resulting in 55±5.5 Hz for the FSCB-transient period, 48±4.8 Hz for the FSCB-sustained period, and 47±4.7 Hz for the bar-transient period (as indicated by the thin vertical lines and gray rectangles in Fig. 3.1D-F).

Repetition-related changes in MUA

We investigated repetition-related changes in MUA across trials. We first normalized all MUA values per recording site and per task period, by expressing MUA as percent of the MUA in the gray condition, averaged over the respective task period. These normalized MUA values were subsequently averaged over recording sites and plotted per trial (Fig. 3.2). We separately considered all combinations of color conditions (Fig. 3.2 rows) and task periods (Fig. 3.2 columns). Note that the bar-transient period during the red condition contained six different contrast conditions. Therefore, we also compiled a plot of repetition-related MUA changes, for which we averaged the data first per contrast condition and then over contrast conditions (Fig. 3.2D).

For several of the combinations of color condition and task period, MUA showed an initial repetition-related decrease followed by an increase. Similar breakpoints had been previously observed by us in several other datasets, both for MUA and gamma in awake macaque V1 (Peter, Stauch et al. 2021, Psarou, Parto-Dezfouli et al. 2025) and for gamma in human MEG (Stauch, Peter et al. 2021). In these datasets, the breakpoints had been determined by eye and occurred at trial 4-10 for gamma-band LFP power and 4-20 for MUA. In the current dataset, visual inspection of the MUA results suggested that breakpoints could occur around trial 20 when we considered the gray condition (Fig. 3.2E-G), and around trial 120 when we considered the

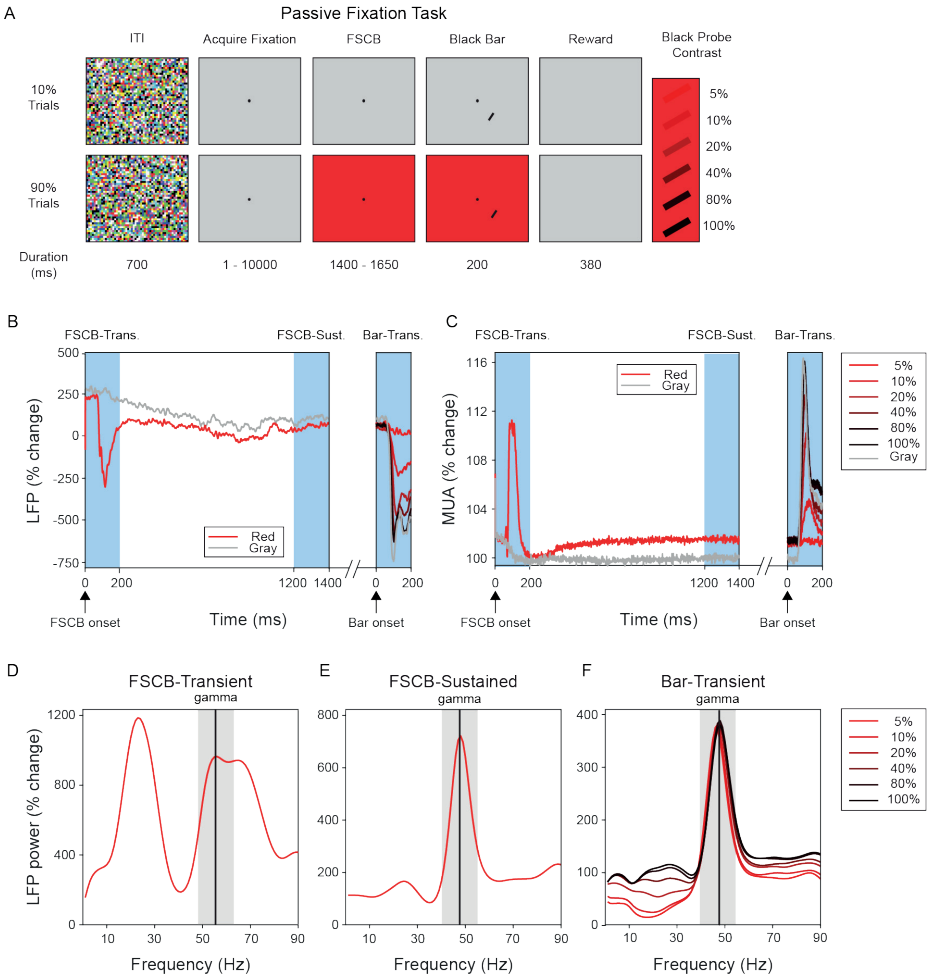

Fig. 3.1. Stimuli, paradigm, task periods, and stimulus evoked and induced MUA and LFP responses. (*A*) Schematic illustration of stimuli and task periods for the gray condition (upper row) and red condition (lower row). (*B*) LFP averaged over trials and recording sites, separately for the gray and the red conditions, shown in the corresponding colors. (*C*) Same as *B*, but for MUA. (*D*) LFP power spectra during the FSCB-transient period for the red condition, averaged over recording sites and trials. Power is expressed as percentage change relative to the corresponding task period of the gray condition. (*E*) Same as *D*, but for FSCB-sustained period. (*F*) Same as D, but for bar-transient period. For the bar-transient period (B, C, F), the different bar-contrast conditions are color coded according to the legend to the right of panel *C* and panel *F*.

red condition (Fig. 3.2A). We noticed that the red condition contained 6 different contrast conditions for the bar that was flashed into the RF, whereas the gray condition contained only 1 contrast condition. We further noticed that the breakpoint appeared around trial number 20 times the number of contrast

conditions. We hypothesize that this might be related to the fact that the bar was temporally predictive of the reward (see Discussion for details). With this in mind, we opted for a segmented regression, where we fixed the number of segments to two, and the breakpoint to occur between trial 4-20 times the number of contrast conditions. This indeed provided excellent fits. For consistency, we applied this approach also to the combinations of color condition and task period, for which visual inspection did not reveal a breakpoint (Fig. 3.2B-D).

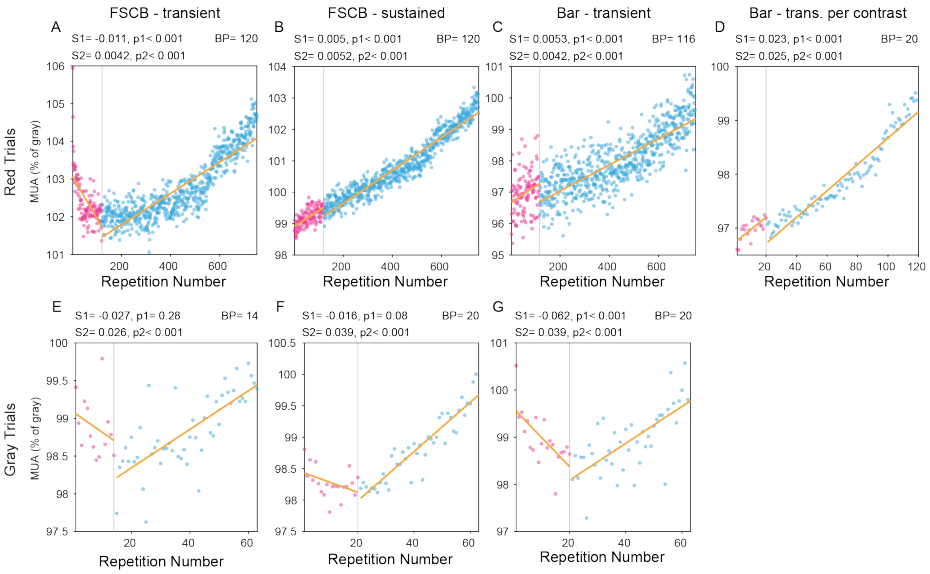

Fig. 3.2. Trial-by-trial analysis of repetition-related changes in MUA responses. (*A*) MUA responses for the FSCB-transient period of the red condition, expressed as percent change to the corresponding gray condition, averaged over recording sites and sessions, separately per trial. Repetition-related changes were fitted with a segmented linear regression, whose results are shown as yellow regression lines, separated by a vertical line at the break point. The text above the plot provides the trial number of the break point (BP), and the slope and p-value for the first regression segment (S1, p1) and the second segment (S2, p2). The respective data points were colored magenta and blue. (*B*) Same as *A*, but for the FSCB-sustained period. (C) Same as *A*, but for the probe-transient period. (*D*) Same as *A*, but for the probe-transient period after averaging separately per bar-contrast condition. (*E*) Same as *A*, but for the FSCB-transient period of the gray condition. (*F*) Same as *A*, but for the FSCB-sustained period of the gray condition. (*G*) Same as *A*, but for the bar-transient period of the gray condition.

Most importantly, this analysis revealed that after the initial MUA decrease, which occurred for some conditions and task periods, all conditions and task periods showed repetition-related MUA increases until the end of the session. This was opposite to many previous reports, including our own, of repetition-related MUA

decreases (Brunet, Bosman et al. 2014, Peter, Stauch et al. 2021, Stauch, Peter et al. 2021, Psarou, Parto-Dezfouli et al. 2025).

We also investigated those repetition-related MUA changes as a function of time within the three task periods. For this, we pooled trials over red and gray conditions, and we focused on the trials after the breakpoint. After pooling, per task period, we determined the breakpoint (Suppl. Fig. 3.2) and divided the remaining trials into three equal-sized trial bins, the early, middle and late trials (Fig. 3.3). Within each trial bin, we averaged the normalized MUA (blue, yellow and magenta lines in Fig. 3.3A-C), and we statistically compared the late to the early trials (Fig. 3.3D-F). This showed that repetition-related MUA increases occurred throughout all three task periods.

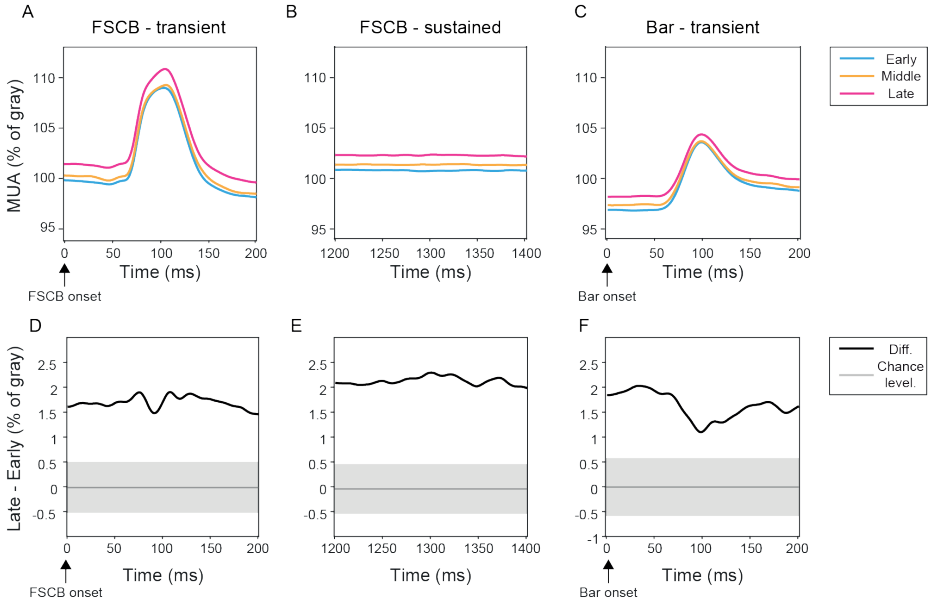

Fig. 3.3. Time-course analysis of repetition-related changes in MUA responses. (*A*) MUA responses, expressed as percent change relative to the average FSCB-sustained period of the gray condition, for the FSCB-transient period of both the red and gray condition combined, separately for the early, middle and late trial group as indicated by the color legend right of panel *C*. The trial groups were defined after excluding the trials before the break point identified by the segmented linear regression. (*B*) Same as *A*, but for the FSCB-sustained period. (*C*) Same as *A*, but for the bar-transient period. (*D*) The black line shows the difference of the late minus the early trial group in *A*. The gray-shaded region indicates the range of differences expected by chance. All observed differences were significant. (*E*) Same as *D*, but corresponding to panel *B* for the FSCB-sustained period. (*F*) Same as *D*, but corresponding to panel *C* for the bar-transient period.

Repetition-related changes in LFP gamma power

We next investigated repetition-related changes in LFP gamma-band power, using the same approaches as used for MUA. Gamma showed initial repetition-related increases followed by decreases, consistently for all combinations of color condition and task period (Fig. 3.4A-F) except for the bar-transient period in the gray condition (Fig. 3.4G). The segmented regression located the breakpoint to trial number 8-16 for the gray condition with one bar-contrast condition (Fig. 3.4E-G), at trial number 7 when we averaged over bar-contrast conditions in the red condition (Fig. 3.4D), and at trial number 30-50 for the red condition, which corresponds to trial number 5-8.3 after dividing by the 6 bar-contrast conditions (see previous paragraph for the rationale of this). These breakpoint positions were consistent with the hypothesis that the breakpoint occurs at trial number 4-20 times the number of bar-contrast conditions.

Most importantly, the observation of repetition-related gamma decreases preceded by initial increases is opposite to our previous studies using other stimuli and task paradigms. In those previous studies, we had consistently found repetition-related gamma increases, preceded in some cases by initial decreases for 4-10 trials.

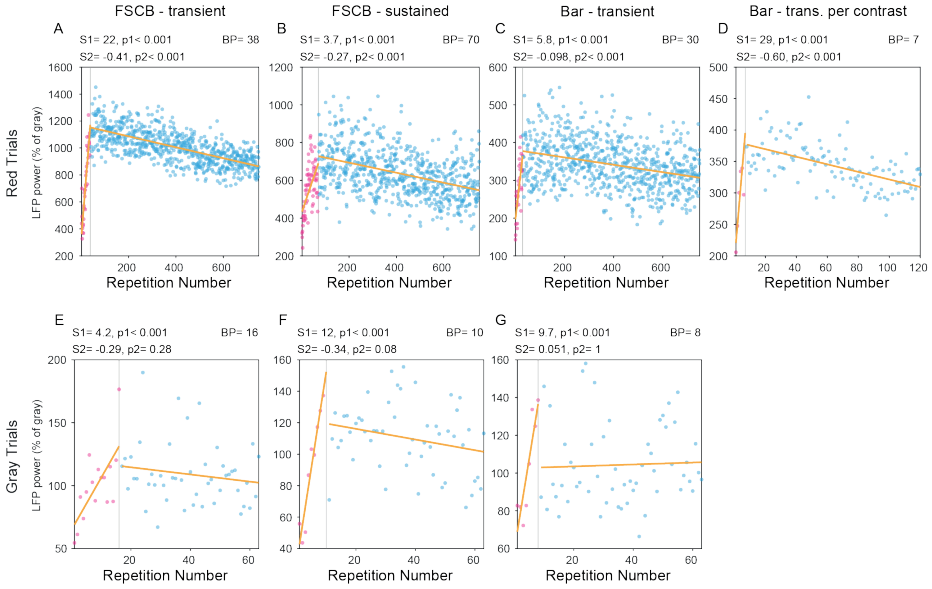

Fig. 3.4. Trial-by-trial analysis of repetition-related changes in LFP gamma-band responses. Same as Fig. 3.2, but for LFP gamma-band power instead of MUA responses.

We also investigated those repetition-related LFP-power changes as a function of frequency within the three task periods, following the same approach as for MUA

(for trial-pooled gamma results and breakpoints see Suppl. Fig. 3.3). This revealed, for the FSCB-transient period, repetition-related LFP power increases in the alpha band and decreases in both the beta and gamma bands (Fig. 3.5A, D). For the FSCB-sustained and the bar-transient period, repetition-related changes were dominated by gamma decreases (Fig. 3.5B, C, E, F). Note that both the FSCB-transient and the bar-transient period most likely contained event-related potentials (ERPs), both for the red and the gray conditions. As we used the gray condition for normalization, the ERP-related spectral perturbations might have influenced the normalized spectra. Therefore, we also considered an alternative normalization, in which the different task periods of the red conditions were always normalized by the FSCB-sustained period of the gray condition. This left the results essentially unchanged (Suppl. Fig. 3.4).

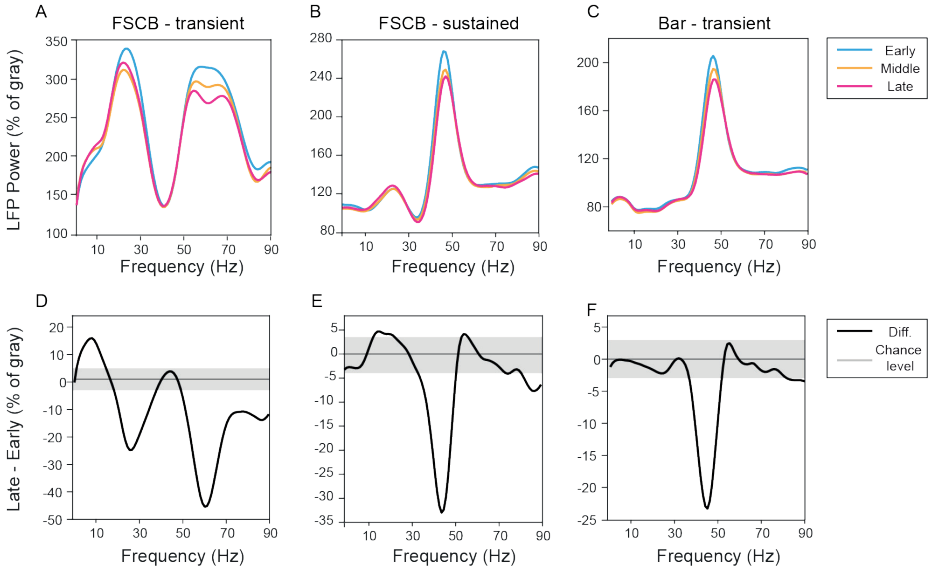

Fig. 3.5. Spectral analysis of repetition-related changes in LFP power. Same as Fig. 3.3, but for LFP power changes during the different task periods, expressed as percent change relative to the corresponding task periods of the gray condition.

Repetition-related changes in MUA-LFP gamma synchronization

We also investigated MUA-LFP synchronization, quantified by the MUA-LFP pairwise phase consistency metric (Vinck, van Wingerden et al. 2010). As the PPC is poorly defined for single trials, we used the same trial-binning approach as in Figs. 3.3 and 3.5.

During the FSCB-transient (Fig. 3.6A, D) and the bar-transient periods (Fig. 3.6C, F), MUA-LFP PPC spectra were dominated by low-frequency synchronization, most

likely due to the transient neuronal responses jointly evoked in MUA and LFP by the FSCB and bar onset, respectively. Those low-frequency components were the only that showed repetition-related changes, namely an increase during the FSCB-transient period and a decrease during the bar-transient period.

During the FSCB-sustained period (Fig. 3.6B, E), the MUA-LFP PPC spectrum showed a low-frequency and a gamma component. Both showed repetition-related decreases. The MUA-LFP PPC gamma component and its repetition-related decrease corresponds closely to the gamma component in the LFP power spectra, suggesting that the LFP power spectra reflect local neuronal synchronization.

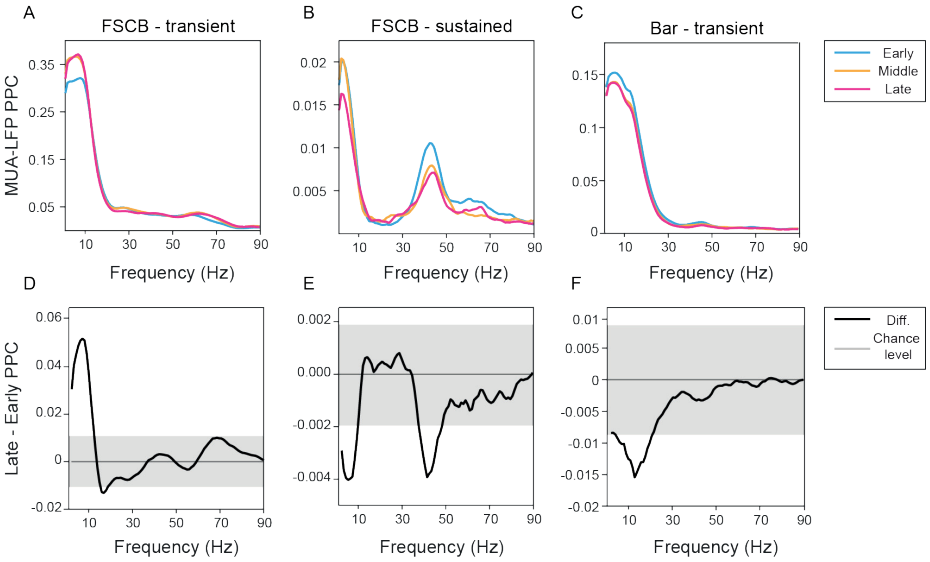

Fig. 3.6. Spectral analysis of repetition-related changes in MUA-LFP PPC. Same as Fig. 3.3, but for MUA-LFP PPC spectra, which are intrinsically normalized.

Isolating responses to the bar and their repetition-related changes

As mentioned above, the repetition-related changes observed for the current stimuli and task were largely opposite to the changes observed previously (Brunet, Bosman et al. 2014, Stauch, Peter et al. 2021, Psarou, Parto-Dezfouli et al. 2025). Those previous studies had used gratings or photos of objects to induce neuronal activity, and those stimuli underwent changes or offsets that temporally predicted the reward. In the present study, the stimulus that temporally predicted reward was the bar. We have already analyzed the neuronal responses to the bar on top of the FSCB. Yet, this response to the compound FSCB + bar stimulus might be dominated by the response to the FSCB, and we therefore set out to isolate the response to the bar by subtracting

the response to the FSCB alone. As a good estimate for this isolated FSCB response, we used the FSCB-sustained period. We subtracted the FSCB-sustained results from the bar-transient results, and refer to the difference as bar-only results (Fig. 3.7). We analyzed this separately for all red-condition trials pooled (Fig. 3.7A, D), for the red-condition trials averaged per bar-contrast condition (Fig. 3.7B, E), and for the gray trials (Fig. 3.7C, F). To our great surprise, those bar-only results showed again the same repetition-related changes that we had found in previous studies, namely for MUA a monotonic decrease (see Fig. 3.7AC for significances), and for gamma an initial decrease followed by an increase for the rest of the trials (Fig. 3.7D-F, both highly significant for most conditions).

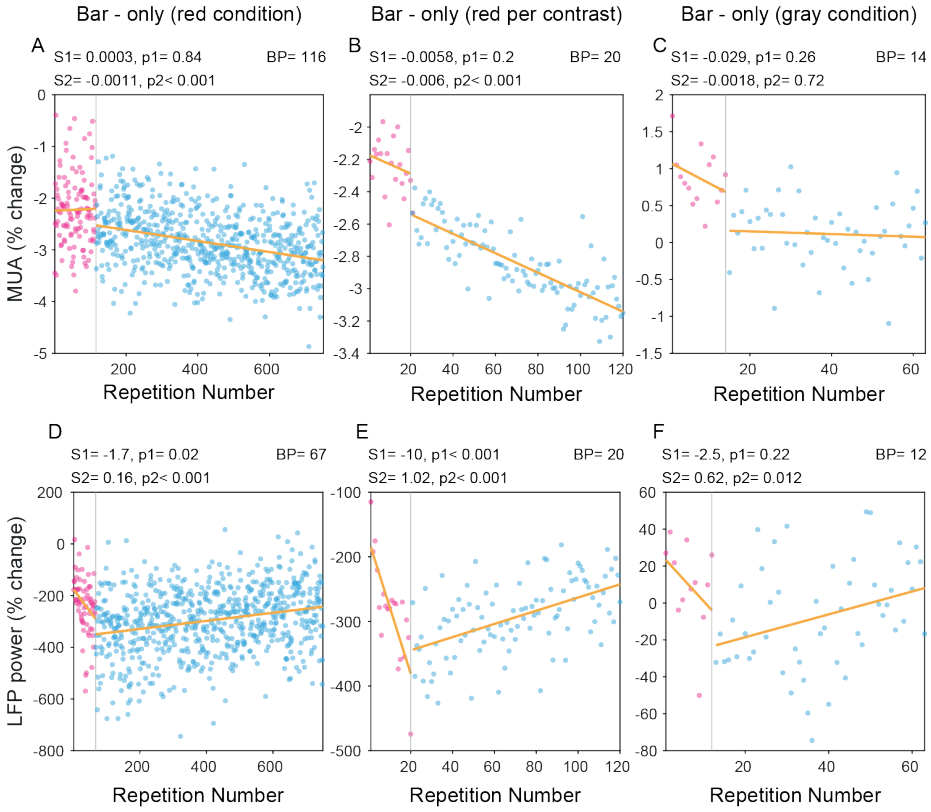

Fig. 3.7. Isolation of MUA (upper row) and LFP gamma power (lower row) responses during the bar-transient period after subtracting the responses to the FSCB-sustained period. (*A*) Same as Fig. 3.2C, but after subtracting the data from the FSCB-sustained period. (*B*) Same as Fig. 3.2D, but after subtracting the data from the FSCB-sustained period. (*C*) Same as Fig. 3.2G, but after subtracting the data from the FSCB-sustained period. (*D*) Same as Fig. 3.4C, but after subtracting the data from the FSCB-sustained period. (*E*) Same as Fig. 3.4D, but after subtracting the data from the FSCB-sustained period. (*F*) Same as Fig. 3.4G, but after subtracting the data from the FSCB-sustained period.

Correlations between repetition-related and stimulus-driven changes

Finally, we tested whether repetition-related changes in neuronal activity were correlated with stimulus-driven changes in neuronal activity. MUA in V1 can be enhanced by many stimuli, and the repetition of those stimuli typically causes MUA response reductions. By contrast, we found, for all conditions except the bar-only condition, repetition-related MUA response increases. Intriguingly, the MUA response in awake macaque V1 to large uniform red surfaces had previously been reported to be a reduction below baseline (Peter, Uran et al. 2019). If this stimulus-induced MUA reduction were itself reduced by stimulus repetition, just like stimulus repetition typically reduces stimulus-induced MUA enhancements, then this might explain our surprising observation of repetition-related MUA increases. If so, the repetition-related MUA increases should be negatively correlated with stimulus-induced MUA changes: the larger the stimulus-induced MUA decrease, the larger the repetition-related MUA increase. We quantified stimulus-induced MUA changes as the ratio of the red condition over the gray condition, and refer to this as the stimulus-related response ratio (SR). We quantified repetition-related MUA changes as the ratio of the last 30 trials over the first 30 trials, and refer to this as the repetition-related response ratio (RR). RR values were positively correlated to SR values during all task periods (Fig. 3.8A-C). This analysis also revealed that the stimuli in this dataset mostly did not suppress but enhance MUA, leading to positive SR values. Both of these observations do not support the possibility that the repetition-related MUA increases were due to repetition-related reductions in stimulus-induced response reductions.

We repeated the same analysis for gamma-band power. For gamma, RR values were not correlated to SR values during the FSCB-transient period (Fig. 3.8D), and they were negatively correlated during the FSCB-sustained and bar-transient period (Fig. 3.8E, F).

Discussion

Summary

We report surprising serendipitous findings from investigating repetition-related changes in MUA and neuronal gamma-band activity in a new dataset. Such repetition-related changes have been reported in several previous publications, whose overall results can be summarized as follows: When a given stimulus is repeatedly presented, (1) MUA responses decrease monotonically with stimulus repetition, with a slope that is steep for the initial ~20 trials and then flattens,

(2) neuronal gamma-band responses increase with stimulus repetition, and this increase can be preceded by a decrease for the initial 4-10 trials. These repetition-related effects were largely reversed in the present dataset: (1) MUA responses decreased for the initial trials in some of the conditions or task periods, but subsequently, MUA responses increased for the remaining trials; (2) neuronal gamma-band responses consistently increased for the initial trials in both the red and the gray conditions and all task periods, and subsequently, neuronal gamma-band responses decreased for the remaining trials for all red-condition task periods and showed the same trend for the gray-condition task periods. However, when we isolated the bar-only response by analyzing the bar-transient minus the FSCB-sustained period, this largely reverted the effects back to those found previously.

Limitations of the study

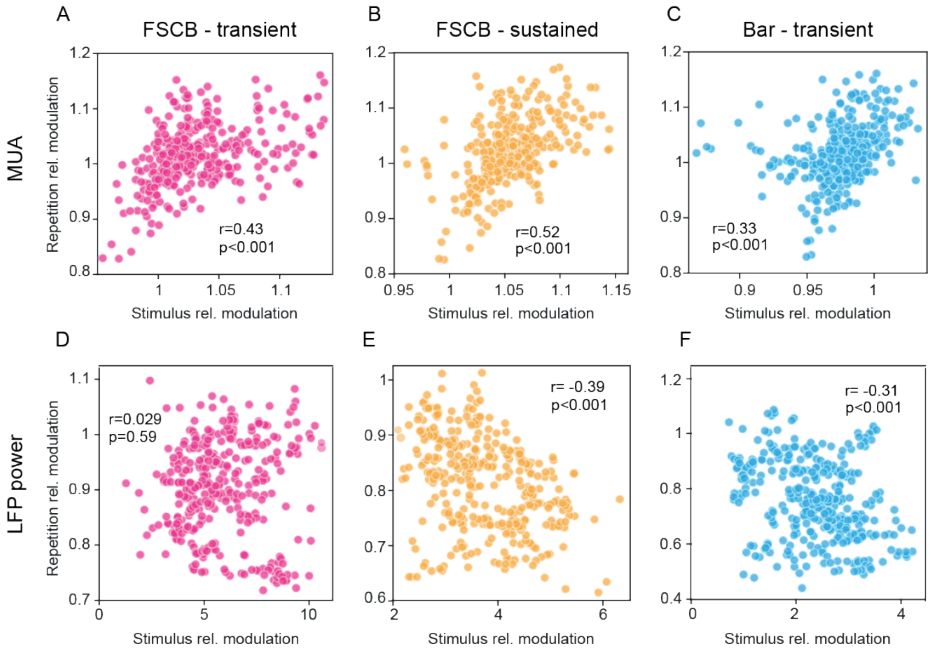

Fig. 3.8. Analysis of correlation between repetition-related and stimulus related modulation. In all plots, each dot represents one recording site, the x-axis value represents the site's stimulus-related modulation (stimulation-over-baseline ratio), and the y-axis value represents the site's repetition-related modulation (late-over-early ratio). The upper row shows the MUA data, the lower row shows the LFP gamma power data. The three columns show the results separately for the three task periods, as indicated on the top. The insets in each plot provide the respective Pearson correlation coefficients and the corresponding p-values.

These surprising findings have been obtained from an experiment that investigated a different effect, namely gamma-rhythmic gain modulation (Ni, Wunderle et al. 2016), and this latter purpose determined stimuli and task. This experimental design leaves several possible explanations for the surprising findings, and it will require future experiments to arbitrate between them. Yet, the observations reported here and in our previous studies on repetition-related gamma changes do allow to argue against some and in favor of some other, intriguing, explanations, and we will spend most of this discussion on this exercise.

Note that also our original report of repetition-related gamma increases was based on a serendipitous finding in a dataset that had been obtained to study selective visual attention (Brunet, Bosman et al. 2014).

The surprising findings are most likely due to experimental differences compared to previous studies. The main differences that appear plausible are: (1) Differences between animals, (2) differences between stimuli, (3) differences between tasks.

An effect of the specific animal?

The animal used in the present study is different from the ones used in Brunet, Bosman et al. (2014) and Peter, Stauch et al. (2021), but the same as used in one previous study: Psarou, Parto-Dezfouli et al. (2025). This latter study with this same animal showed repetition-related changes in MUA and gamma-band responses that were highly similar to the ones reported in Brunet, Bosman et al. (2014) and Peter, Stauch et al. (2021). Thus, the specific animal used in the present study is likely not the reason for the surprising findings. Yet, this one previous study with this same animal also used similar stimuli and tasks as parts of Peter, Stauch et al. (2021) and Stauch, Peter et al. (2021), leaving open the possibility that differences in the present study in either one of those aspects were relevant.

An effect of the specific stimuli?

An effect of using uniform, colored stimuli?

The previous studies reporting repetition-related gamma increases had used gratings (Brunet, Bosman et al. 2014, Peter, Stauch et al. 2021, Stauch, Peter et al. 2021), and one of them had additionally used photos of natural objects (Peter, Stauch et al. 2021). None of them had used uniform, colored surfaces. Thus, this specific choice of stimuli might appear like a plausible candidate to explain the surprising findings. However, we had six recording sessions from the same animal, in which we used uniform colored discs in a task that was highly similar to Psarou,

Parto-Dezfouli et al. (2025). While this was a very limited dataset, the results were fully in line with our previously published reports (Suppl. Fig. 3.5) and do not support an explanation of the surprising findings as a result of using these stimuli.

An effect of using full-screen stimuli?

The previous studies reporting repetition-related gamma increases had mostly used stimuli that did not cover the full screen. However, the original report demonstrated the effect first and very clearly for full-screen gratings (Fig. 1A-C of Brunet, Bosman et al. (2014)). Thus, the use of full-screen stimuli could clearly be eliminated as explanation for the surprising findings.

An effect of the specific task?

This leaves the specific task as an intriguing candidate explanation. To explore this, we first review the main aspects of the tasks that have induced repetition-related gamma increases in previous studies.

In the original report of repetition-related gamma increases (Brunet, Bosman et al. 2014), several different datasets were used. Most of the data were recorded while macaques performed selective attention tasks, during which two patches of drifting grating were presented and one was cued as behaviorally relevant. One of the patches was inside the RF of the recorded neurons, the other one outside, and attention was randomly cued per trial to the stimulus inside or outside. The cued stimulus had to be monitored for a randomly timed change in shape (for the ECoG data in that study) or color (for the V4 microelectrode data in that study), which the animal needed to report by releasing a bar. The behavioral response prompted the disappearance of both the attended and the non-attended stimulus, and their disappearance immediately preceded reward delivery. This same study also reported repetition-related gamma increases for another ECoG dataset. For this dataset, a monkey monitored the fixation point for a color change, while the neuronal activity was induced by a full-field patch of drifting grating. Similar to the attention tasks, the behavioral report of the fixation-point color change prompted the disappearance of the stimulus, which immediately preceded reward delivery.

In the subsequent study (Peter, Stauch et al. 2021), macaques monitored stimuli for randomly timed changes, which were small localized contrast decrements randomly positioned on the stimuli. Those stimuli were either natural stimuli (color photos of isolated leaves, flowers, sweets, fruits, vegetables) or grating patches. Change detection was again reported manually, which prompted stimulus disappearance and subsequent reward delivery.

In the next study (Stauch, Peter et al. 2021), human subjects monitored a large grating patch for a suprathreshold (50%) contrast decrement of the entire grating combined with a near-threshold orientation change. The contrast change prompted the behavioral report of the orientation change. The behavioral report in turn prompted stimulus disappearance and subsequent presentation of a smiley, which provided positive feedback irrespective of behavioral response correctness.

In the most recent study (Psarou, Parto-Dezfouli et al. 2025), macaques fixated while patches of grating were presented in the RFs of the recorded neurons. The duration of stimulus presentation was either 0.8-0.9 s for variable-stimulus blocks, or 1-1.3 s for fixed-stimulus blocks (see ref for details), and the stimulus offset was immediately followed by reward delivery.

In summary, in the previous datasets for which a repetition-related gamma increase has been reported (Brunet, Bosman et al. 2014, Peter, Stauch et al. 2021, Stauch, Peter et al. 2021), the stimulus that activated the recorded neurons was behaviorally relevant for obtaining the reward, and/or stimulus changes or stimulus offsets were predictive of the upcoming reward.

In the present study, as soon as the animal acquired fixation, the FSCB appeared and stayed on throughout the trial. After 1400 to 1650 ms, randomly timed, the bar was presented inside the RF of the recorded neurons for 200 ms. After the bar disappeared, the FSCB turned gray, which was a change for the red-condition trials and no change for the gray-condition trials, and this was followed by reward delivery after a constant interval of 100 ms. Thereby, the bar was predictive of the upcoming reward. Note that when we isolated the neuronal responses to the bar by subtracting the responses to the FSCB, we found similar repetition-related changes as in previous studies. In comparison, the FSCB was less predictive of the reward, as it was presented for a variable amount of time before reward delivery, and it also did not contain any temporal structure predictive of the upcoming bar and/or reward. For the FSCB, the main findings were opposite to the previous studies. Based on these considerations, we would like to speculate as follows.

We will first focus on the changes that we have observed for many repetitions. In the previous studies, that was the repetition-related firing-rate decrease and gamma increase; we will later discuss the changes observed in some datasets (including the present one) for the initial repetitions. Those many-repetition-related changes might be explained by a statistical dependence of the reward on the stimuli. When a stimulus repeatedly predicted a reward, we observed that the stimulus-

induced neuronal responses showed firing-rate decreases and gamma increases. By contrast, and this is the main novel insight from the present study, when a stimulus was repeatedly presented but not reward predictive, or at least there was another stimulus that was much more tightly reward-predictive, then the stimulus-induced neuronal responses showed firing-rate increases and gamma decreases.

We next turn to the changes that we have observed for the initial repetitions in some of the previous studies. In those previous studies this was mainly a firing-rate decrease that was steeper than for the later repetitions, and a gamma decrease for the initial 4-10 repetitions preceding the later gamma increase. This gamma decrease was observed for non-overtrained natural stimuli in macaques and for non-overtrained gratings in human subjects (Peter, Stauch et al. 2021, Stauch, Peter et al. 2021), and it was not observed for highly-overtrained gratings in macaques (Brunet, Bosman et al. 2014, Peter, Stauch et al. 2021, Psarou, Parto-Dezfouli et al. 2025). Therefore, we have previously suggested that the initial presentations of non-overtrained stimuli induce an arousal reaction, which leads to increased gamma, and that this arousal and its enhancing effect on gamma decline over the course of few trials. In the present study, we find similar initial gamma decreases when we isolate the response to the bar, and we find opposite changes, i.e., initial gamma increases when we analyze the response to the FSCB.

In addition, we here make one intriguing observation, which holds both for the responses to the FSCB and the responses to the black bar: the number of those initial trials was similar to previous studies, i.e., in the range of 7 to 20 when we analyzed the gray condition, for which only one bar contrast was used, and when we analyzed the red condition after averaging over the different bar conditions. However, when we concatenated all trials of the red condition, the number of those initial trials was larger, in the range of 30 to 120. When this larger number was divided by 6, i.e., the number of bar-contrast conditions for the red condition, then we ended up with similar initial-trial numbers as in the other cases. This suggests that the changes observed for the initial trials "count" the number of repetitions of a particular black-bar. This might be related to the abovementioned, speculative, mechanism that results from the pairing of a particular stimulus with reward. Yet note, that this putative explanation departs from our previous interpretation of the initial-trial related changes as an arousal-related effect. The arousal in response to the FSCB is not expected to be modulated by the pairing of the preceding black bar with reward.

We emphasize that these latter paragraphs offer speculations intended to explain all observations as parsimoniously as possible, namely as the learning of a stimulus' reward predictability. Yet, those observations have partly been made serendipitously – this applies to the original study (Brunet, Bosman et al. 2014) and the present one – and therefore the stimuli and tasks were not optimized to investigate the observed phenomena, to minimize confounds, and to dissect different possibilities of explanation. At the same time, the observed effects are so striking and appear so fundamental, and the datasets from invasive recordings in awake non-human primates are so precious, that we think those serendipitous findings deserve to be reported. That said, the speculations offered as putative interpretations definitively require rigorous testing in other datasets and experiments that allow the dissection of different possibilities, and we anticipate that this will be a highly fruitful avenue for future research.

Supplementary Material

Supplementary Figures

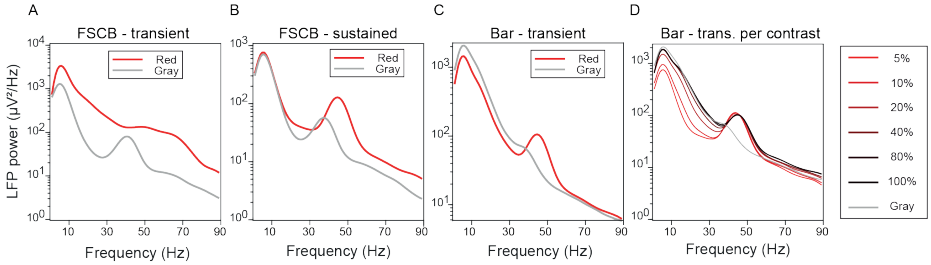

Suppl. Fig. 3.1. Raw LFP power spectra, without normalization. Each plot shows the raw LFP power spectrum, averaged over trials and recording sites, separately for the red and gray condition as indicated by the inset legends. The different plots show the data for the different task periods. For the bar-transient period, the data were either averaged over all contrast conditions (*C*), or separately per contrast condition (*D*), as indicated by the color legend to the right.

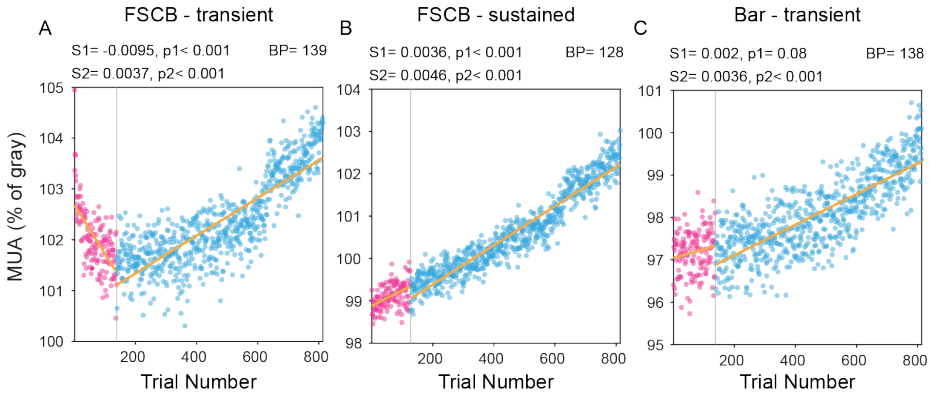

Suppl. Fig. 3.2. Same as Fig. 3.2, but for red- and gray-condition trials combined. As this combines trials of different conditions, those trials do not constitute repetitions of the same stimulus, and correspondingly, the x-axis is not labeled "Repetition number" but "Trial number".

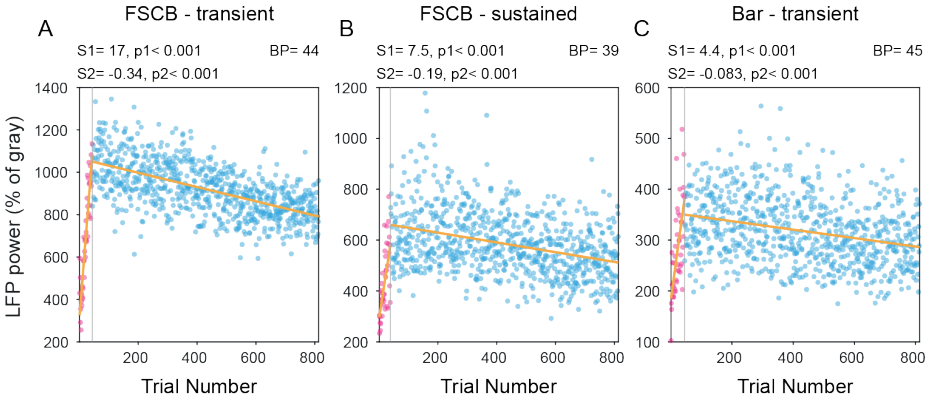

Suppl. Fig. 3.3. Same as Fig. 3.4, but for red- and gray-condition trials combined. As this combines trials of different conditions, those trials do not constitute repetitions of the same stimulus, and correspondingly, the x-axis is not labeled "Repetition number" but "Trial number".

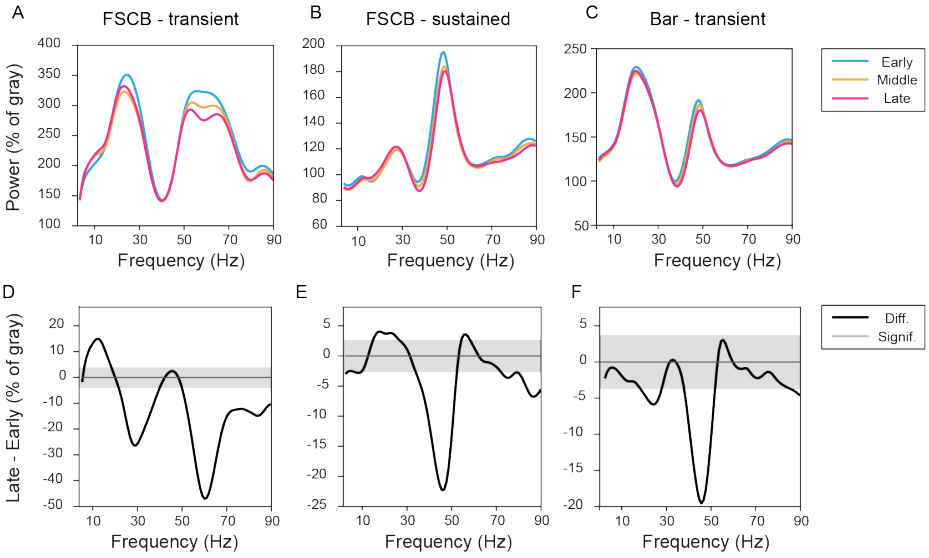

Suppl. Fig. 3.4. Same as Fig. 3.5, but always using the FSCB-sustained periodof the grey condition for normalization.

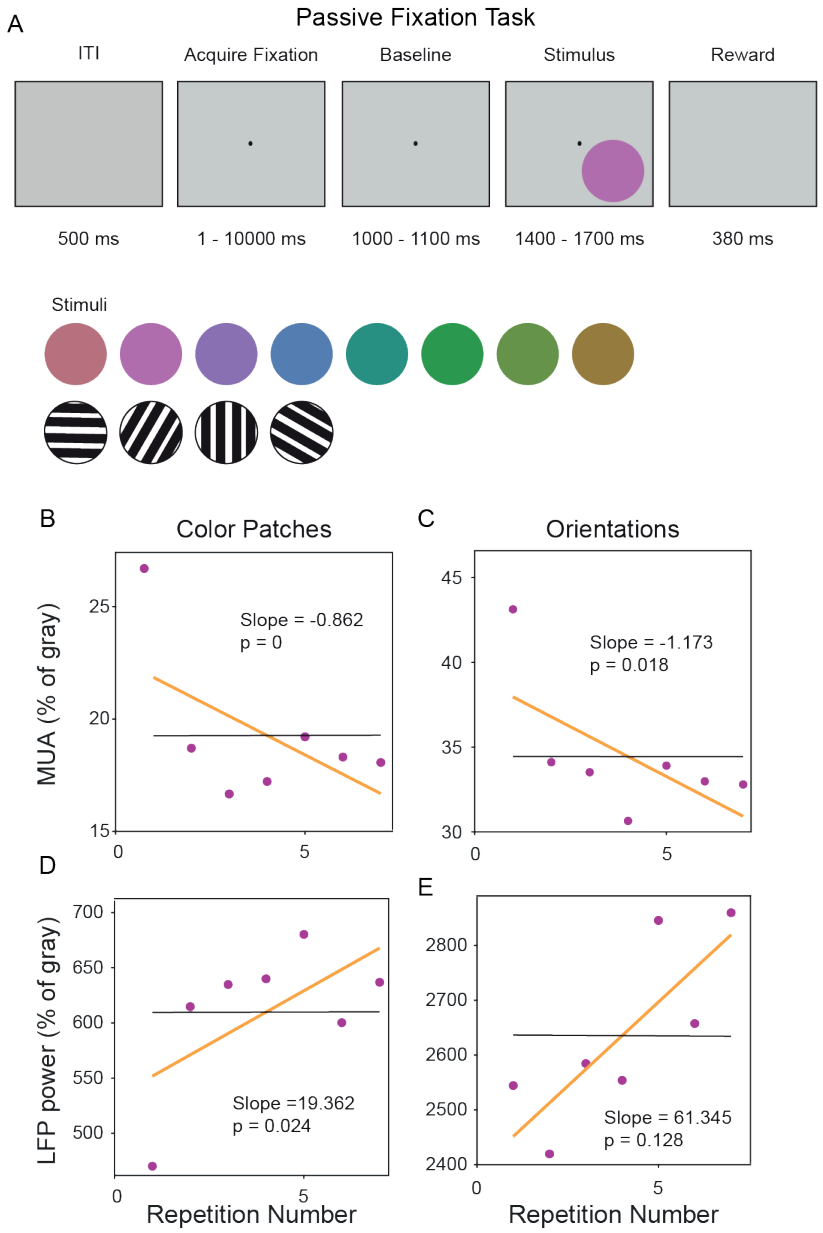

Suppl. Fig. 3.5. Classical results obtained in the same animal for different stimuli and task. (*A*) Illustration of task paradigm and stimuli. (*B*) Trial-by-trial analysis of repetition-related changes in MUA responses to the red-color disk stimuli. MUA responses for the stimulation period, averaged over recording sites and sessions, separately per trial. The yellow line shows the linear regression, whose slope and p-value are given as inset. (*C*) Same as *B*, but for grating patches. (*D*) Same as *B*, but for LFP gamma power. (*E*) Same as *C*, but for LFP gamma power.

Acknowledgments
This work was supported by DFG (FR2557/11, FR2557/21, FR2557/51, FR2557/71), EU (HEALTH-F2-2008-200728-BrainSynch, FP7-604102-HBP), NIH (1U54MH091657-WU-Minn-Consortium-HCP). We thank Dr. Alina Peter for the most useful scientific input, and Rasmus Roese for the invaluable day to day assistance and supervision in the laboratory work.

Author contributions
Conceptualization: M.P., E.P., P.F.; investigation: M.P., E.P., I.G.; methodology: M.P., E.P., I.G., P.F.; software: M.P., M.P.D., E.P.; formal analysis: M.P., M.P.D., E.P., P.F.; writing – original draft; M.P., P.F. writing – review & editing, all authors; visualization: M.P., M.P.D., P.F.; supervision: P.F.; funding acquisition, P.F.

Declaration of interests
P.F. has a patent on thin-film electrodes and is a member of the Advisory Board of CorTec GmbH (Freiburg, Germany).

Materials and Methods

The data used for the current experiment were acquired in the same experimental setup used for the (Psarou, Parto-Dezfouli et al. 2025) study, and by the same collaborators. Moreover, because the (Psarou, Parto-Dezfouli et al. 2025) study also addressed the question of stimulus repetition, some of the analysis methods and statistical testing procedures presented here are very similar to those reported in the above-mentioned study. For this reason, the following descriptions will contain pieces of text that are copies or close to literal copies of (Psarou, Parto-Dezfouli et al. 2025), while avoiding the placement of those sentence parts in quotes, which would have impoverished readability.

Surgical procedures
All experiments on NHP were performed in compliance with the German and European ethical guidelines and regulations for the protection of animals. The experimental procedures were reviewed and approved by the German regional authority, the Regierungspräsidium Darmstadt.

One adult male macaque monkey (*Macaca Mulatta*), 19 years of age, weighing 13 kg, was used in this study. We used one rather than the more typical two or three animals, because we recently showed that the inference with the addition of

a second or third animal is still limited to the sample (Fries and Maris 2022, Laurens 2022, Psarou, Katsanevaki et al. 2024). Thus, doubling or tripling the number of used animals would not change the quality of the inference, and ethical considerations mandate the use of one animal. All surgical procedures performed on the animal were carried out under general anesthesia, and analgesic and antibiotic treatments were administered in the postoperative time period.

The procedure for head-post implantation followed a two-step approach, described in detail in Psarou, Vezoli et al. (2023). Subsequently, a modular custom-made titanium recording chamber for acute recordings was implanted. The chamber was fixed over the occipital area of the skull corresponding to visual area V1, on the left hemisphere. AAV virus injections into V1, used for other experiments, were performed at locations remote from the recording locations used here.

Visual Stimulation

Visual stimuli were presented on an LG 32GK850G-B monitor (LG Electronics Inc., Seoul, South Korea), and gamma correction was applied in all tasks (gamma: 1.57). The monkey's eyes were at a distance of 83.5 cm from the screen. The precise times of black-bar presentation were recorded by simultaneously presenting a small stimulus in the corner of the monitor, occluded from the monkey's view, and recording that small stimulus with a custom-made photo-diode signal.

Receptive field (RF) estimation

The RF position and orientation preference were determined after averaging neuronal responses over all electrode contacts on the laminar probe that were deemed to be located inside the cortex, as is explained in the corresponding section below. The electrode contacts were densely spaced, such that RF positions and orientation preferences were expected to be similar across simultaneously recorded contacts.

RF position was determined at the beginning of each recording session by using the back-projection method described in Fiorani, Azzi et al. (2014). Per trial, one bar moving in one of eight possible directions across the entire monitor was presented while the monkey kept fixation on a central fixation spot. The moving bar was 0.1 deg wide and had a speed of 8 deg/s. Ten correct trials for each direction were collected, for a total of 80 correct trials.

The MUA spike density functions were accumulated over time to reconstruct a spatial response map that indicated the position of the receptive field, after

correcting for the response latency which maximized the back-projection response. The MUA's response-based receptive field position was inferred by smoothing MUA responses with a Gaussian function for each direction of movement, and taking the 10th and 90th percentile and fitting an ellipse to the resulting data points.

Orientation tuning task

The orientation preference of the located RF was inferred with a dedicated orientation tuning task. Per trial, a 0.1 degrees of visual angle (dva) wide and 0.3 dva long bar of one of six possible orientations, was presented at the location of the RF, while the monkey was required to keep fixation on the central fixation spot. A trial was considered correctly performed if fixation was maintained. Ten correct trials for each orientation were collected for a total of 60 trials. The preferred orientation was inferred by directly comparing the MUA (or LFP in case of low MUA signal) response amplitude across the 6 orientations and choosing the orientation with the highest related MUA response. The screen background during the orientation-tuning task was gray (RGB 128, 128, 128).

Behavioral task

During training and recordings, the monkey sat in a primate chair located inside a fully shielded recording booth, with dim illumination. All recordings were performed under head fixation. The behavioral paradigm was created using ARCADE (Dowdall, Schmiedt et al. 2018), a custom software built in house using MATLAB.

The monkey performed a fixation task. The animal acquired fixation on a central black fixation dot, 0.3 dva diameter, positioned in the center of the gray screen, and maintained fixation in a tolerance radius of 0.5 dva from the fixation spot. A trial was considered correctly performed when the monkey kept fixation for the whole duration of a trial (1600 to 1850 ms), and was rewarded with the delivery of grape juice.

Each trial consisted of the presentation of a sequence of visual stimuli on the monitor. Each trial began by showing a gray background screen (RGB coordinates [128, 128, 128]) together with the central fixation dot. The monkey was allowed a time period of maximally 10 seconds to acquire fixation, yet they typically attained fixation much quicker.

As soon as the animal started fixating, a full-screen colored background (FSCB) was shown. The FSCB was red colored (RGB coordinates [255,0,0]) in 90% of the trials (red-condition), while in 10% of the trials, the screen maintained the same

gray color as the initial background (gray-condition). The gray trials were taken as a baseline reference for the red trials. The FSCB time period had a constant duration of 1400 ms, plus a time jitter ranging from 0 to 250 ms to precede the following section of the trial.

After the FSCB time period, the FSCB, red or gray, was kept in place, and an additional visual stimulus in the shape of a black bar was presented inside the previously determined RF for 200 ms. The black bar had a length of 0.3 dva, a thickness of 0.1 dva and was oriented according to the preference of the recorded neurons. In the red condition, the black bar stimulus was presented at 6 contrast levels (see below), while in the gray condition, the black bar stimulus was always shown at full contrast. After bar offset, a waiting period of 100 ms elapsed after which the animal was rewarded. Fixation breaks led to immediate termination of the trial, and no reward was given.

During each inter-trial interval (ITI, 700 ms), a colorful noise mask was presented on the screen. The noise mask was composed of squares of height and width ranging from 0.1 to 0.5 dva in steps of 0.01 dva, and each square had a color randomly selected from the possible RGB color coordinates. This mask was intended to counteract color adaptation effects.

Color contrast and normalized color space

In the red condition, the black bar stimulus was presented at six contrast levels: 5%, 10%, 20%, 40%, 80%, 100%. The contrast was calculated based on the Weber contrast formula:

$$\frac{I - Ib}{Ib}$$

where I indicates the luminance of the stimulus, and I_b indicates the luminance of the background. In order to define contrast levels appropriately, color coordinates for the red background and for the black bar foreground stimulus were chosen from the CIELAB standardized color space (Gravesen 2015), then translated to RGB coordinates.

Color patches and oriented gratings task

Results shown in Suppl. Fig. 3.5 were obtained by analyzing data collected with a dedicated task. Every trial of the task started with an inter-trial interval (ITI) of 500 ms, presenting a grey screen (RGB [128,128,128]). An acquire-fixation time window started right after the ITI. A central fixation dot of 0.5 dva, dark gray in color

(RGB [204,204,204]), was presented on the screen. In this time window, the monkey was allowed a maximum of 10000 ms to acquire fixation. After fixation was acquired, the monkey was required to maintain fixation for the duration of a baseline time window of 1000 – 1300 ms, during which the screen kept the initial grey color. At the end of the baseline window, the visual stimulus was presented during a 1300 – 1800 ms long time window. The stimulus consisted in a circular patch of uniform color or of grating. The circular-colored patch had a 7 dva diameter, covering RFs, and could assume one of the following colors: RGB [149,112,198], [188,107,180], [191,115,129], [160,130,60], [103,143,6], [44,147,59], [37,140,128], [90,126,179]. The grating stimulus was also circular, had a 3.5 dva diameter, a spatial period of 0.5 dva, and was approximately centered on the RF. The grating could assume one of four possible orientations: 0, 45, 90 or 135 degrees. If the monkey maintained fixation for the whole trial duration, the trial was considered correct, and the monkey was rewarded with delivery of grape juice.

Eye position

Eye position was recorded at 1000 Hz using an Eyelink 1000 system (Eyelink Inc., SR research Ottawa, Canada). The system was calibrated on the left eye at the beginning of every recording session, and the left-eye signal was recorded.

Recordings

In each recording session, one laminar probe was introduced through the intact dura into the cortex. Laminar probes featured 16 channels in one column, spaced by 50 micron (linear V-probes from Plexon Inc., Dallas, Texas, USA). The probe was guided by a guide tube that rested on the dura. For the recordings, the guide tube served as ground and the shank of the probe as reference. Recordings were performed in a fully shielded booth acting as a Faraday cage that prevented disturbance of the electrophysiological signal by line noise. Correspondingly, line-noise removal was not necessary and not performed.

Electrophysiological data were acquired using Tucker Davis Technologies (TDT, Alachua, Florida, USA) systems. Raw data were recorded and digitized by a TDT PZ2 pre-amplifier at 24.4140625 kHz.

Data Analysis

All analyses were carried out in MATLAB and using the FieldTrip toolbox (Oostenveld, Fries et al. 2011).

Preprocessing

Raw data were downsampled to 1000 Hz. For the LFP, this entailed upsampling to 3,125,000 Hz, downsampling to 25,000 Hz, filtering with a stop-band at 500 Hz (IIR filter) and downsampling to 1000 Hz. For the MUA, this entailed upsampling to 3,125,000 Hz, band-pass filtering at 300-12000 Hz, rectification, stop-band filtering at 500 Hz (IIR filter) and downsampling to 1000 Hz.

Recording site selection

During each recording session, we performed one penetration with one laminar probe. The probe was positioned under online visual inspection of the neuronal signals and their general responsiveness to visual stimulation, such that typically all recording sites provided good MUA and LFP responses. Yet, some recording sites did not provide clear RFs, and those recording sites were identified by visual inspection and not used for further analyses. The remaining recordings sites will be referred to as "selected recording sites", or "selected sites".

Spectral analysis

For the spectral analysis, the LFP in the 200 ms long FSCB-transient, FSCB-sustained or bar-transient periods was multiplied with a Hann taper, zero-padded to 1s, and Fourier transformed using the FieldTrip function ft_freqanalysis.

Baseline normalization

All analyses except Fig. 3.1B, C and Suppl. Fig. 3.4 use the gray condition as baseline, separately per task period. For the MUA, separately per recording site, each task period provided one value for the gray condition, averaged over time points and trials. This gray-condition value was used to express the corresponding red-condition MUA as percent change relative to the gray condition. The same was done for the LFP, except that the LFP was first transformed to a spectrum, and the averaging and normalization was done per frequency, providing a frequency-wise LFP power change spectrum during the red condition relative to the gray condition.

For Suppl. Fig. 3.4, the same procedure was followed, except that the normalization was not by the corresponding task period of the gray condition, but always by the FSCB-sustained period of the gray condition.

For Fig. 3.1B, C the signals, both the raw LFP and the MUA, were expressed as percent change relative to the average respective values during the gray-condition FSCB-sustained period. This was done per recording site, with subsequent averaging over sites.

Estimation of gamma peak frequency and gamma band

The LFP power change spectra as compiled for the main analyses were used to determine the gamma peak frequency. The gamma peak frequency was estimated after averaging over all recording sites from all sessions, yet separately for the FSCB-transient, FSCB-sustained and bar-transient. The frequency associated with the maximum power change value in the 3090 Hz range was defined as the gamma peak frequency, and a band of +/- 10% around the peak was defined as the gamma band.

Analysis of repetition-related changes across trials

To visualize and quantify repetition-related changes across trials, LFP gamma power and MUA were averaged over recording sites and sessions, separately per trial. For this, only the trials present in all sessions were used. In other words, the session with the smallest number of trials for the respective stimulation condition determined the number of trials that was used from all other sessions. When all trials of both the red and the gray condition were considered together, this resulted in 813 trials (Suppl. Fig. 3.2 and Suppl. Fig. 3.3). When all trials of the red condition were considered, this resulted in 750 trials (Fig. 3.2A, B, C, Fig. 3.4A, B, C, Fig. 3.7A, D). When all trials of the red condition were considered, yet averaged separately per bar-contrast condition, this resulted in 120 trials (Fig. 3.2D, Fig. 3.4D, Fig. 3.7B, E). When all trials of the gray condition were considered, this resulted in 63 trials (Fig. 3.2E, F, G, Fig. 3.4E, F, G, Fig. 3.7C, F).

Visual inspection of the resulting trial-by-trial MUA and gamma values suggested that they could generally be described as a linear increase, or a linear decrease, or a combination of those two with a relatively well-defined break point in between. Furthermore, as discussed in the results and discussion sections, visual inspection suggested that the break point occurred at approximately trial number 4 to 20, times the number of bar-contrast conditions that was relevant for the respective analysis. Finally, we intended to treat all data as uniformly as possible. Therefore, we fitted the data with two linear regression lines, separated at a break point that was constrained to lie at trial 4 to 20, times the number of bar-contrast conditions that was relevant for the respective analysis. The number of bar contrast conditions that was relevant for the respective analysis was seven for the all-trials condition (Suppl. Fig. 3.2 and Suppl. Fig. 3.3), six for the red condition (Fig. 3.2A, B, C; Fig. 3.4A, B, C; Fig. 3.7A, D), one for the gray condition (Fig. 3.2E, F, G; Fig. 3.4E, F, G; Fig. 3.7C, F), and also one for the red condition after averaging over bar-contrast conditions (Fig. 3.2D; Fig. 3.4D; Fig. 3.7B, E). The decision about the precise trial constituting the break point was made objectively by using the approach described in (Bogartz 1968). This approach

is one version of a segmented linear regression. The algorithm iteratively considers each trial as a potential break point, and subsequently selects that trial as break point that minimizes the sum of the squared errors of the two regression lines.

PPC analysis

Local neuronal synchronization was assessed by calculating the Pairwise Phase Consistency (PPC) (Vinck, van Wingerden et al. 2010) between MUA and the LFP (Fig. 3.6), as implemented in the FieldTrip toolbox (Oostenveld, Fries et al. 2011). For each session, respectively for each laminar-probe penetration, we calculated PPC between all combinations of MUA and LFP from all selected recording sites, except between MUA and LFP from the same recording site. This latter exclusion was made to minimize spectral bleeding of spikes into the LFP. We used the "unipolar" LFP, i.e., the LFP referenced against the laminar-probe shaft. Subsequently, the MUA-LFP PPC was averaged over site-pair combinations. PPC was based on Fourier transforms of the MUA and the LFP during the task period and trial groups as described in the results section.

Statistical analysis

Statistical testing was performed (1) for the segmented linear regressions quantifying the trial-by-trial MUA or gamma responses (Fig. 3.2, 3.4, 3.7, Suppl. Fig. 3.2, Suppl. Fig. 3.3), (2) for the simple linear regression quantifying the trial-by-trial MUA or gamma responses in the very few trials with color or grating patches (Suppl. Fig. 3.5), (3) for the comparison of MUA change time courses, LFP change spectra, or MUA-LFP PPC spectra between late and early trial groups, including correction for multiple comparisons across time points or frequencies (Fig. 3.3, 3.5, 3.6, Suppl. Fig. 3.4).

Regarding the statistical tests for case (1): The segmented linear regression was performed on the observed trial-by-trial data, giving two observed regression slopes. Subsequently, the trial numbers were randomized, and the segmented linear regression repeated, and this randomization was performed 1000 times. The slopes obtained across randomizations were collected in two randomization distributions, one for each segment. Per segment, we first determined whether the observed slope was positive or negative and then determined the number of randomization slopes with the same sign that exceeded the observed slope. This number was divided by the total number of randomizations and multiplied by two, and the resulting value was taken as p-value of a two-sided test.

Regarding the statistical tests for case (2): This followed the same approach as case (1), except that the regression was not segmented, but performed across all of the few available trials.

Regarding the statistical tests for case (3): We first obtained the observed difference time course or observed difference spectra of the late minus the early trial group. Subsequently, we randomly exchanged trials between the late and the early trial groups and recalculated the differences, and this was performed 1000 times. Importantly, for each randomization, only the minimal and the maximal difference – across all time points or frequencies - was retained and placed into the minimal randomization distribution and the maximal randomization distribution, respectively. The 2.5^{th} percentile of the minimal randomization distribution and the 97.5^{th} percentile of the maximal randomization distribution were taken as thresholds for statistical significance at a false-positive level of 5%, including correction for the multiple comparisons across time points or frequencies, respectively (Nichols and Holmes 2002).

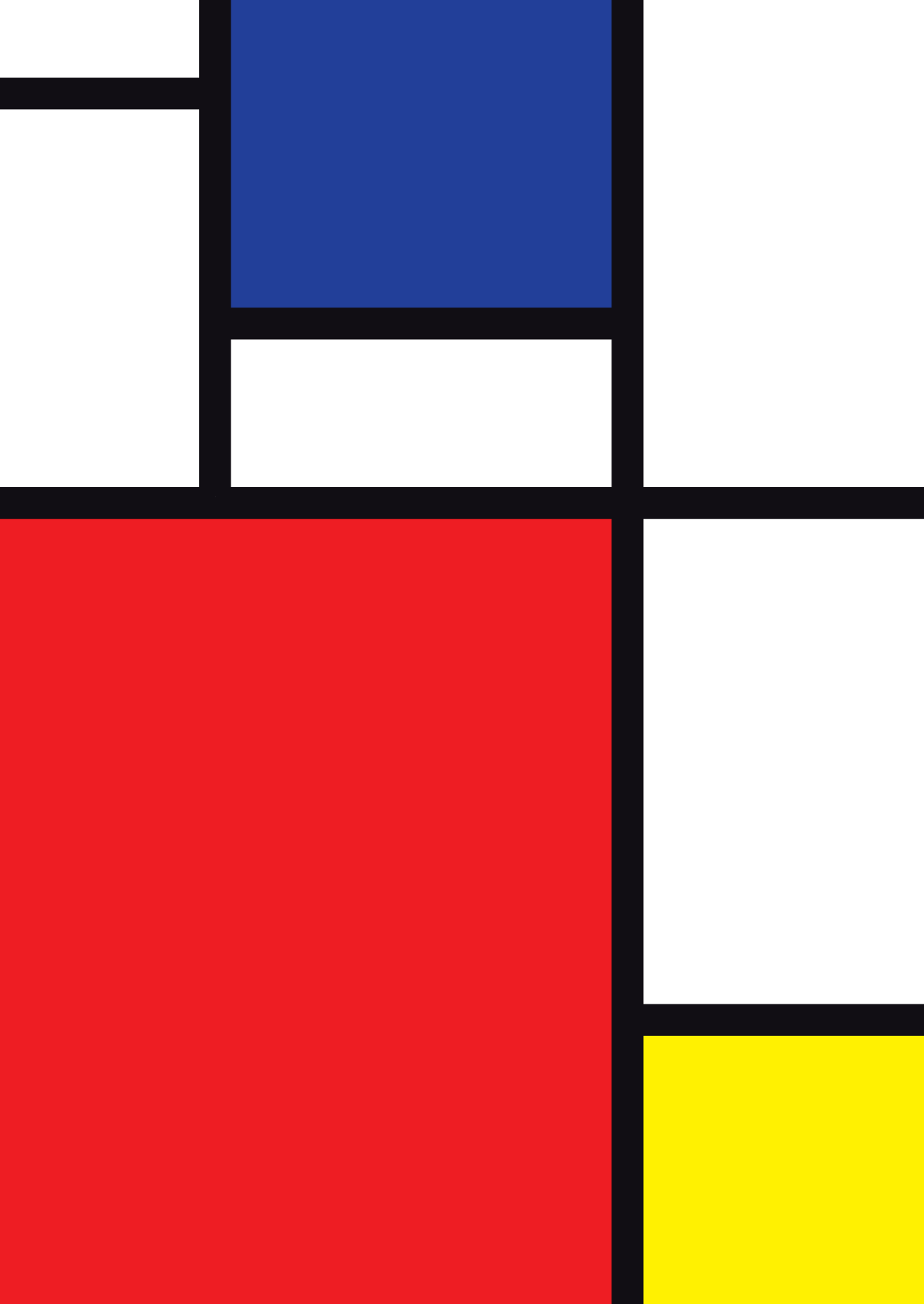

Chapter 4

General Discussion

Summary

The scientific questions that motivated this thesis work mainly revolved around revisiting in a new light some long-standing concepts in neuroscience: the rhythmic activity in the gamma-band and the neuronal spiking (as in a continuous MUA trace), and the relationship they entertain with each other. These concepts were investigated in the context of gamma-rhythmic gain modulation of the MUA, by revisiting an older study on the same topic (Ni, Wunderle et al. 2016) in Chapter 2, and in the context of a stimulus repetition paradigm, in Chapter 3. Whilst the study presented in Chapter 2 managed to replicate the results of the original Ni, Wunderle et al. (2016) only partially, the study presented in Chapter 3 yielded interesting new insights on the topic of stimulus repetition, expanding the notion of this paradigm to consider behaviorally relevant reward prediction effects.

Gamma rhythmic gain modulation

Chapter 2 focused on assessing the effect of gamma-band oscillatory activity on neuronal gain, and if this effect could correspond to a multiplicative modulation, and also on trying to define the absolute phase of this modulation, and the model of gain modulation – input or output – put in place by gamma on V1 cortical neurons. The experimental paradigm involved triggering the activation of a strong gamma-band rhythmic activity with the use of a red-colored FSCB, and then testing how the phase of this gamma rhythm impacted on the neuronal response to the presentation of a test stimulus, a black bar, at a random time. It was possible to demonstrate that gamma band activity rhythmically modulates the neuronal gain, replicating the 2016 study findings, but not that this effect is specific to gamma, since significant modulation was exerted also by alpha beta and high gamma frequency bands. The absolute preferred phase of the modulation imposed by gamma ranged always between -30˚ and +30˚. The evidence that mid-level contrasts, like 40% contrast, were subject to the highest phase modulation effect indicated that the modulation model imposed by gamma on MUA was consistent with an input-gain model, even though this could not be unequivocally demonstrated.

Stimulus repetition effects

Chapter 3 reported a study about the effect of stimulus repetition. The study presented serendipitous observations for the set of stimuli that were included in the visual stimulation paradigm used in Chapter 2: the FSCB in red or gray color, and the FSCB with the superposition of a black bar. The effect of stimulus repetition was studied on both oscillatory activity in the gamma band, and MUA. The effects reported in this study were surprising, as they were opposite to the

results commonly described in classical literature about repetition for a plethora of different stimuli and stimulation conditions (Brunet, Bosman et al. 2014, Peter, Stauch et al. 2021, Stauch, Peter et al. 2021, Psarou, Parto-Dezfouli et al. 2025). Gamma-rhythmic activity is classically described as mainly increasing – sometimes after an initial decrease - with stimulus repetition, while in the context of Chapter 3 study, it was steadily decreasing, after an initial set of trials that showed increase in gamma band power, for both the FSCB and the FSCB in combination with the black bar. The opposite pattern of results was observed for the MUA: while it is classically described to decrease over the course of repetitions, it was steadily increasing after an initial decrease (the latter only for some conditions). Interestingly, the reported results reverted again when isolating the effect of the black bar from the FSCB, and went back to classical results where gamma band activity is increasing while neuronal spiking (MUA) is decreasing.

Considerations and future perspectives for gamma rhythmic gain modulation studies

Chapter 2 revealed that gamma-band activity multiplicatively modulates gain affecting neuronal sensitivity, with a model consistent with an input gain. Some considerations will be presented here regarding the gamma-band gain modulation. First, some observations will be made about the specificity feature of the gain modulation predicted by CTC, recalling what was explained in the *Gain modulation and gamma-band oscillatory activity* paragraph, and in the *Mechanisms implementing gain modulation* paragraph in Chapter 1. Then, the input gain feature of the modulation will be discussed. Finally, because frequencies other than gamma were also found to modulate MUA gain, some considerations will be expressed on the topic.

Gamma-rhythmic gain modulation, stimulus specificity, and input gain model

The *Gain modulation and gamma-band oscillatory activity* paragraph in Chapter 1, described some predictions stemming from the CTC hypothesis about the kind of modulatory influence that gamma-band activity would impose on the neuronal gain. Specifically, one of these predictions regarded the fact that gamma band activity should be able to implement gain modulation with a mechanism that would manage to keep stimulus specificity, and act on the precise synaptic input carrying information about a specific stimulus. Nevertheless, in the *Mechanisms implementing gain modulation* paragraph, several currently known mechanisms were listed to describe how a modulation of the neuron's I/O response curve can

be put in action, and it emerged that a mechanism that would implement gain modulation on a specific input to the cell is not known or has not been described yet. The mechanisms mentioned were, for example, a change in the neuron's V_m, GABAergic inhibitory activity like shunting inhibition, or the regulation of the synaptic input drive to a neuron. These mechanisms are capable of implementing different kinds – input, output, multiplicative, additive - of gain modulation, but all of them affect the post-synaptic neuron as a whole, or at least they affect the cumulative input drive to the cell, without providing any distinction between single synaptic inputs to the neuron that participate to the global summed input drive. Shunting inhibition, to mention one, is thought to act on the apical dendrite of a neuron, close to the soma (Callaway 2004, Bartos, Vida et al. 2007, Ferguson and Cardin 2020), so it will influence the overall input drive that is constituted by the single synaptic inputs the neuron summed all together. It could be argued that top-down synapses synapsing onto bottom-up synapses could be able to specifically modulate the gain of the latter (Callaway 2004), but this would require that top-down synapses' activation pattern contain information that is typically carried by the top-down ones. Moreover, this hypothesis would still leave open the problem of the combinatorial explosion of synapses that would be required to represent every possible stimulus –selective gain modulatory projection combination to achieve gain modulation specificity, as more extensively argued in the introduction of Katsanevaki, Bastos et al. (2023). Evidently, a convincing cellular-level mechanism capable of implementing an input-specific gain modulation has not been described yet, and it was also not possible to investigate this aspect with the results at our disposal in this dissertation. One hypothesis that is possible to advance considering the CTC framework is based on the idea of multiplexing. The synaptic input related to a specific stimulus could entertain a preferential relationship with the inhibition clock timing the reset of each gamma cycle, via a temporal channel. This means that the inhibitory neurons involved in the generation of a gamma cycle act, so to say, as gatekeepers, and the input relative to the specific stimulus could be sent forward at a preferential time point, right before the gate favoring synaptic integration is closed by inhibition. This could explain the specificity feature of the gain modulation effect, but further research on the topic will be needed to shed light and try to bring evidence to support this prediction from CTC.

Stimulus-specific modulation of the neuronal gain has to be distinguished from the feature of non-changing stimulus selectivity implied in the definition of multiplicative gain modulation. While both concepts refer to an aspect of "stimulus specificity", this assumes a very different meaning in the two contexts. The stimulus-specific modulation of the neuronal gain described above and in Chapter 1,

is a prediction stemming from CTC, related in particular to the implementation of selective attention processes at neuronal level. In this case, gain modulation must be selective, or specific, for the attended stimulus and not change. On the other hand, gain modulation of the multiplicative kind is described as a transformation that affects neuronal sensitivity to a stimulus, without affecting stimulus selectivity (see also Chapter 1). This entails the preservation of the tuning curve of a neuron that has in this sense to keep its specificity, or selectivity, so that the curve does not change. Regarding the latter aspect, consistency in neuronal stimulus selectivity related to multiplicative gain modulation was not directly tested in Chapter 2 with appropriate task conditions: this could represent an interesting follow up study to the results reported in this thesis.

Lastly, the study in Chapter 2 revealed that the modulation imposed by gamma is consistent with an input response model, rather than an output one. This is also in line with the predictions stemming from CTC (Fries 2009), as rhythmic synchronization in time windows of few milliseconds guaranteed by gamma rhythm, not only affects the efficacy of local spike output by grouping the action potentials in windows of excitability, but also affects the input to the local network engaged in gamma activity, because the inhibitory cells activate cyclically inhibiting the involved postsynaptic cells, hence the input gain modulation. An output gain modulation model would impact on the spiking output of the local network, by multiplicatively scaling it according to gamma phase, and this would probably represent a less energy efficient mechanism to potentiate neuronal response, because the gamma rhythm already increases the efficacy of the spiking output by grouping it according to its phase.

Rhythmic-gain modulation: frequency ranges other than gamma, local circuits and stimuli

The gamma rhythmic gain modulation study showed that frequency bands other than gamma were significantly modulating the neuronal gain in a multiplicative way. While some potential explanations of this phenomenon were elucidated already in the Discussion section of Chapter 2, it is interesting to connect these findings to one of the basic properties of the brain-wide oscillatory activity described in the Chapter 1 of this thesis, which is the tendency of brain rhythms to act in concert one with the other (Buzsáki and Draguhn 2004, Canolty, Edwards et al. 2006). Brain rhythms can be nested into each other, specifically, slower rhythms will tend to create rhythmic scaffolds where faster rhythms can be embedded, and therefore be modulated or reset. Brain rhythms can also engage in complex interactions due to cross-frequency coupling, and this way support the encoding of

nested relations so to represent complex objects (Buzsaki, Logothetis et al. 2013). In this light, modulation of the neuronal gain could be studied and interpreted as a result of the interaction of multiple frequency bands, rather than associated to the specific activity of a single one. Future experiments specifically tailored to this scope will be necessary to address the topic and shed further light on the possibility that modulation of the neuronal gain is supported by the interaction of multiple frequency bands.

Another important point to further investigate in the future, in order to reach a convincing explanation of the phenomena observed in Chapter 2, lies in the precise structure of the circuits generating gamma band oscillation, and the type of inhibitory cells participating to the rhythmic activation. As mentioned in Chapter 1, the specific cell types involved in the generation of gamma-rhythmic activity in NHP have not been extensively studied yet, so it will be crucial to elucidate more details about the cellular composition of the local circuits. In addition to this, it will also be of importance to broaden the understanding of the role of lateral and long range connections in local circuits, by connecting their anatomical connectivity and functional implications with the effects here described, since these kind of connections can strongly impact the gamma rhythmic synchronization and the modulation of the neuronal gain (Vinck and Bosman 2016). One initial step directed towards this goal in the context of the studies presented in the current dissertation could be to analyze layer specificity of the effects described here, and put them in relation with the literature describing primate V1 structural architecture in terms of feedback and feedforward connections and neuronal types (Callaway 1998, Callaway 2004).

The two points indicated above, about the necessity of further studies to fully elucidate the brain mechanisms leading to the results described in Chapter 2, will have to be considered together with the possibility that the effect witnessed in the context of this experiment are due to the specific conditions of the visual stimulation used. A full-screen background and a full-screen background in conjunction with a black bar represent a set of stimuli which is quite different from those used in other studies, with effects that might diverge from those described in the study that has been here replicated, which used traditional gratings (Ni, Wunderle et al. 2016). More in general, the stimulation protocols used to investigate aspects of the visual system and the processing of the stimuli, have always been of a very artificial kind, significantly distant from the everyday stimulation conditions the brain is commonly subject to in the process of vision. This represents a *caveat* for the interpretation and the generalization of these findings. In the future, it will

be necessary to reproduce the results described here and in the previous studies with more naturalistic stimulation conditions, in order to make more general and possibly more valid claims about the nature of the functioning of the brain. The studies conducted under more unnatural stimulation conditions will offer anyways valid insights, because they could serve to test in case of more extreme stimulation conditions the validity of certain hypotheses made under naturalistic condition testing.

Surprising repetition effects: more on the relation with classical studies and the reward prediction framework

The study about stimulus repetition presented in Chapter 3 led to interesting serendipitous findings, opposite to the ones classically described by repetition related studies. It is necessary to stress that the study was not tailored to the scope of investigating repetition effects, so in the future it will be necessary to carry out more research to evaluate again the findings that are presented in Chapter 3, and control with a better precision all the variables that could have played a role in determining the results opposite to the classical literature. In any case, some interesting considerations can be made in the context of this study about stimulus homogeneity and reward prediction.

Repetition in the context of stimulus homogeneity and mechanistic models of brain computational efficiency

The experimental task described in Chapter 3 can be considered homogeneous for its structure, as the same stimuli in the same order of presentation were repeated over and over again in each trial during the course of a recording session. Many studies have described the resulting brain responses to the presentation of stimuli, or to stimulation conditions that can be considered homogeneous in time and/or in space for some of their constitutive features. Neuronal responses in terms of firing rate and gamma band oscillatory activity were investigated in many contexts involving at least one aspect of stimulus homogeneity, for example: temporal consistency, like in the case of the continuous uninterrupted presentation of the same stimulus for long time intervals (Peter, Uran et al. 2019), or spatial continuity, like in the case of large uniform surfaces (Shirhatti and Ray 2018, Peter, Uran et al. 2019), and even homogeneity in terms of stimulation structure, like in the case of the repetition studies (Brunet, Bosman et al. 2014, Peter, Stauch et al. 2021, Stauch, Peter et al. 2021, Psarou, Parto-Dezfouli et al. 2025). Interestingly, all of these studies conducted in different conditions, but with the common factor of investigating

some kind of stimulus-related feature of homogeneity, reported consistently a reduction in neuronal firing rates concomitantly to an increase in gamma band activity power and/or even coherence between brain areas.

Mechanistic models were hypothesized to describe these activity patterns, all converging around the idea that gamma-rhythmic activity would support computational processes in the context of reduced firing rates, optimizing the computation by reducing energy consumption. Hence, stimulus repetition effects are associated with an efficient processing of the sensory stimuli that is maintained by increasing the temporal precision of the lower spike number thanks to the oscillatory activity in the gamma range, so that behavioral performance results are not affected (Grill-Spector, Henson et al. 2006, Gotts, Chow et al. 2012). Similarly, for spatially homogeneous stimuli, Vinck and Bosman (2016) hypothesized that gamma synchronization reflects contextual integration processes, so that gamma increases when input to the central RF can be predicted by the surround, because it is homogeneous to it. At a cellular level, a mechanism was also hypothesized to explain how the increase in gamma synchronization and/or power could be accompanied by the reduction in neuronal firing rates (Stauch, Peter et al. 2021). E – I neurons involved in the generation of the gamma cycle will tend to fire in a temporally alternating sequence, reinforcing their connection, while other *e* neurons of the network not involved in the gamma cycle would be firing asynchronously or even be inhibited, so that the connection with the E – I gamma generating loop would be weakened and consequently, the global firing rate reduced (see also Chapter 1).

How do the findings from Chapter 3 relate with the classical findings of the repetition literature, and with the mechanistic and cellular models described above? The results from the repetition of an FSCB and an FSCB with a superimposed black bar show a decrease of power in the gamma band together with an increase of MUA spiking activity over the course of many trials. It seems that the E – I connections responsible for the generation of the gamma cycle in the cellular model described above are not being reinforced, therefore the other *e* neurons not connected to the gamma cycle do not get as strongly inhibited due to their asynchronous firing, and consequently are free to increase their activity rate, acting independently from the gamma cycle in a de-synchronized way. The de-synchronization was also demonstrated by the LFP-MUA PPC analysis results presented in Chapter 3. On one hand, the de-synchronization could be due to some kind of fatigue or interference mechanism acting on interneurons. Inhibitory interneurons are mostly responsible for the activation of a gamma cycle, therefore their weakening paired with an increased spiking of the excitatory cells might indicate some kind of effect

of inhibition of the inhibition or fatigue weighing on the interneurons that reduces the power of the gamma-band activity, while letting neuronal spiking increase freely. On the other hand, it is possible that the de-synchronization between the firing and the gamma activity is due to some sort of feedback connection sending information from higher cortical areas. To expand this concept, it is necessary to first remember that situations of heightened firing rate paired with lower gamma-band activity power are usually connected with center-surround information mismatch in the recorded RF (Peter, Uran et al. 2019). Moreover, it is helpful to highlight that in the trial structure of the experiment presented in Chapter 3, the presentation of the black bar in the RF generates a mismatch in the uniform FSCB that precedes it. It is therefore possible that mismatch anticipation mechanisms due to trial history and based on feedback information sent by higher cortical areas could be put in place, thereby generating a heightened MUA activity and decreased gamma band power.

Interestingly, Peter, Uran et al. (2019) already had noted that when a FSCB is consistently presented for long periods of time during one trial, gamma band power weakened. In this case, two factors could play a role in determining the reduction of gamma power, namely the size of the stimulus as a full-screen colored surface, or the prolonged presentation of the FSCB, for a total of 3.3 seconds. Further analyses clarified that the effect witnessed was due to stimulus history, so to the prolonged presentation, rather than its size. Anyways, it is interesting to notice how two types of stimulus homogeneity were at play in this context: homogeneity in space, as for the full-screen surface, and homogeneity in time, as the prolonged presentation. Similarly, in the context of the Chapter 3 experiment, where the reduction in gamma power was found, several features of the visual stimulation on top of the repeated presentation could be addressed as homogeneities of a certain kind: the full-screen surface, as homogeneity in space, the prolonged presentation of the FSCB (1.4 to 1.7 s in the case of Chapter 3 experiment) as homogeneity in time. A fascinating new perspective for future investigation could be to study these different kinds of stimulus homogeneity together and how they affect each other and the neuronal response.

Repetition and reward prediction

The specific stimulus features that could have caused the effects of Chapter 3 were already discussed in the Chapter 3 Discussion. The last point that was made in that context was that the most plausible explanation for the opposite effects found for the FSCB stimuli repetition was that the FSCB is in fact less relevant for the brain as it is not predictive of the upcoming behavioral reward, while on the contrary the black bar is, and this is why the results are reverted again to classical when analyzing the

effect of the black bar in isolation. This finding indicates that probably repetition effects on gamma-band activity and MUA spiking are not fixed, but are modulated by contextual factors such as reward prediction. The role of reward in modulating repetition effects can be positioned in a broader framework of evidence supporting that attention and reward can modulate gamma synchronization by boosting task-relevant information and concomitantly suppressing irrelevant inputs (Fries, Reynolds et al. 2001, Fries 2005, Bosman, Schoffelen et al. 2012, Fries 2015). Reward prediction, in the sense of the prediction of the reward associated with the behavioral response to an attended stimulus, has been shown to selectively enhance gamma coherence between visual areas, suggesting that gamma synchronization may serve as a flexible mechanism for prioritizing behaviorally relevant stimuli (Bosman, Schoffelen et al. 2012). Moreover, it has been shown that gamma synchronization is actively regulated depending on behavioral goals and reward contingencies (Fries, Reynolds et al. 2001, Bastos, Vezoli et al. 2015). These findings support the notion that repetition effects might not be a consequence of the sensory stimuli alone, but are instead determined and modulated by contextual factors such as, in the case of the current experiment, reward prediction. The modulation of repetition effects could be a general mechanism through which the brain efficiently allocates processing resources to behaviorally relevant stimuli (Fries 2005, Fries 2015). Future studies will need to add experimental proof to this hypothesized mechanism.

General final considerations

Many of the findings highlighted in this thesis work will require further experiments to be fully elucidated and clarified. Notably, both Chapter 2 and Chapter 3 results' Discussions led to address a common set of mechanisms that may underlie the observed effects—mechanisms that remain interesting open topics for future investigation. Two aspects stand out in particular: the local circuit structure that represents the biological substrate generating neuronal responses to stimuli, and the central role of inhibitory interneurons. On one hand, the structure of local circuits and their reciprocal connections in conjunction with feedback, lateral and long-range network connections, represent the anatomical substrate of neuronal activity: clarifying this structure and describing it in detail will lead to a better understanding of the resulting neuronal activity. On the other hand, studying brain activity, it is fascinating to notice how neuronal responses and the mechanisms proposed in various contexts to explain cognitive outcomes revolve around the organization of the neuronal spiking through inhibition. Inhibition sets itself as

one of the most important regulating principles of the brain, because it is capable of building a temporal structure to organize an otherwise dysregulated excitatory firing activity. More insights on these two interesting aspects of brain anatomical and functional structure could lead the way to a deeper understanding of the brain computation in relation to the visual system, LFP power in the gamma band, MUA, and beyond.

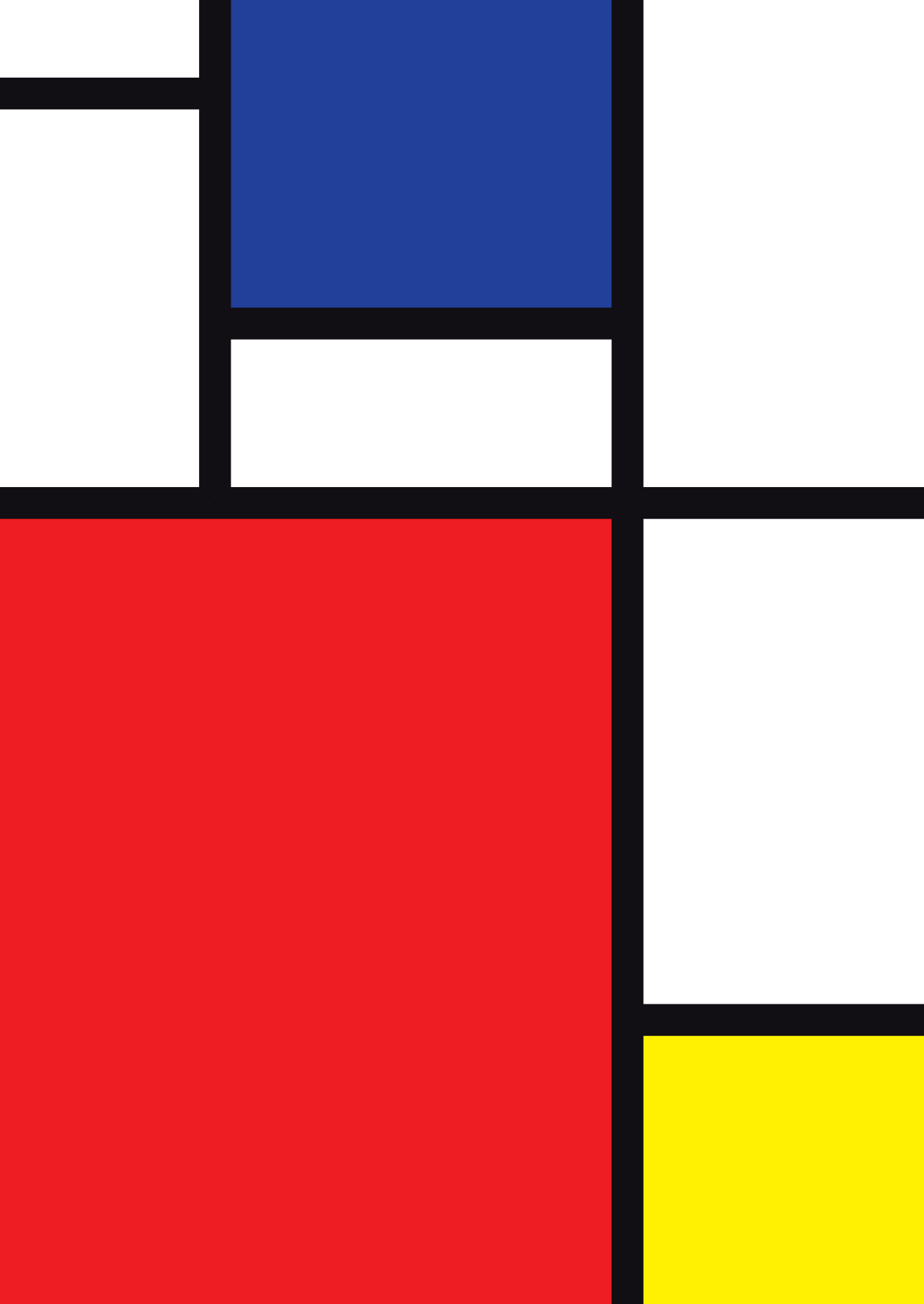

Bibliography

Ahissar, E. (1998). "Temporal-code to rate-code conversion by neuronal phase-locked loops." Neural Comput **10**(3): 597-650.

Ainsworth, M., S. Lee, M. O. Cunningham, R. D. Traub, N. J. Kopell and M. A. Whittington (2012). "Rates and rhythms: a synergistic view of frequency and temporal coding in neuronal networks." Neuron **75**(4): 572-583.

Alitto, H. J. and W. M. Usrey (2004). "Influence of contrast on orientation and temporal frequency tuning in ferret primary visual cortex." J Neurophysiol **91**(6): 2797-2808.

Andersen, R. A. and V. B. Mountcastle (1983). "The influence of the angle of gaze upon the excitability of the light-sensitive neurons of the posterior parietal cortex." J Neurosci **3**(3): 532-548.

Angelucci, A., M. Bijanzadeh, L. Nurminen, F. Federer, S. Merlin and P. C. Bressloff (2017). "Circuits and Mechanisms for Surround Modulation in Visual Cortex." Annu Rev Neurosci **40**: 425-451.

Ardid, S., X. J. Wang, D. Gomez-Cabrero and A. Compte (2010). "Reconciling coherent oscillation with modulation of irregular spiking activity in selective attention: gamma-range synchronization between sensory and executive cortical areas." J Neurosci **30**(8): 2856-2870.

Azouz, R. and C. M. Gray (2003). "Adaptive coincidence detection and dynamic gain control in visual cortical neurons in vivo." Neuron **37**(3): 513-523.

Azouz, R. and C. M. Gray (2008). "Stimulus-selective spiking is driven by the relative timing of synchronous excitation and disinhibition in cat striate neurons in vivo." Eur J Neurosci **28**(7): 1286-1300.

Bartos, M., I. Vida and P. Jonas (2007). "Synaptic mechanisms of synchronized gamma oscillations in inhibitory interneuron networks." Nat Rev Neurosci **8**(1): 45-56.

Bastos, A. M., J. Vezoli, C. A. Bosman, J. M. Schoffelen, R. Oostenveld, J. R. Dowdall, P. De Weerd, H. Kennedy and P. Fries (2015). "Visual areas exert feedforward and feedback influences through distinct frequency channels." Neuron **85**(2): 390-401.

Bauer, M., R. Oostenveld, M. Peeters and P. Fries (2006). "Tactile spatial attention enhances gamma-band activity in somatosensory cortex and reduces low-frequency activity in parieto-occipital areas." J Neurosci **26**(2): 490-501.

Bazhenov, M., M. Stopfer, T. J. Sejnowski and G. Laurent (2005). "Fast odor learning improves reliability of odor responses in the locust antennal lobe." Neuron **46**(3): 483-492.

Bichot, N. P., A. F. Rossi and R. Desimone (2005). "Parallel and serial neural mechanisms for visual search in macaque area V4." Science **308**(5721): 529-534.

Blasdel, G. and D. Campbell (2001). "Functional retinotopy of monkey visual cortex." J Neurosci **21**(20): 8286-8301.

Bogartz, R. S. (1968). "A least squares method for fitting intercepting line segments to a set of data points." Psychological Bulletin **70**(6): 749-755.

Börgers, C., S. Epstein and N. J. Kopell (2005). "Background gamma rhythmicity and attention in cortical local circuits: a computational study." Proc Natl Acad Sci U S A **102**(19): 7002-7007.

Börgers, C. and N. Kopell (2003). "Synchronization in networks of excitatory and inhibitory neurons with sparse, random connectivity." Neural Comput **15**(3): 509-538.

Börgers, C. and N. Kopell (2005). "Effects of noisy drive on rhythms in networks of excitatory and inhibitory neurons." Neural Comput **17**(3): 557-608.

Bosman, C. A., J. M. Schoffelen, N. Brunet, R. Oostenveld, A. M. Bastos, T. Womelsdorf, B. Rubehn, T. Stieglitz, P. De Weerd and P. Fries (2012). "Attentional stimulus selection through selective synchronization between monkey visual areas." Neuron **75**(5): 875-888.

Bragin, A., G. Jandó, Z. Nádasdy, J. Hetke, K. Wise and G. Buzsáki (1995). "Gamma (40-100 Hz) oscillation in the hippocampus of the behaving rat." J Neurosci **15**(1 Pt 1): 47-60.

Brown, P., S. Salenius, J. C. Rothwell and R. Hari (1998). "Cortical correlate of the Piper rhythm in humans." J Neurophysiol **80**(6): 2911-2917.

Brunel, N. and X. J. Wang (2003). "What determines the frequency of fast network oscillations with irregular neural discharges? I. Synaptic dynamics and excitation-inhibition balance." J Neurophysiol **90**(1): 415-430.

Brunet, N., M. Vinck, C. A. Bosman, W. Singer and P. Fries (2014). "Gamma or no gamma, that is the question." Trends Cogn Sci **18**(10): 507-509.

Brunet, N. M., C. A. Bosman, M. Vinck, M. Roberts, R. Oostenveld, R. Desimone, P. De Weerd and P. Fries (2014). "Stimulus repetition modulates gamma-band synchronization in primate visual cortex." Proc Natl Acad Sci U S A **111**(9): 3626-3631.

Bulsara, A. R., R. D. Boss and E. W. Jacobs (1989). "Noise effects in an electronic model of a single neuron." Biol Cybern **61**(3): 211-222.

Buzsáki, G. (2006). Rhythms of the Brain, Oxford University Press.

Buzsáki, G. (2010). "Neural syntax: cell assemblies, synapsembles, and readers." Neuron **68**(3): 362-385.

Buzsáki, G., C. A. Anastassiou and C. Koch (2012). "The origin of extracellular fields and currents--EEG, ECoG, LFP and spikes." Nat Rev Neurosci **13**(6): 407-420.

Buzsáki, G. and J. J. Chrobak (1995). "Temporal structure in spatially organized neuronal ensembles: a role for interneuronal networks." Curr Opin Neurobiol **5**(4): 504-510.

Buzsáki, G. and A. Draguhn (2004). "Neuronal oscillations in cortical networks." Science **304**(5679): 1926-1929.

Buzsaki, G., N. Logothetis and W. Singer (2013). "Scaling brain size, keeping timing: evolutionary preservation of brain rhythms." Neuron **80**(3): 751-764.

Buzsáki, G. and E. I. Moser (2013). "Memory, navigation and theta rhythm in the hippocampal-entorhinal system." Nat Neurosci **16**(2): 130-138.

Buzsáki, G. and X. J. Wang (2012). "Mechanisms of gamma oscillations." Annu Rev Neurosci **35**: 203-225.

Callaway, E. M. (1998). "Local circuits in primary visual cortex of the macaque monkey." Annu Rev Neurosci **21**: 47-74.

Callaway, E. M. (2004). "Feedforward, feedback and inhibitory connections in primate visual cortex." Neural Netw **17**(5-6): 625-632.

Canolty, R. T., E. Edwards, S. S. Dalal, M. Soltani, S. S. Nagarajan, H. E. Kirsch, M. S. Berger, N. M. Barbaro and R. T. Knight (2006). "High gamma power is phase-locked to theta oscillations in human neocortex." Science **313**(5793): 1626-1628.

Caporale, N. and Y. Dan (2008). "Spike timing-dependent plasticity: a Hebbian learning rule." Annu Rev Neurosci **31**: 25-46.

Carandini, M. and D. J. Heeger (2011). "Normalization as a canonical neural computation." Nat Rev Neurosci **13**(1): 51-62.

Cardin, J. A., M. Carlén, K. Meletis, U. Knoblich, F. Zhang, K. Deisseroth, L. H. Tsai and C. I. Moore (2009). "Driving fast-spiking cells induces gamma rhythm and controls sensory responses." Nature **459**(7247): 663-667.

Cardin, J. A., L. A. Palmer and D. Contreras (2008). "Cellular mechanisms underlying stimulus-dependent gain modulation in primary visual cortex neurons in vivo." Neuron **59**(1): 150-160.

Chance, F. S., L. F. Abbott and A. D. Reyes (2002). "Gain modulation from background synaptic input." Neuron **35**(4): 773-782.

Chow, C. C., J. A. White, J. Ritt and N. Kopell (1998). "Frequency Control in Synchronized Networks of Inhibitory Neurons." Journal of Computational Neuroscience **5**(4): 407-420.

Csicsvari, J., B. Jamieson, K. D. Wise and G. Buzsáki (2003). "Mechanisms of gamma oscillations in the hippocampus of the behaving rat." Neuron **37**(2): 311-322.

Defelipe, J., M. C. González-Albo, M. R. Del Río and G. N. Elston (1999). "Distribution and patterns of connectivity of interneurons containing calbindin, calretinin, and parvalbumin in visual areas of the occipital and temporal lobes of the macaque monkey." J Comp Neurol **412**(3): 515-526.

Demb, J. B. (2007). "Cellular mechanisms for direction selectivity in the retina." Neuron **55**(2): 179-186.

Desimone, R. (1996). "Neural mechanisms for visual memory and their role in attention." Proc Natl Acad Sci U S A **93**(24): 13494-13499.

Di Dona, G. and L. Ronconi (2023). "Beta oscillations in vision: a (preconscious) neural mechanism for the dorsal visual stream?" Front Psychol **14**: 1296483.

Donoghue, T., M. Haller, E. J. Peterson, P. Varma, P. Sebastian, R. Gao, T. Noto, A. H. Lara, J. D. Wallis, R. T. Knight, A. Shestyuk and B. Voytek (2020). "Parameterizing neural power spectra into periodic and aperiodic components." Nat Neurosci **23**(12): 1655-1665.

Dou, W., A. Morrow, L. Iemi and J. Samaha (2022). "Pre-stimulus alpha-band phase gates early visual cortex responses." Neuroimage **253**: 119060.

Dowdall, J., J. Schmiedt, M. Stephan and P. Fries (2018). "Arcade: a modular multithreaded stimulus presentation software for the Real-Time control of stimuli, actions and reward during behavioral experiments." SfN **2018**(254.18): 2018.

Drebitz, E., L. P. Rausch and A. K. Kreiter (2025). "Gamma-band synchronization between neurons in the visual cortex is causal for effective information processing and behavior." Nat Commun **16**(1): 7380.

Eckhorn, R., R. Bauer, W. Jordan, M. Brosch, W. Kruse, M. Munk and H. J. Reitboeck (1988). "Coherent oscillations: a mechanism of feature linking in the visual cortex? Multiple electrode and correlation analyses in the cat." Biol Cybern **60**(2): 121-130.

Economo, M. N. and J. A. White (2012). "Membrane properties and the balance between excitation and inhibition control gamma-frequency oscillations arising from feedback inhibition." PLoS Comput Biol **8**(1): e1002354.

Effenberger, F., P. Carvalho, I. Dubinin and W. Singer (2025). "The functional role of oscillatory dynamics in neocortical circuits: A computational perspective." Proc Natl Acad Sci U S A **122**(4): e2412830122.

Engel, A. K., P. König, A. K. Kreiter and W. Singer (1991). "Interhemispheric synchronization of oscillatory neuronal responses in cat visual cortex." Science **252**(5009): 1177-1179.

Engel, A. K., A. K. Kreiter, P. Konig and W. Singer (1991). "Synchronization of oscillatory neuronal responses between striate and extrastriate visual cortical areas of the cat." Proc Natl Acad Sci U S A **88**(14): 6048-6052.

Farley, B. J., M. C. Quirk, J. J. Doherty and E. P. Christian (2010). "Stimulus-specific adaptation in auditory cortex is an NMDA-independent process distinct from the sensory novelty encoded by the mismatch negativity." J Neurosci **30**(49): 16475-16484.

Ferguson, K. A. and J. A. Cardin (2020). "Mechanisms underlying gain modulation in the cortex." Nat Rev Neurosci **21**(2): 80-92.

Fernandez-Ruiz, A., A. Sirota, V. Lopes-Dos-Santos and D. Dupret (2023). "Over and above frequency: Gamma oscillations as units of neural circuit operations." Neuron **111**(7): 936-953.

Ferster, D. and K. D. Miller (2000). "Neural mechanisms of orientation selectivity in the visual cortex." Annu Rev Neurosci **23**: 441-471.

Finn, I. M., N. J. Priebe and D. Ferster (2007). "The emergence of contrast-invariant orientation tuning in simple cells of cat visual cortex." Neuron **54**(1): 137-152.

Fiorani, M., J. C. Azzi, J. G. Soares and R. Gattass (2014). "Automatic mapping of visual cortex receptive fields: a fast and precise algorithm." J Neurosci Methods **221**: 112-126.

Fishman, Y. I. and M. Steinschneider (2012). "Searching for the mismatch negativity in primary auditory cortex of the awake monkey: deviance detection or stimulus specific adaptation?" J Neurosci **32**(45): 15747-15758.

Fries, P. (2005). "A mechanism for cognitive dynamics: neuronal communication through neuronal coherence." Trends Cogn Sci **9**(10): 474-480.

Fries, P. (2009). "Neuronal gamma-band synchronization as a fundamental process in cortical computation." Annu Rev Neurosci **32**: 209-224.

Fries, P. (2015). "Rhythms for Cognition: Communication through Coherence." Neuron **88**(1): 220-235.

Fries, P. and E. Maris (2022). "What to Do If N Is Two?" J Cogn Neurosci **34**(7): 1114-1118.

Fries, P., J. H. Reynolds, A. E. Rorie and R. Desimone (2001). "Modulation of oscillatory neuronal synchronization by selective visual attention." Science **291**(5508): 1560-1563.

Fries, P., R. Scheeringa and R. Oostenveld (2008). "Finding gamma." Neuron **58**(3): 303-305.

Gerster, M., G. Waterstraat, V. Litvak, K. Lehnertz, A. Schnitzler, E. Florin, G. Curio and V. Nikulin (2022). "Separating Neural Oscillations from Aperiodic 1/f Activity: Challenges and Recommendations." Neuroinformatics.

Gieselmann, M. A. and A. Thiele (2008). "Comparison of spatial integration and surround suppression characteristics in spiking activity and the local field potential in macaque V1." Eur J Neurosci **28**(3): 447-459.

Gieselmann, M. A. and A. Thiele (2022). "Stimulus dependence of directed information exchange between cortical layers in macaque V1." Elife **11**.

Gilbert, C. D. and W. Li (2013). "Top-down influences on visual processing." Nat Rev Neurosci **14**(5): 350-363.

Gilbert, J. R., S. J. Gotts, F. W. Carver and A. Martin (2010). "Object repetition leads to local increases in the temporal coordination of neural responses." Front Hum Neurosci **4**: 30.

Glatigny, M., F. Geffroy and T. van Kerkoerle (2024). "Comparison of the cortical hierarchy between macaque monkeys and mice based on cell-type specific microcircuits." bioRxiv: 2024.2010.2031.621258.

Gotts, S. J. (2003). Mechanisms underlying enhanced processing efficiency in neural systems, Carnegie Mellon University.

Gotts, S. J., C. C. Chow and A. Martin (2012). "Repetition priming and repetition suppression: A case for enhanced efficiency through neural synchronization." Cogn Neurosci **3**(3-4): 227-237.

Gravesen, J. (2015). "The metric of colour space." Graphical Models **82**: 77-86.

Gray, C. M., P. König, A. K. Engel and W. Singer (1989). "Oscillatory responses in cat visual cortex exhibit inter-columnar synchronization which reflects global stimulus properties." Nature **338**(6213): 334-337.

Gray, C. M. and W. Singer (1989). "Stimulus-specific neuronal oscillations in orientation columns of cat visual cortex." Proc Natl Acad Sci U S A **86**(5): 1698-1702.

Gray, C. M. and G. Viana Di Prisco (1997). "Stimulus-dependent neuronal oscillations and local synchronization in striate cortex of the alert cat." J Neurosci **17**(9): 3239-3253.

Grill-Spector, K., R. Henson and A. Martin (2006). "Repetition and the brain: neural models of stimulus-specific effects." Trends Cogn Sci **10**(1): 14-23.

Grill-Spector, K. and R. Malach (2001). "fMR-adaptation: a tool for studying the functional properties of human cortical neurons." Acta Psychol (Amst) **107**(1-3): 293-321.

Grothe, I., S. D. Neitzel, S. Mandon and A. K. Kreiter (2012). "Switching neuronal inputs by differential modulations of gamma-band phase-coherence." J Neurosci **32**(46): 16172-16180.

Grothe, I., D. Rotermund, S. D. Neitzel, S. Mandon, U. A. Ernst, A. K. Kreiter and K. R. Pawelzik (2018). "Attention Selectively Gates Afferent Signal Transmission to Area V4." J Neurosci **38**(14): 3441-3452.

Hakim, R., K. Shamardani and H. Adesnik (2018). "A neural circuit for gamma-band coherence across the retinotopic map in mouse visual cortex." Elife **7**.

Harvey, B. M. and S. O. Dumoulin (2011). "The relationship between cortical magnification factor and population receptive field size in human visual cortex: constancies in cortical architecture." J Neurosci **31**(38): 13604-13612.

Hubel, D. H. and T. N. Wiesel (1962). "Receptive fields, binocular interaction and functional architecture in the cat's visual cortex." J Physiol **160**(1): 106-154.

Hubel, D. H. and T. N. Wiesel (1968). "Receptive fields and functional architecture of monkey striate cortex." J Physiol **195**(1): 215-243.

Hubel, D. H. and T. N. Wiesel (1979). "Brain mechanisms of vision." Sci Am **241**(3): 150-162.

Jinno, S., T. Klausberger, L. F. Marton, Y. Dalezios, J. D. Roberts, P. Fuentealba, E. A. Bushong, D. Henze, G. Buzsáki and P. Somogyi (2007). "Neuronal diversity in GABAergic long-range projections from the hippocampus." J Neurosci **27**(33): 8790-8804.

Kandel, E. R., J. D. Koester, S. H. Mack and S. A. Siegelbaum (2021). Principles of Neural Science, 6e. New York, NY, McGraw Hill.

Katsanevaki, C., A. M. Bastos, H. Cagnan, C. A. Bosman, K. J. Friston and P. Fries (2023). "Attentional effects on local V1 microcircuits explain selective V1-V4 communication." Neuroimage **281**: 120375.

Katzner, S., L. Busse and M. Carandini (2011). "GABAA inhibition controls response gain in visual cortex." J Neurosci **31**(16): 5931-5941.

Kohn, A. and J. A. Movshon (2003). "Neuronal adaptation to visual motion in area MT of the macaque." Neuron **39**(4): 681-691.

Kopell, N., G. B. Ermentrout, M. A. Whittington and R. D. Traub (2000). "Gamma rhythms and beta rhythms have different synchronization properties." Proc Natl Acad Sci U S A **97**(4): 1867-1872.

Lakatos, P., G. Karmos, A. D. Mehta, I. Ulbert and C. E. Schroeder (2008). "Entrainment of neuronal oscillations as a mechanism of attentional selection." Science **320**(5872): 110-113.

Lamme, V. A. (1995). "The neurophysiology of figure-ground segregation in primary visual cortex." J Neurosci **15**(2): 1605-1615.

Laurens, J. (2022). "The statistical power of three monkeys." bioRxiv: 2022.2005.2010.491373.

Laurent, G. (2002). "Olfactory network dynamics and the coding of multidimensional signals." Nat Rev Neurosci **3**(11): 884-895.

Lee, S. H., A. C. Kwan, S. Zhang, V. Phoumthipphavong, J. G. Flannery, S. C. Masmanidis, H. Taniguchi, Z. J. Huang, F. Zhang, E. S. Boyden, K. Deisseroth and Y. Dan (2012). "Activation of specific interneurons improves V1 feature selectivity and visual perception." Nature **488**(7411): 379-383.

Lewis, C. M., J. Ni, T. Wunderle, P. Jendritza, A. Lazar, I. Diester and P. Fries (2021). "Cortical gamma-band resonance preferentially transmits coherent input." Cell Rep **35**(5): 109083.

Li, L., E. K. Miller and R. Desimone (1993). "The representation of stimulus familiarity in anterior inferior temporal cortex." J Neurophysiol **69**(6): 1918-1929.

Livingstone, M. and D. Hubel (1988). "Segregation of form, color, movement, and depth: anatomy, physiology, and perception." Science **240**(4853): 740-749.

Lytton, W. W. and T. J. Sejnowski (1991). "Simulations of cortical pyramidal neurons synchronized by inhibitory interneurons." J Neurophysiol **66**(3): 1059-1079.

McAdams, C. J. and R. C. Reid (2005). "Attention modulates the responses of simple cells in monkey primary visual cortex." J Neurosci **25**(47): 11023-11033.

Michalareas, G., J. Vezoli, S. van Pelt, J. M. Schoffelen, H. Kennedy and P. Fries (2016). "Alpha-Beta and Gamma Rhythms Subserve Feedback and Feedforward Influences among Human Visual Cortical Areas." Neuron **89**(2): 384-397.

Mitchell, S. J. and R. A. Silver (2003). "Shunting inhibition modulates neuronal gain during synaptic excitation." Neuron **38**(3): 433-445.

Natan, R. G., I. M. Carruthers, L. Mwilambwe-Tshilobo and M. N. Geffen (2017). "Gain Control in the Auditory Cortex Evoked by Changing Temporal Correlation of Sounds." Cereb Cortex **27**(3): 2385-2402.

Natan, R. G., W. Rao and M. N. Geffen (2017). "Cortical Interneurons Differentially Shape Frequency Tuning following Adaptation." Cell Rep **21**(4): 878-890.

Ni, J., T. Wunderle, C. M. Lewis, R. Desimone, I. Diester and P. Fries (2016). "Gamma-Rhythmic Gain Modulation." Neuron **92**(1): 240-251.

Nichols, T. E. and A. P. Holmes (2002). "Nonparametric permutation tests for functional neuroimaging: a primer with examples." Hum Brain Mapp **15**(1): 1-25.

Niell, C. M. and M. P. Stryker (2010). "Modulation of visual responses by behavioral state in mouse visual cortex." Neuron **65**(4): 472-479.

Ohshiro, T., D. E. Angelaki and G. C. DeAngelis (2011). "A normalization model of multisensory integration." Nat Neurosci **14**(6): 775-782.

Olshausen, B. A. and D. J. Field (1996). "Emergence of simple-cell receptive field properties by learning a sparse code for natural images." Nature **381**(6583): 607-609.

Oostenveld, R., P. Fries, E. Maris and J. M. Schoffelen (2011). "FieldTrip: Open source software for advanced analysis of MEG, EEG, and invasive electrophysiological data." Comput Intell Neurosci **2011**: 156869.

Patel, S., E. Psarou, G. Mönke and P. Fries (2024). "Spectral estimation at the edge." bioRxiv.

Peter, A. (2020). Effect of stimulus repetition, color and context on visual cortical gamma

Der Effekt von Stimuluswiederholung, Farbe und Kontext auf visuelle kortikale Gamma-Oszillationen.

Peter, A., B. J. Stauch, K. A. Shapcott, K. Kouroupaki, J. T. Schmiedt, L. Klein, J. Klon-Lipok, J. R. Dowdall, M. L. Schölvinck, M. Vinck, M. C. Schmid and P. Fries (2021). "Stimulus-specific plasticity of macaque V1 spike rates and gamma." Cell Reports **37**(10): 110086.

Peter, A., C. Uran, J. Klon-Lipok, R. Roese, S. van Stijn, W. Barnes, J. R. Dowdall, W. Singer, P. Fries and M. Vinck (2019). "Surface color and predictability determine contextual modulation of V1 firing and gamma oscillations." Elife **8**.

Poort, J., M. W. Self, B. van Vugt, H. Malkki and P. R. Roelfsema (2016). "Texture Segregation Causes Early Figure Enhancement and Later Ground Suppression in Areas V1 and V4 of Visual Cortex." Cereb Cortex **26**(10): 3964-3976.

Priebe, N. J. and D. Ferster (2012). "Mechanisms of neuronal computation in mammalian visual cortex." Neuron **75**(2): 194-208.

Psarou, E. (2024). Neural recordings, implant refinement, and rethinking sample sizes in non-human primate research, Radobud University.

Psarou, E., C. Katsanevaki, E. Maris and P. Fries (2024). "Would you agree if N is three? On statistical inference for small N." bioRxiv: 2024.2008. 2026.609821.

Psarou, E., M. Parto-Dezfouli, I. Grothe, A. Peter, R. Roese and P. Fries (2025). "Repetition-related gamma plasticity in macaque V1 and V2 is highly stimulus specific and robust to stimulus set size." bioRxiv: 2025.2006. 2020.660699.

Psarou, E., J. Vezoli, M. L. Schölvinck, P. A. Ferracci, Y. Zhang, I. Grothe, R. Roese and P. Fries (2023). "Modular, cement-free, customized headpost and connector-chamber implants for macaques." J Neurosci Methods **393**: 109899.

Ray, S. and J. H. Maunsell (2015). "Do gamma oscillations play a role in cerebral cortex?" Trends Cogn Sci **19**(2): 78-85.

Reynolds, J. H., L. Chelazzi and R. Desimone (1999). "Competitive mechanisms subserve attention in macaque areas V2 and V4." J Neurosci **19**(5): 1736-1753.

Reynolds, J. H. and R. Desimone (1999). "The role of neural mechanisms of attention in solving the binding problem." Neuron **24**(1): 19-29, 111-125.

Reynolds, J. H. and D. J. Heeger (2009). "The normalization model of attention." Neuron **61**(2): 168-185.

Reynolds, J. H., T. Pasternak and R. Desimone (2000). "Attention increases sensitivity of V4 neurons." Neuron **26**(3): 703-714.

Roberts, M. J., E. Lowet, N. M. Brunet, M. Ter Wal, P. Tiesinga, P. Fries and P. De Weerd (2013). "Robust gamma coherence between macaque V1 and V2 by dynamic frequency matching." Neuron **78**(3): 523-536.

Roelfsema, P. R. (2006). "Cortical algorithms for perceptual grouping." Annu Rev Neurosci **29**: 203-227.

Rohenkohl, G., C. A. Bosman and P. Fries (2018). "Gamma Synchronization between V1 and V4 Improves Behavioral Performance." Neuron **100**(4): 953-963 e953.

Salinas, E. and T. J. Sejnowski (2000). "Impact of correlated synaptic input on output firing rate and variability in simple neuronal models." J Neurosci **20**(16): 6193-6209.

Salinas, E. and T. J. Sejnowski (2001). "Correlated neuronal activity and the flow of neural information." Nat Rev Neurosci **2**(8): 539-550.

Salinas, E. and P. Thier (2000). "Gain modulation: a major computational principle of the central nervous system." Neuron **27**(1): 15-21.

Schoffelen, J. M., R. Oostenveld and P. Fries (2005). "Neuronal coherence as a mechanism of effective corticospinal interaction." Science **308**(5718): 111-113.

Schwartz, O., A. Hsu and P. Dayan (2007). "Space and time in visual context." Nat Rev Neurosci **8**(7): 522-535.

Self, M. W., T. van Kerkoerle, H. Super and P. R. Roelfsema (2013). "Distinct roles of the cortical layers of area V1 in figure-ground segregation." Curr Biol **23**(21): 2121-2129.

Shirhatti, V. and S. Ray (2018). "Long-wavelength (reddish) hues induce unusually large gamma oscillations in the primate primary visual cortex." Proc Natl Acad Sci U S A **115**(17): 4489-4494.

Shu, Y., A. Hasenstaub, M. Badoual, T. Bal and D. A. McCormick (2003). "Barrages of synaptic activity control the gain and sensitivity of cortical neurons." J Neurosci **23**(32): 10388-10401.

Silver, R. A. (2010). "Neuronal arithmetic." Nat Rev Neurosci **11**(7): 474-489.

Sincich, L. C. and J. C. Horton (2005). "The circuitry of V1 and V2: integration of color, form, and motion." Annu Rev Neurosci **28**: 303-326.

Singer, W. (2018). "Neuronal oscillations: unavoidable and useful?" Eur J Neurosci **48**(7): 2389-2398.

Singer, W. (2021). "Recurrent dynamics in the cerebral cortex: Integration of sensory evidence with stored knowledge." Proc Natl Acad Sci U S A **118**(33).

Singer, W. and F. Effenberger (2025). "Oscillations in Natural Neuronal Networks; An Epiphenomenon or a Fundamental Computational Mechanism?" Human Arenas.

Singer, W. and C. M. Gray (1995). "Visual feature integration and the temporal correlation hypothesis." Annu Rev Neurosci **18**: 555-586.

Sirota, A., S. Montgomery, S. Fujisawa, Y. Isomura, M. Zugaro and G. Buzsáki (2008). "Entrainment of neocortical neurons and gamma oscillations by the hippocampal theta rhythm." Neuron **60**(4): 683-697.

Solomon, S. G. (2021). "Retinal ganglion cells and the magnocellular, parvocellular, and koniocellular subcortical visual pathways from the eye to the brain." Handb Clin Neurol **178**: 31-50.

Stauch, B. J., A. Peter, I. Ehrlich, Z. Nolte and P. Fries (2022). "Human visual gamma for color stimuli." Elife **11**.

Stauch, B. J., A. Peter, H. Schuler and P. Fries (2020). "Stimulus-specific plasticity in human visual gamma-band activity and functional connectivity." bioRxiv: 2020.2011.2013.381467.

Stauch, B. J., A. Peter, H. Schuler and P. Fries (2021). "Stimulus-specific plasticity in human visual gamma-band activity and functional connectivity." Elife **10**: e68240.

Stopfer, M. and G. Laurent (1999). "Short-term memory in olfactory network dynamics." Nature **402**(6762): 664-668.

Tootell, R. B., N. K. Hadjikhani, W. Vanduffel, A. K. Liu, J. D. Mendola, M. I. Sereno and A. M. Dale (1998). "Functional analysis of primary visual cortex (V1) in humans." Proc Natl Acad Sci U S A **95**(3): 811-817.

Torralba, A. and A. Oliva (2003). "Statistics of natural image categories." Network **14**(3): 391-412.

Traub, R. D., A. Bibbig, A. Fisahn, F. E. LeBeau, M. A. Whittington and E. H. Buhl (2000). "A model of gamma-frequency network oscillations induced in the rat CA3 region by carbachol in vitro." Eur J Neurosci **12**(11): 4093-4106.

Trujillo, C. A., R. Gao, P. D. Negraes, J. Gu, J. Buchanan, S. Preissl, A. Wang, W. Wu, G. G. Haddad, I. A. Chaim, A. Domissy, M. Vandenberghe, A. Devor, G. W. Yeo, B. Voytek and A. R. Muotri (2019). "Complex Oscillatory Waves Emerging from Cortical Organoids Model Early Human Brain Network Development." Cell Stem Cell **25**(4): 558-569.e557.

Tschechne, S. and H. Neumann (2014). "Hierarchical representation of shapes in visual cortex-from localized features to figural shape segregation." Front Comput Neurosci **8**: 93.

van Kerkoerle, T., M. W. Self, B. Dagnino, M. A. Gariel-Mathis, J. Poort, C. van der Togt and P. R. Roelfsema (2014). "Alpha and gamma oscillations characterize feedback and feedforward processing in monkey visual cortex." Proc Natl Acad Sci U S A.

Varela, F., J. P. Lachaux, E. Rodriguez and J. Martinerie (2001). "The brainweb: phase synchronization and large-scale integration." Nat Rev Neurosci **2**(4): 229-239.

Varela, F. J. (1995). "Resonant cell assemblies: a new approach to cognitive functions and neuronal synchrony." Biol Res **28**(1): 81-95.

Veit, J., R. Hakim, M. P. Jadi, T. J. Sejnowski and H. Adesnik (2017). "Cortical gamma band synchronization through somatostatin interneurons." Nat Neurosci **20**(7): 951-959.

Veit, J., G. Handy, D. P. Mossing, B. Doiron and H. Adesnik (2021). "Cortical VIP neurons locally control the gain but globally control the coherence of gamma band rhythms." bioRxiv: 2021.2005.2020.444979.

Veit, J., G. Handy, D. P. Mossing, B. Doiron and H. Adesnik (2023). "Cortical VIP neurons locally control the gain but globally control the coherence of gamma band rhythms." Neuron **111**(3): 405-417 e405.

Vinck, M., R. Batista-Brito, U. Knoblich and J. A. Cardin (2015). "Arousal and locomotion make distinct contributions to cortical activity patterns and visual encoding." Neuron **86**(3): 740-754.

Vinck, M. and C. A. Bosman (2016). "More Gamma More Predictions: Gamma-Synchronization as a Key Mechanism for Efficient Integration of Classical Receptive Field Inputs with Surround Predictions." Front Syst Neurosci **10**: 35.

Vinck, M., M. van Wingerden, T. Womelsdorf, P. Fries and C. M. Pennartz (2010). "The pairwise phase consistency: A bias-free measure of rhythmic neuronal synchronization." Neuroimage **51**(1): 112-122.

Vinck, M., T. Womelsdorf, E. A. Buffalo, R. Desimone and P. Fries (2013). "Attentional modulation of cell-class-specific gamma-band synchronization in awake monkey area V4." Neuron **80**(4): 1077-1089.

Vogels, T. P. and L. F. Abbott (2009). "Gating multiple signals through detailed balance of excitation and inhibition in spiking networks." Nat Neurosci **12**(4): 483-491.

von Stein, A. and J. Sarnthein (2000). "Different frequencies for different scales of cortical integration: from local gamma to long range alpha/theta synchronization." Int J Psychophysiol **38**(3): 301-313.

Wachtler, T., T. J. Sejnowski and T. D. Albright (2003). "Representation of color stimuli in awake macaque primary visual cortex." Neuron **37**(4): 681-691.

Wang, X. J. and G. Buzsáki (1996). "Gamma oscillation by synaptic inhibition in a hippocampal interneuronal network model." J Neurosci **16**(20): 6402-6413.

Weber, A. I. and A. L. Fairhall (2019). "The role of adaptation in neural coding." Curr Opin Neurobiol **58**: 135-140.

Wehr, M. and G. Laurent (1996). "Odour encoding by temporal sequences of firing in oscillating neural assemblies." Nature **384**(6605): 162-166.

Wilming, N., S. Harst, N. Schmidt and P. König (2013). "Saccadic momentum and facilitation of return saccades contribute to an optimal foraging strategy." PLoS Comput Biol **9**(1): e1002871.

Womelsdorf, T., J. M. Schoffelen, R. Oostenveld, W. Singer, R. Desimone, A. K. Engel and P. Fries (2007). "Modulation of neuronal interactions through neuronal synchronization." Science **316**(5831): 1609-1612.

Wyart, V. and C. Tallon-Baudry (2008). "Neural dissociation between visual awareness and spatial attention." J Neurosci **28**(10): 2667-2679.

Zweig, S., G. Zurawel, R. Shapley and H. Slovin (2015). "Representation of Color Surfaces in V1: Edge Enhancement and Unfilled Holes." The Journal of Neuroscience **35**(35): 12103-12115.

B

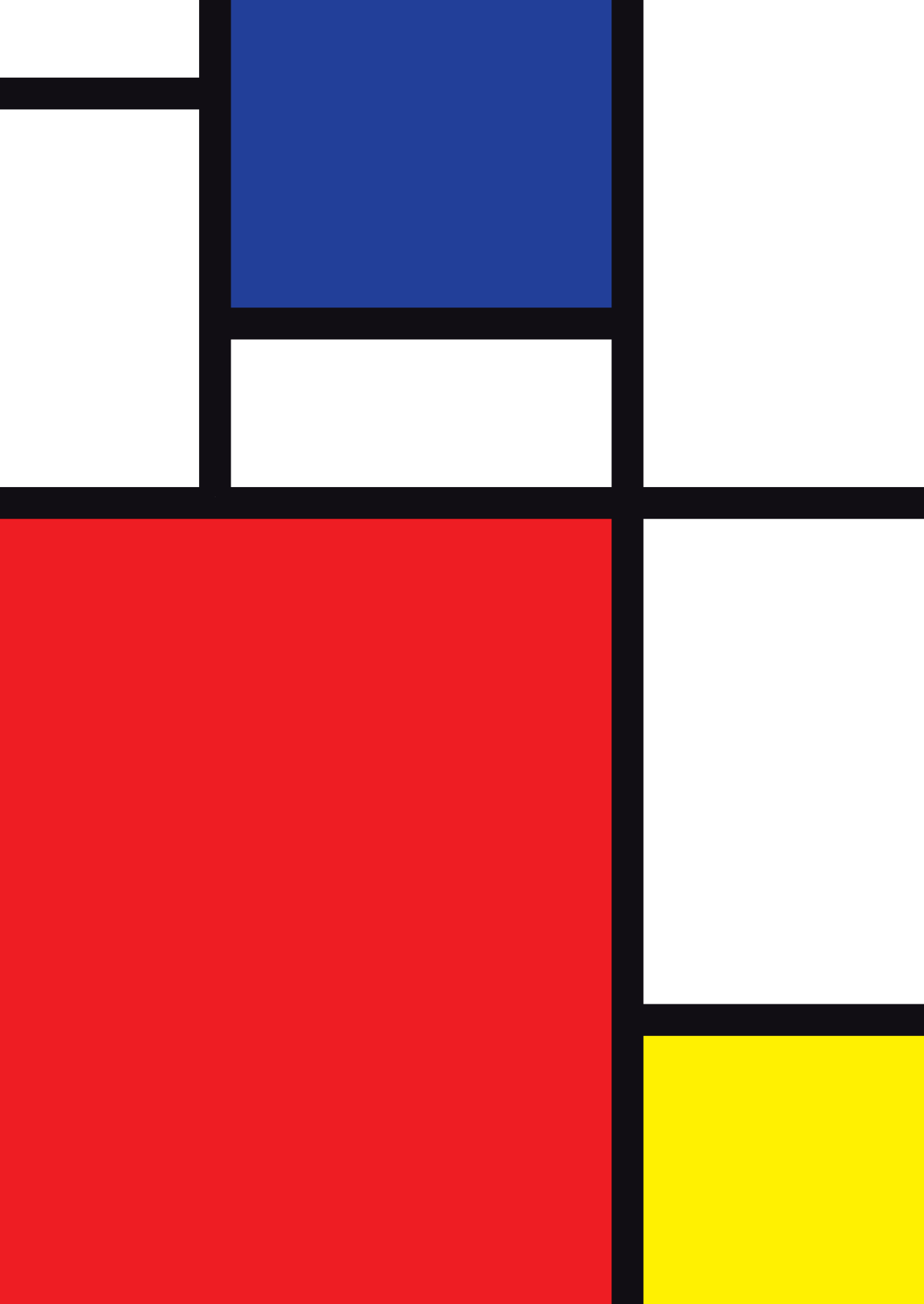

Appendices

A1 - Dutch Summary

Deze thesis is het resultaat van experimenteel onderzoek uitgevoerd in het Fries lab, met als doel het neurowetenschappelijke begrip te vergroten van hoe de hersenen informatie coderen en doorgeven. Alle experimenten werden uitgevoerd in een niet-menselijk primaten (NHP) experimenteel model en omvatten intracraniële opnames van neuronale activiteit in de vorm van lokale veldpotentialen (LFP's) en multi-unit activiteit (MUA), in het primaire visuele hersengebied V1, terwijl het dier wakker was en een fixatietaak uitvoerde. Het onderzoek richtte zich op het herzien van twee goed bestudeerde onderwerpen in de neurowetenschappen, namelijk de oscillatoire hersenactiviteit in het gamma-bereik (≈40-90 Hz) en de neuronale piekactiviteit, en op het verder verduidelijken van hun onderlinge relatie en hun gedrag onder specifieke stimulatiecondities. In dit kader werden twee wetenschappelijke vragen onderzocht:

1. Hoe moduleert gamma-ritmische activiteit de gain van de MUA-respons op een visuele stimulus?
2. Hoe gedragen de gamma-bandoscillatoire activiteit en MUA zich in de context van onconventionele stimulusherhaling?

Vraag 1 werd behandeld in Hoofdstuk 2 door een eerdere studie (Ni, Wunderle et al. 2016) te herzien met een nieuw stimulatieparadigma en nieuwe analysemethoden. Het onderzoek beoordeelde het effect van de fase van gamma-bandoscillaties op de modulatie van de MUA-gain in reactie op een visuele stimulus. De werkhypothese van de studie was dat gamma een multiplicatieve modulatie van de gain oplegt, dat wil zeggen dat gamma in staat is de gevoeligheid van neuronen voor een stimulus te veranderen. Het multiplicatieve karakter van dit gain-modulatie-effect houdt in dat de MUA-respons op de presentatie van een stimulus niet kan worden beschreven als louter een som van een constante stimulusrespons opgeteld bij gammafasen van hogere of lagere prikkelbaarheid, bepaald door de lopende gamma-oscillatie. De studie karakteriseerde ook de modulatie die door het gamma-ritme op MUA werd opgelegd door het model te identificeren (input- of output-gain) volgens welk gamma de MUA-gain moduleert, en bepaalde daarnaast de absolute fase van gamma-modulatie.

Vraag 2 werd behandeld in Hoofdstuk 3 en herzag eveneens eerdere bevindingen, namelijk dat stimulusherhaling er doorgaans toe leidt dat de vuursnelheden in V1 afnemen en de gamma-activiteit toeneemt. Het idee om het gedrag van gamma-bandoscillatoire activiteit en MUA in relatie tot stimulusherhaling opnieuw te onder-

zoeken ontstond door de overvloed aan trials die tijdens de opnames werden verzameld, en door de vaststelling dat de visuele stimuli die in het paradigma van Hoofdstuk 2 werden gebruikt onconventioneel waren en nog niet in verband met het herhalingseffect waren bestudeerd. Klassieke studies over stimulusherhaling rapporteerden consequent dezelfde resultaten voor gamma-oscillatoire activiteit en MUA (Brunet, Bosman et al. 2014, Peter, Stauch et al. 2021, Stauch, Peter et al. 2021, Psarou, Parto-Dezfouli et al. 2025). Daarom had de studie tot doel te beoordelen of de klassieke effecten ook konden worden teruggevonden voor de nieuwe set visuele stimuli die in Hoofdstuk 2 werd gebruikt.

De bevindingen van het onderzoek worden tot slot besproken. Er worden overwegingen gepresenteerd over de noodzaak om vervolgonderzoek uit te voeren om rekening te houden met storende variabelen. Er worden enkele gedachten geuit over de generaliseerbaarheid van de resultaten en de reproduceerbaarheid van de studie. Ten slotte worden de belangrijkste vragen die uit de twee onderzoekshoofdstukken naar voren komen en die richting kunnen geven aan toekomstig onderzoek beschreven.

A2 - English Summary

This thesis is the result of experimental work conducted in the Fries lab, to the end of broadening the neuroscientific understanding of how the brain encodes and transmits information. All the experiments were carried out in a non-humane primate (NHP) experimental model, and involved intra-cranial recordings of neuronal activity in the form of local field potentials (LFPs) and multi-unit activity (MUA), in the primary visual cortical area, V1, while the animal was awake and performing a fixation task. The research work carried out focused on revisiting two well-studied topics in neuroscience, namely the brain oscillatory activity in the gamma range (≈40-90 Hz), and the neuronal spiking activity, and on further clarifying the relationship they entertain with each other and their behavior in particular stimulation conditions. To this end, the scientific questions that were addressed in the thesis were mainly two:

1. How does gamma rhythmic activity modulate the gain of the MUA response to a visual stimulus?
2. How do gamma band oscillatory activity and MUA behave in the context of unconventional stimuli repetition?

Questions 1 was addressed in Chapter 2 by revisiting a previous study (Ni, Wunderle et al. 2016), with a new stimulation paradigm and new analysis methods. The study assessed the effect of gamma-band oscillation phase on the MUA gain modulation in response to a visual stimulus. The working hypothesis of the study was that gamma imposes a multiplicative gain modulatory effect, i.e. that gamma is capable of changing the neurons' sensitivity to a stimulus. The multiplicative nature of this gain modulation effect entails that the MUA response to the presentation of a stimulus cannot be described as a mere sum of a constant stimulus response added on top of gamma phases of higher or lower excitability determined by the ongoing gamma oscillatory activity. The study also characterised the modulation imposed by the gamma rhythm on MUA by identifying the model, input or output gain, according to which gamma is modulating the MUA gain, and assessed the absolute phase of gamma modulation.

Question 2 was addressed in Chapter 3 and also revisited previous findings, namely that stimulus repetition typically leads to V1 firing rates to decrease and gamma activity to increase. The idea to re-investigate the behavior of gamma-band oscillatory activity and MUA in relation to stimulus repetition stemmed from the abundance of trials collected during the recordings, and from the realization that

the visual stimuli presented in the paradigm used in Chapter 2 were unconventional and had not yet been studied in relation to the repetition effect. Classical studies about stimulus repetition consistently reported the same results for gamma-oscillatory activity and MUA (Brunet, Bosman et al. 2014, Peter, Stauch et al. 2021, Stauch, Peter et al. 2021, Psarou, Parto-Dezfouli et al. 2025), so the study aimed to assess if the classical effects could be found for the novel set of visual stimuli used in Chapter 2.

The findings of the research work are finally discussed. Considerations about the necessity to conduct further studies to account for confounding variables are presented. Some thoughts are expressed regarding result generalizability and study reproducibility. Finally, the main questions emerging from the two research chapters to lead to future investigation are described.

A3 - Data Management

Ethical approval

All the procedures described in this thesis involving the use of experimental animals were carried out in compliance with the German and European law for the protection of animals (EU Directive 2010/63/EU for animal experiments). The housing conditions for the NHP also complied with the abovementioned law. The experimental and surgical procedures described in Chapter 2 and Chapter 3 were reviewed and approved by the German regional authority, the Regierungspräsidium Darmstadt.

Findability and Accessibility

The raw data collected and analyzed for the studies in Chapter 2 and Chapter 3 are stored in in the archive of the Ernst Strüngmann Institute (ESI) for Neuroscience in Cooperation with Max Planck Society in Frankfurt am Main, (Germany), where the experiments were conducted and the data were collected.

Interoperability and Reusability

The MUA and LFP raw and preprocessed trial data used in the analysis, together with the custom MATLAB (Chapter 3) and Python (Chapter 2) code used to analyze the data have been documented and stored in the archives of the Ernst Strüngmann Institute (ESI) for Neuroscience.

The preprocessed data used in Chapter 2 and Chapter 3 can be provided upon reasonable request.

A4 - Abbreviations

(In alphabetical order)

AM	=	Additive modulation
BOLD	=	Blood-oxygenation level dependent (response or imaging)
CO	=	cytochrome oxidase
CR	=	Constant response
CTC	=	Communication through coherence
dva	=	degrees of visual field
E – I	=	Excitatory – inhibitory network of neurons
E	=	excitatory neuron connected to a network
e	=	excitatory neuron NOT connected to a network
EPSP	=	Excitatory post-synaptic potential
fMRI	=	functional magnetic resonance imaging
FOOOF	=	fitting-oscillations-and-one-over-f method
FSB	=	Full-screen background
FSCB	=	Full-screen-colored background
GABA	=	Gamma-aminobutyric acid
I – I	=	inhibitory – Inhibitory network of neurons
I	=	inhibitory neuron connected to a network
I/O	=	Input-output (referred to input-output response curve of a neuron)
ING	=	Interneuron-network gamma
IPSP	=	Inhibitory post-synaptic potential
L1	=	Layer 1
L2	=	Layer 2
L3	=	Layer 3
L4	=	Layer 4
L5	=	Layer 5
L6	=	Layer 6
LFP	=	Local field potential
LGN	=	Lateral geniculate nucleus
MD	=	Modulation depth
MM	=	Multiplicative modulation
MUA	=	Multi-unit activity
NHP	=	Non-human primates
OM	=	Ongoing modulation
PING	=	Pyramidal-interneuron network gamma
PPC	=	Pairwise phase consistency metric

PV^+	=	Parvalbumin-positive interneurons
RF	=	Receptive field
RR	=	Repetition-related response ratio
RT	=	Reaction times
SR	=	Stimulus-related response ration
SST	=	Somatostatin-expressing interneurons
STDP	=	Spike time-dependent plasticity
sTP	=	surrogate time point
TP	=	time point
V1	=	Visual area 1 (Primary visual area)
V2	=	Visual area 2
V4	=	Visual area 4
VIP	=	Vasoactive intestinal peptide expressing interneurons
V_m	=	Membrane potential

A5 - Curriculum Vitae

Education

- M.Sc. in Neuroscience
  International Master Degree in Neuroscience, University of Trieste and SISSA (Trieste, Italy)
- Supplementary superior education
  Excellence University College 'Luciano Fonda' (Trieste, Italy)
- B.Sc. in Biological Sciences
  University of Florence (Florence, Italy)

Research Experience

- 04/10/2021 – present. PhD candidate
  Fries lab, Ernst Strüngmann Institute (ESI) for Neuroscience in cooperation with the Max Planck Society (Frankfurt am Main, Germany)
- 01/10/2018 – 24/03/2021 Master Thesis
  "Role of Locus Coeruleus – Noradrenergic system in sleep dependent memory consolidation", University of Trieste (Trieste, Italy) and Eberhard Karls Universität Tübingen (Tübingen, Germany)
- 15/09/2015 – 26/09/2018 Bachelor Thesis
  "Establishment and molecular characterization of AGS-5FUr, AGS-CISr and AGS-TAXr chemoresistant cell lines obtained from a human gastric cancer cell line", University of Florence (Firenze, Italy)

Publications

Pandinelli, M., Parto-Dezfouli, M., Psarou, E., Grothe, I. and Fries, P. (2025). "Surprising effects of stimulus repetition on neuronal firing rates and gamma-band synchronization in awake macaque V1." bioRxiv 2025.07.09.663517. doi: https://doi.org/10.1101/2025.07.09.663517

Näher, T., Zhang, Y., Pandinelli, M. and Fries, P. (2024). "Primate Saccade Rhythmicity." bioRxiv 2023.09.27.559710; doi: https://doi.org/10.1101/2023.09.27.559710

Durán, E., Pandinelli, M., Logothetis, N. K., and Eschenko, O. (2023). "Altered norepinephrine transmission after spatial learning impairs sleep-mediated memory consolidation in rats." Sci Rep 13(1): 4231. https://doi.org/10.1038/s41598-023-31308-1

A6 - Acknowledgements

I have been trying to start writing these acknowledgements about a million times, and about a million times I stopped and got stuck with the clear feeling of being incapable to express in words how grateful I actually am to all the people that belonged to this incredibly intense journey. I wanted to use creative words that would sound special and elevated, and funny, and deep at the same time, and inevitably failed to accomplish that. The truth is, you all deserve a poem worth the Divine Comedy, and I am only capable of writing very simple, probably banal words that cannot possibly express the magnitude of my gratitude for you all. Nevertheless, I shall try, and I hope you will still be able to perceive, at least in part, how big my love and appreciation for you are. I am the luckiest person in the universe to know such beautiful people, I cannot say it often enough.

Pascal, thank you for your supervision and your guidance during this complicated journey. Thank you for sharing with me your smart insights about the brain, and for allowing me to take part to your vision and translating it into scientific work. I will remain especially grateful to you for your singing "Il canto del cucù" to me, trying to cheer me up in one of the darkest moments of these past years. Your delicate and polite humor never failed to leave a smile on my face.

A huge and heartfelt thank you goes to two incredible people, near and far, whose support I never missed when I needed it, and that I was lucky enough to have by my side: Saskia and Renata. Saskia, I really admire the brilliant scientist you are, and I thank you for always providing me with precious, sharp and to-the-point comments on my scientific work as part of my TAC committee. I also hold the most profound respect for you, for the person you are, and for your dedication to remain in academia, trying to make it a better world. Many more people like you are desperately needed. Renata, your commitment to support me in navigating the complex political dynamics at ESI, and in always trying to find a solution to any problem is unprecedented. I cherish that we became closer during this journey. Your beautiful emotional depth, and the care you demonstrate towards all of us will always be dear to me.

Lothar, thank you for your help and support in the last part of this journey. I was glad to be able to interact with a professional and trustworthy person like you.

Marieke, thank you for taking up the role of my co-supervisor and checking in with me every once in a while, for scientific and any other kind of help I might have needed.

Georg, thank you for your constant support with my technical challenges. You were always there, even on a Friday evening, ready to help me repair the dead battery of an RS4, always with a smile on your face and nice chats. Our "Freitag ist Deutschtag" moment was always the best part of my week.

Joshua, thank you for always visiting me in the office to chat and see how I am doing. I will miss our conversations. It all started when Frederike and Dorothee were still in that same room, and I am glad we kept the tradition going.

Frede and Doro, a huge thank you to you, beautiful women and fantastic scientists. My original office mates, the two people who welcomed me at ESI, helped me immensely with moving my first steps in navigating the PhD, and the difficult situation at the institute. The years we shared together were possibly the hardest of our journeys: I am glad I had the two of you to share hardships, a lot of funny moments, and our memorable emergency cupboard with. I am forever grateful for learning so much from you both. Since the moment I moved desk in that office, I knew things were never going to be the same.

With Frede and Doro my gratitude goes also to Yufeng, Ben, Elena, Tina, Rasmus, Mohsen, Shivangi, Tim (Näher), Tim (Schäfer), Diljit, Tianlu, Matthias, Jackson, Nanni, Sabrina, all the wonderful colleagues that belonged to the Fries Lab when I first joined, and that I shared offices, labs, and great memories with. It breaks my heart to think that the lab was dismembered, and that we had to part in such awful circumstances. We could have accomplished so much more together, it was really a huge loss of potential, and mostly of great people. Every one of you gave me something that goes well beyond the scientific help, which was already great. I deeply thank you for that, and I hope wherever you are in your life right now you are happy and fulfilled.

Yufeng and Tim, a special thanks to you for your help and support until the very last moment of your presence at ESI and beyond. You are both brilliant minds I was constantly inspired by, and I learnt a huge amount form you. My thesis would not be here without Tim's precious contribution. I am glad I could give a bit back to you guys by joining some of your experiments.

Mohsen, a huge thank you goes to you as well. My latest office mate, who joined me in the loneliness of my empty office, and made it a comfortable and lively space again. I am happy we could share these past years together, and I am thankful that I could have next to me a person whose presence was always calming, reassuring,

and respectful. Thank you for all of your help, without you another big part of this work would not be there. And thank you for sharing with me your professional, and personal life as friends.

Elena. Here the words really fail me, I cannot express how much help I received from you, and how much I have learnt as a scientist and as a person. From a professional point of view, you taught me all I know about being a neuroscientist, and I admire you for how knowledgeable and skilled you are. But this is only a small part. You have been the one and only working together with me side by side, since day one, with dedication and consistency, to make it happen for real. Despite the difficulty of your journey, and how much was on your plate, and despite the fact that you were left alone to learn everything, you decided to stick with me and give me the guidance you did not received, to avoid that yet another PhD student would have to suffer through what you did. This really takes courage, moral integrity, and great strength. Many people should be inspired by you and your choice to try to make science a healthier place, replacing toxic ego and competition with support and guidance. I am forever grateful to you for this and I am happy to call you a friend even outside the lab.

Rasmus. Something very similar goes for you. Thank you for being a constant presence I could always count on during this journey. The last one standing next to me, you never failed to be there to provide me with scientific guidance and assistance, together with moral and emotional support whenever I needed it. I have always felt at ease working with you: every learning moment was also a moment where we could learn about each other and bond. I had a lot of fun working together, training and cleaning monkeys, and being good friends outside of work. You are a great person, fun, witty, big-hearted, and always ready to right wrongs you see happening around you. Except for your tic-tac gun. Put that away.

Speaking of monkeys, my greatest gratitude, appreciation and love for two tireless coworkers, without whom REALLY this thesis would not be here. Gandalf and Homer, you have offered me the invaluable opportunity to work with you to collect the data that are here analyzed, trying to shed a small light on the biggest mystery, the brain. You beautiful creatures with the best personalities: Gandalf, always on charge and fearless, old and wise. Homer, sweet and quiet, with your big deep eyes. Working with you was a huge learning experience in patience, respect, and care.

Natalie, thank you for being my foster post-doc. During my years of being a free-lance PhD student without a lab, I have always found of the biggest help

the scientific feedback you were available to provide me with. I am glad to have you amongst my friends. From day to day texting about fitting functions, to recommendations on what journals to publish, to our gossip sessions and support group for finding a job, and to the "ESI summer Feierabend" hangouts protocols, you are such a smart, caring and fun person to be around. I really thank you for that.

Together with this group of amazing colleagues and friends that I have just mentioned and I have had around from day one, I am lucky enough to say that many more have joined the gang during the years, some newly come, some have always been there but we discovered each other after a while. Rob, Mina, Shivangi, Ryan, Ana, Nisa, Moad, Ece, Amr, Petros, Lana, and Janina. I couldn't be happier and more grateful to have such fantastic and brilliant people sharing interests, discussions, hangouts, great parties, amazing music sessions, deep moments of connections through thick and thin with me. Thank you for always being there for me, you are the greatest gift from my Frankfurt experience.

Rob, I was especially grateful for the late blooming of a deeper friendship between the two of us. I cannot help but smile thinking about how we danced around each other for a while, keeping a distance because intimidated by the idea we had of one another. I am so happy that this culminated in a strong, fun, honest and supportive friendship, to the point that I still ask myself how we did not become friends sooner. You are such a precious person, I admire your openness and directness in communicating your feelings, how much you practice this in your everyday life, and the confidence that stems from it. I am very inspired by you, and by the hard work you put in everything you do. Thank you for being a great friend, advising me on how to be less boomer, showing me the ways of fashion, and simply E-slaying.

Un grandissimo grazie va anche a colleghi e amici che sono dispersi per il mondo, ma il cui affetto non mi manca mai: Matteo e Ana. Grazie per la vostra gioiosa allegria, empatia e vitalita'. Matteo sai quanto sono felice che ci siamo incontrati e abbiamo connesso in modo cosi' intuitivo e spontaneo. Le nostre conversazioni e la tua speciale sensibilita' le ho portate sempre con me in questo percorso e mi hanno aiutato profondamente.

Francesca, Alberto: grazie per essere la mia casa a Francoforte. Un pezzo di Italia che mi accoglie e mi fa sentire curata e amata. Grazie per le nostre cene, il ragu' spaziale di Berto, gli Spritz fenomenali di Fra, la vostra splendida generosita' e voglia di far stare bene le persone in compagnia. Mi sento sempre accolta e circondata da un caldo affetto quando siamo insieme, siete delle persone stupende e davvero ho la

sensazione di stare in famiglia quando passo del tempo con voi. Fra, grazie speciale a te per esserci sempre stata in questi anni, per le nostre fantastiche sessioni di gossip in ufficio, e tutte le risate che ci siamo fatte.

Elena, grazie anche a te. La mia prima supervisor in un laboratorio, ci siamo conosciute quando eravamo ancora etrambe quasi delle "bambine", appena approdate nel mondo della scienza. Le nostre lunghe passeggiate durante il Covid, le letture che ci siamo consigliate e scambiate, le nostre chiacchierate sono ricordi molto cari che porto con me. Grazie per la tua magnifica presenza, sempre positiva e delicata, piena di gioia e voglia di fare. Ho imparato moltissimo da te, a non farmi abbattere dalle difficolta' e a rialzarmi sempre reinventandomi ancora una volta. Grazie per il tuo ascolto costante e la tua vicinanza.

Dario, Lorenzo, Camilla, Clara and Adrianna. Thank you for being my amazing friends outside work. The people I could always turn to when I needed a break from the institute drama, and with whom I am always so excited to spend my time. I love that we can share so much together, from going to exhibitions, museums and cinemas and do a lot of brainy talk about books, ideas and ideals, to letting loose, partying and dancing like crazy and being out and about discovering the city, doing every sort of fun things together.

Cami, tu specialmente sei sempre in grado di illuminarmi con la tua luce serena. Con i tuoi consigli che mi hanno sempre messo su una buona strada quando ero confusa o in difficolta'. Sono incredibilmente grata che ci siamo conosciute quella sera al Naxos: non tutti possono essere cosi fortunati da dire di avere un'amica cosi meravigliosa che li ispira ogni giorno con la sua arte stupenda e con la sua forza d'animo di donna forte e consapevole. E' sempre bellissimo parlare e danzare con te, grazie per darmi questa opportunita di esprimermi con te con e senza le parole.

Darione, grazie davvero perche' tu sei quella persona su cui posso sempre contare, che e' li accanto a me e non esita mai a finire le birre che inizio e non finisco perche non mi piacciono. Grazie per essere sempre felice di partecipare a qualunque evento strambo ti propongo, per essere una presenza che sa sia ascoltare che condividere quello che pensa. Grazie perche' piano piano ci siamo aperti l'uno con l'altra e abbiamo condiviso tante cose profonde di noi stessi, a partire da quei tempi remoti in cui sia tu che io avevamo ancora i capelli lunghi, ed eravamo un po' impauriti da noi stessi.

Grazie alle mie pazze, splendide, favolose ragazze Francesca, Chiara, Bianca, Anna, Tiziana. Abbiamo condiviso insieme gli albori del nostro percorso di Neuroscienziate, e sono grata che siamo rimaste vicine e sempre desiderose di aggiornarci sulla vita di ognuna. Dalle nostre avventure fra gli scogli di Barcola fino alle diverse strade che le nostre vite hanno preso, e' bello sapere di poter contare su di voi per chiacchiere di ogni tipo, allegre e spensierate e profonde. Grazie per essere donne incredibili, ognuna di voi mi ispira costantemente nella propria unicita'.

Grazie anche ai miei amici di sempre, quelli che davvero mi hanno vista crescere e che, in un modo o nell'altro sono ancora vicini, anche se ci vediamo poco e viviamo lontani. Matteo, Angelo, Lorenzo, Simone, Giacomo. Sono felice che ancora facciamo parte gli uni del cammino degli altri e che siamo stati spettatori di alti e bassi della vita di tutti e siamo presenti per sostenerci a vicenda. Lollo, grazie perche' con alle tue magliette grandi e accoglienti il tuo abbraccio rassicurante non mi e' mai mancato anche da cosi lontano. Simo, sono piena di gioia al pensiero che tu sia "tornato" e rientrato a far parte delle nostre vite. Mi mancava tantissimo la tua presenza viva e positiva, sempre attenta ai sentimenti e alle esigenze di tutti, la tua incredibile simpatia e voglia di fare amicizia anche con i tavoli. Giaco, grazie per essere il mio amico giramondo che condivide con me la passione e anche le difficolta' di avere una vita che si svolge sempre in 50 luoghi diversi allo stesso tempo. Grazie per le risate che ci siamo sempre fatti insieme, per le nostre stupidaggini, e per tutte le foto ridicole che mi hai fatto.

Grazie a Susanna e Annalisa, le mie amiche di una vita – una vita davvero! – da quando avevamo sei anni sempre insieme, coltivando la nostra amicizia con giochi, corse al mare, diari e lettere invernali. Grazie per essere ancora nella mia vita con la vostra dolcezza e semplicita'.

Frederique, sei un'amica fenomenale. Adoro fare mille avventure sempre diverse con te, cavalli, salite ripide dove tutti ci odiano perche' li trasciniamo a camminare, le serate dalla mitica Silvia di Dio, non ci anniamo mai. Hai uno spirito fantastico, sei sempre pronta e piena di voglia di fare, mi trascini in un'onda di energia positiva. Le nostre chiacchierate durante le mie migrazioni fra Germania, Olanda e Belgio mi danno sempre un sacco di carica. Grazie per la tua costante presenza e per i mille reel che mi fanno sentire che non sono mai sola. Apprezzamento speciale per il mio Pippino, la stella magica del mio cuore.

Grazie dal profondo del mio cuore a tutta la mia famiglia, che ha da sempre seguito il mio percorso con affetto, fiducia e stima. Grazie a zio Giacomo, zia Francy, Gabriele,

Giovanni e alla mia amata Nina per essere parte del mio cammino, e per mostrare sempre gioia nello stare insieme e nel condividere sfide e traguardi di ognuno di noi.

Grazie a babbo, Andrea, Susanna e Luciana. Grazie per il vostro amore e il vostro supporto. Grazie babbo per la tua presenza nello spronarmi e nell'elaborare con me piani strategici per affrontare le difficolta'del mondo del lavoro. Andre, Susy, sento la vostra ammirazione nei miei confronti, ma non perdete mai tempo a seguire le mie orme. Mi rendete fiera di voi seguendo il vostro personale cammino e diventendo delle splendide persone cosi' come state facendo. Sono contenta che possiamo condividere ogni giorno qualcosa in piu' e far parte sempre di piu' gli uni della vita degli altri, vi voglio bene.

Giammi grazie per aver condiviso con me gli ultimi quattro intensissimi anni. Grazie per la tua presenza in ogni momento del mio dottorato, sei stato tu il mio vero mentore e post-doc di riferimento in tante circostanze, con la tua incredibile intelligenza e abilita' nell'analizzare problemi e situazioni di ogni tipo. Ti ringrazio infinitamente per la tua capacita' di sapermi spronare a non fermarmi davanti alle paure e a scavalcare i limiti che mi frenano, nel mio percorso professionale e nella vita. Sopra ogni cosa pero', ti ringrazio per essere stato il mio compagno in tutto questo tempo, e per avermi vista cambiare, crescere, ed essere anche tu cresicuto e cambiato con me. Abbiamo attraversato mari tempestosi e scogli, e visto spiagge bellissime e tranquille. Scalato montagne e visto notti di stelle stupende insieme, nelle nostre avventure in giro per il mondo e nella nostra relazione allo stesso modo. Questo nostro percorso e' stato straordinariamente vario e movimentato, ti ringrazio perche' lo abbiamo affrontato insieme imparando a conoscerci e volerci bene per quello che siamo. Non c'e' cosa piu' preziosa.

Giuli, la mia roccia, il mio punto fisso. Grazie di essere sempre e da sempre quella persona che non si stanca mai di essere al mio fianco, di occuparsi di estendere il proprio se' per favorire la propria e la mia crescita in tutti i campi. Ho rubato le belle parole di Bell Hooks per descrivere questa nostra amicizia, che mi sento corrisponda in pieno alla sua definizione. Grazie perche' non mi hai mai fatto sentire, neanche per un momento, di dovermi meritare il tuo affetto, di dover comportarmi in un certo modo per avere la tua amicizia. Grazie per avermi fatto sempre sentire libera di essere me stessa e di fare le mie scelte, anche quando queste ci hanno allontanato per un po' di tempo. Grazie perche' continui ad essere sempre incredibilmente presente nella mia vita con complicita' e fiducia. Sono felice che dopo tutti questi anni camminiamo ancora insieme, l'una a fianco dell'altra sempre pronte a sostenerci e trainarci a vicenda quando l'altra e' in difficolta'. E sono grata perche'

mi permetti di imparare da te, specialmente la cura e l'attenzione che poni nei tuoi rapporti con gli altri. Avere un'amicizia come la tua e' un dono davvero inestimabile.

Un piccolo ringraziamento lo vorrei fare anche a me stessa, concedendomi questa liberta', anche se magari sembrera' un po' arrogante. Sento di dovermi ringraziare per tutta questa strada fatta fino ad adesso, in questi 30 anni di vita. Per la determinazione con cui ho cercato di affrontare tutte le cose con cui mi sono dovuta confrontare e per avere sempre cercato di fare del mio meglio. Grazie per quando ci sono riuscita e anche per quando non ci sono riuscita. Grazie per le cose belle e quelle brutte, per le cose giuste e per tutti gli errori che mi hanno concesso di imparare qualcosa. Grazie per non aver mollato mai, anche quando le difficolta' sembravano troppe, e per aver intrapreso un percorso per conoscermi sempre di piu' e stare sempre meglio con me stessa, a prescindere da chiunque altro. Grazie per essermi presa cura di me stessa e per cercare di imparare a farlo sempre meglio ogni giorno, anche se a volte e' tanto difficile.

Mamma per te il grazie piu grande. Grazie di non avermi mai fatto mancare nulla, soprattutto il tuo amore incodizionato e smisurato. E' sempre stato con me e sempre lo sara', e' forse l'unica certezza che porto nella vita. Anche Joyce lo diceva nell'Ulisse, "Amor matris, genitivo soggettivo e oggettivo, e' probabilmente l'unica cosa vera della vita". Grazie per i sacrifici che hai fatto per me e per avermi sempre accompagnata nel mio percorso. Grazie per avermi saputo lasciar andare e spiccare le ali verso la mia vita in una terra straniera, dove sto cercando ogni giorno di scoprire me stessa. Grazie per essere sempre pronta ad accogliermi in qualunque condizione mi trovi e a darmi una spinta o una rassicurazione quando ne ho bisogno. Grazie per avermi risparmiato e ancora risparmiarmi il peso di molte difficolta' che porti silenziosamente sulle tue spalle. Sappi pero' che adesso posso farlo anche io per te, puoi sempre contare su di me quando hai bisogno. Ti voglio un bene infinito.

Come sempre quando scrivo, non sono riuscita a contenermi, le mie parole hanno travolto le pagine come un fiume in piena, ma non potevo fare altrimenti nel rievocare alla mia mente tutta la gratitudine e i sentimenti che provo per ognuno di voi. Per concludere, vorrei dedicare questo lavoro frutto di tanti sforzi e tanta fatica, alla mia nonna Grazia, che non c'e' piu'. Nonna, so che oggi sei la piu' fiera di tutti, piu' fiera anche di me stessa e della mamma perche' ho raggiunto questo traguardo. Anche se probabilmente ancora non hai ancora capito che cosa faccio o come si scrive la parola Neuroscienze. So che insieme avremmo riso molto di questo. Grazie di avermi cresciuta e di avermi sempre fatto sentire di essere speciale. Mi manchi molto.

Donders Graduate School

For a successful research Institute, it is vital to train the next generation of scientists. To achieve this goal, the Donders Institute for Brain, Cognition and Behaviour established the Donders Graduate School in 2009. The mission of the Donders Graduate School is to guide our graduates to become skilled academics who are equipped for a wide range of professions. To achieve this, we do our utmost to ensure that our PhD candidates receive support and supervision of the highest quality.

Since 2009, the Donders Graduate School has grown into a vibrant community of highly talented national and international PhD candidates, with over 500 PhD candidates enrolled. Their backgrounds cover a wide range of disciplines, from physics to psychology, medicine to psycholinguistics, and biology to artificial intelligence. Similarly, their interdisciplinary research covers genetic, molecular, and cellular processes at one end and computational, system-level neuroscience with cognitive and behavioural analysis at the other end. We ask all PhD candidates within the Donders Graduate School to publish their PhD thesis in de Donders Thesis Series. This series currently includes over 600 PhD theses from our PhD graduates and thereby provides a comprehensive overview of the diverse types of research performed at the Donders Institute. A complete overview of the Donders Thesis Series can be found on our website: https://www.ru.nl/donders/donders-series

The Donders Graduate School tracks the careers of our PhD graduates carefully. In general, the PhD graduates end up at high-quality positions in different sectors, for a complete overview see https://www.ru.nl/donders/destination-our-former-phd. A large proportion of our PhD alumni continue in academia (>50%). Most of them first work as a postdoc before growing into more senior research positions. They work at top institutes worldwide, such as University of Oxford, University of Cambridge, Stanford University, Princeton University, UCL London, MPI Leipzig, Karolinska Institute, UC Berkeley, EPFL Lausanne, and many others. In addition, a large group of PhD graduates continue in clinical positions, sometimes combining it with academic research. Clinical positions can be divided into medical doctors, for instance, in genetics, geriatrics, psychiatry, or neurology, and in psychologists, for instance as healthcare psychologist, clinical neuropsychologist, or clinical psychologist. Furthermore, there are PhD graduates who continue to work as researchers outside academia, for instance at non-profit or government organizations, or in pharmaceutical companies. There are also PhD graduates who work in education, such as teachers in high school, or as lecturers in higher education. Others continue in a wide range of positions, such as policy advisors,

project managers, consultants, data scientists, web- or software developers, business owners, regulatory affairs specialists, engineers, managers, or IT architects. As such, the career paths of Donders PhD graduates span a broad range of sectors and professions, but the common factor is that they almost all have become successful professionals.

For more information on the Donders Graduate School, as well as past and upcoming defences please visit: http://www.ru.nl/donders/graduate-school/phd/

9 789465 152585 >

DONDERS INSTITUTE

Radboud University

Radboudumc